

**Carbon-carbon Bond Forming Reactions from Bis(carbene)-
platinum(II) Complexes**

-and-

**Olefin Polymerization and Oligomerization Using Group 4 Post-
metallocene Complexes**

Thesis by

Rachel Christine Klet

In Partial Fulfillment for the Requirements for the
Degree of Doctor of Philosophy

California Institute of Technology

Pasadena, California

2014

(Defended August 19, 2013)

© 2014

Rachel Christine Klet

All Rights Reserved

With gratitude to all the teachers, mentors, family, and friends who helped me get to where I am today.

I found Sherlock Holmes alone, however, half asleep, with his long, thin form curled up in the recesses of his armchair. A formidable array of bottles and test-tubes, with the pungent cleanly smell of hydrochloric acid, told me that he had spent his day in the chemical work which was so dear to him.

"Well, have you solved it?" I asked as I entered.

"Yes. It was the bisulphate of baryta."

"No, no, the mystery!" I cried.

*- The Adventures of Sherlock Holmes: A Case of Identity
by Sir Arthur Conan Doyle*

Acknowledgements

Looking back at my time at Caltech, I can sincerely say I've had a wonderful experience here and I'm humbled and extremely thankful to the people who helped me on this path; it's not an easy one!

I'm very lucky to count myself among John's PhD students. I'll never forget when I was deciding where to go for grad school and my undergrad advisor (W. Dean Harman) told me of John: "I've heard a lot of things said about a lot of people, but I've never heard anyone say anything bad about John Bercaw." After six years in his group, I understand why. John is extremely patient – particularly with his students – and brilliant, but he is also humble, despite how successful he's been. He's been a wonderful mentor and teacher to me and I've learned an incredible amount from him. I think he does science the "right way," but he also lives his life the right way – by the way he treats people; he is a great role model and someone I deeply admire and respect. He doesn't like me saying "[he] knows everything," but I'll continue to think it's true. John, thank you for letting me join your group and being my PhD advisor.

Jay Labinger has been my co-advisor throughout my PhD and I've learned as much from him as from John. Jay always has great suggestions for all aspects of science, and although I'm still intimidated by Jay's intelligence, I've learned that it's to my benefit to get over my fear of looking stupid and to ask him questions. I'm particularly grateful that Jay has taken the time to help me become a better science writer and patiently edited everything I've written in grad school.

Jay is a great teacher and much like John, Jay has played a very large role in shaping me into the scientist I am today. Thank you Jay.

My committee as a whole has been wonderful. Theo has been a good friend and extremely supportive of me at times when grad school has been really tough; but, Theo has also been tough on me when I've needed someone to push me. Harry is without a doubt the most generous person I've ever met and has made me realize that I always can and should do more for other people. He also has the most incredible stories and is the reason I came to Caltech; I'm lucky to know him (Go Dodgers!). Sarah has encouraged me and supported me since I started here, and I really look to her as a role model for myself as a woman in chemistry. I've asked her a lot of questions about her experiences and she's always been very honest and insightful. My committee has made all of the Ph.D. hurdles valuable experiences – particularly my prop exam – the pKa of water is 15.7, by the way. Thank you for your support, encouragement, and helping me to become a better scientist.

Finally, I want to thank my friends, family, and the colleagues I've shared a lab with for six years. I've made some really really wonderful friends here, many of whom I expect and hope will be lifelong friends. My friends have helped me with experiments (literally standing by my side when I've set things up), taught me chemistry, and been sounding boards for the scientific process; they've provided shoulders to cry on, and have been people to laugh with; they've been company at memorable meals, enablers of fine wine, partners to explore the

outdoors and LA with, and so much more. All of you mean so much to me and have made my time at Caltech so special; thanks for always being there for me.

Abstract

A long-standing challenge in transition metal catalysis is selective C–C bond coupling of simple feedstocks, such as carbon monoxide, ethylene or propylene, to yield value-added products. This work describes efforts toward selective C–C bond formation using early- and late-transition metals, which may have important implications for the production of fuels and plastics, as well as many other commodity chemicals.

The industrial Fischer-Tropsch (F-T) process converts synthesis gas (syngas, a mixture of CO + H₂) into a complex mixture of hydrocarbons and oxygenates. Well-defined homogeneous catalysts for F-T may provide greater product selectivity for fuel-range liquid hydrocarbons compared to traditional heterogeneous catalysts. The first part of this work involved the preparation of late-transition metal complexes for use in syngas conversion. We investigated C–C bond forming reactions via carbene coupling using bis(carbene)platinum(II) compounds, which are models for putative metal–carbene intermediates in F-T chemistry. It was found that C–C bond formation could be induced by either (1) chemical reduction of or (2) exogenous phosphine coordination to the platinum(II) starting complexes. These two mild methods afforded different products, constitutional isomers, suggesting that at least two different mechanisms are possible for C–C bond formation from carbene intermediates. These results are encouraging for the development of a multicomponent homogeneous catalysis system for the generation of higher hydrocarbons.

A second avenue of research focused on the design and synthesis of post-metallocene catalysts for olefin polymerization. The polymerization chemistry of a new class of group 4 complexes supported by asymmetric anilide(pyridine)phenolate (NNO) pincer ligands was explored. Unlike typical early transition metal polymerization catalysts, NNO-ligated catalysts produce nearly regiorandom polypropylene, with as many as 30–40 mol % of insertions being 2,1-inserted (versus 1,2-inserted), compared to <1 mol % in most metallocene systems. A survey of model Ti polymerization catalysts suggests that catalyst modification pathways that could affect regioselectivity, such as C–H activation of the anilide ring, cleavage of the amine R-group, or monomer insertion into metal–ligand bonds are unlikely. A parallel investigation of a Ti–amido(pyridine)phenolate polymerization catalyst, which features a five- rather than a six-membered Ti–N chelate ring, but maintained a dianionic NNO motif, revealed that simply maintaining this motif was not enough to produce regioirregular polypropylene; in fact, these experiments seem to indicate that only an intact anilide(pyridine)phenolate ligated-complex will lead to regioirregular polypropylene. As yet, the underlying causes for the unique regioselectivity of anilide(pyridine)phenolate polymerization catalysts remains unknown. Further exploration of NNO-ligated polymerization catalysts could lead to the controlled synthesis of new types of polymer architectures.

Finally, we investigated the reactivity of a known Ti–phenoxy(imine) (Ti-FI) catalyst that has been shown to be very active for ethylene homotrimerization in

an effort to upgrade simple feedstocks to liquid hydrocarbon fuels through co-oligomerization of heavy and light olefins. We demonstrated that the Ti-FI catalyst can homo-oligomerize 1-hexene to C₁₂ and C₁₈ alkenes through olefin dimerization and trimerization, respectively. Future work will include kinetic studies to determine monomer selectivity by investigating the relative rates of insertion of light olefins (e.g., ethylene) vs. higher α -olefins, as well as a more detailed mechanistic study of olefin trimerization. Our ultimate goal is to exploit this catalyst in a multi-catalyst system for conversion of simple alkenes into hydrocarbon fuels.

Table of Contents

Acknowledgements	iv
Abstract	vii
Table of Contents	x
List of Schemes	xii
List of Figures	xiv
List of Tables	xvi
Chapter 1	
General Introduction	1
Chapter 2	
Investigations into Pd- and Pt-promoted C–C Bond Formation Using Fischer Carbene Complexes as Stoichiometric Reagents	8
Introduction	9
Results and Discussion	
<i>Attempted Mechanistic Investigations into the Palladium-catalyzed Dimerization Reaction</i>	11
<i>Investigations into C–C Bond Formation from Bis(carbene)platinum(II) Complexes: Implications for the Pd-catalyzed Carbene Dimerization Reaction</i>	24
Conclusions	35
Experimental Section	36
References	54
Chapter 3	
Synthesis and Polymerization Behavior of Asymmetric Group 4 Post-Metallocene Catalysts	56
Introduction	57
Results and Discussion	
<i>NNO Ligand and Complexes</i>	59
<i>^RNNO Ligands and Complexes</i>	76
<i>CNO Ligand and Complex</i>	84
<i>ArNO Ligand and Complexes</i>	87
<i>^{amido}NNO Ligand and Complexes</i>	90
<i>(NNO)TiCl₂: Further Polymerization Studies</i>	95

Chapter 3 (cont'd)

Conclusions and Future Work	101
Acknowledgements	104
Experimental Section	104
References	139

Chapter 4

Improved Synthesis of Fujita's Ti Phenoxy-Imine Catalyst and Initial Studies of 1-Hexene Trimerization	144
Introduction	145
Results and Discussion	
<i>Improved Synthesis of Fujita Catalyst</i>	148
<i>Trimerization of 1-Hexene</i>	150
<i>Investigation of MAO Equivalents</i>	152
Conclusions and Future Work	153
Experimental Section	153
References	157

Appendix A

Compound Numbers by Chapter: A Handy Guide	159
Chapter 2 Compounds	160
Chapter 3 Compounds	161
Chapter 4 Compounds	162

Appendix B

Comparison of ^{13}C NMR Data of Polypropylene from $(\text{NNO})\text{TiCl}_2$ (8) and Reported ^{13}C NMR Data for Regioirregular Propylene	164
---	-----

List of Schemes

Chapter 2:

- Scheme 2.1** Pd-catalyzed carbene dimerization reaction.
- Scheme 2.2** Proposed mechanism for Pd-catalyzed carbene dimerization reaction.
- Scheme 2.3** Synthetic route to Cr carbene complexes 1-3.
- Scheme 2.4** Conversion of Cr carbenes 1-3 to *E/Z*-olefins via Pd-catalyzed carbene dimerization.
- Scheme 2.5** Ratio of *E/Z*-olefinic experiments in crossover experiment between 1 and 2. Ratio of products is shown after approximately 6 h. The reaction took approximately 22 h to reach completion.
- Scheme 2.6** Pd black-promoted carbene dimerization from Cr carbene complex 2 to form 4.
- Scheme 2.7** Synthesis of Cp(CO)(NO)Cr{carbene} complexes 4 and 5.
- Scheme 2.8** Synthesis of (triphos)(PPh₃)Pd 7.
- Scheme 2.9** Pt-catalyzed carbene dimerization of Cr complex 2 to 4 and Pt black.
- Scheme 2.10** Proposed mechanism for carbene formation on Pt complexes from alkynes and alcohols.
- Scheme 2.11** Synthesis of bis(carbene)platinum complexes 9 and 10.
- Scheme 2.12** Synthesis of bis(carbene)platinum complex 11 from 9.
- Scheme 2.13** Reduction of carbene complexes 9 and 10 with cobaltocene to yield *E/Z*-olefinic products 12.
- Scheme 2.14** Reduction of carbene complex 11 with cobaltocene to yield *E/Z*-olefinic products 13.
- Scheme 2.15** Addition of PPh₃ to 9 to form 14 and 15.
- Scheme 2.16** Addition of PPh₃ to 10 in CD₂Cl₂ led to the formation of *cis*- and *trans*-Br(PPh₃)Pt(COMe){C(OMe)(Me)}, MeBr, and unidentified decomposition.
- Scheme 2.17** Addition of PPh₃ to 10 in THF to form 15 and 16.
- Scheme 2.18** Addition of PPh₃ to 11 to form *E/Z*-13, 14, and 17.
- Scheme 2.19** Addition of pyridine to 9 and 10 to yield acetyl methoxycarbene complexes 18 and 19.
- Scheme 2.20** Addition of pyridine to 11 to yield acetyl methoxycarbene complex 20.
- Scheme 2.21** Proposed mechanism for C–C bond formation from bis(carbene)platinum(II) complexes upon addition of PPh₃.
- Scheme 2.22** Proposed mechanism for phosphonium ylide migration to a carbene ligand on a Pt(II) complex.
- Scheme 2.23** Proposed mechanistic pathway for reaction of pyridine with 9–11.
- Scheme 2.24** Addition of chloride salts to 9 to form acyl Pt(II) complex 22.

Chapter 3:

Scheme 3.1 Propylene polymerization with post-metallocene complexes of triaryl dianionic ligands.

Scheme 3.2 Retrosynthetic scheme for anilide(pyridine)phenoxide ligands.

Scheme 3.3 Literature precedent for monoarylation of 2,6-dibromopyridine using a Suzuki coupling.

Scheme 3.4 Synthesis of boronic ester **1**.

Scheme 3.5 Suzuki coupling **1** and 2,6-dibromopyridine led to inconsistent product formation with complete conversion of **1** to the protodeboronated product without any formation of **2** occurring in many instances.

Scheme 3.6 Buchwald-Hartwig coupling to yield 2-bromo-N-(1-phenylethyl)aniline **4**.

Scheme 3.7 Synthesis of ligand **5** from coupling **4** and **2**.

Scheme 3.8 Synthesis of anilide(pyridine)phenoxide Zr, Hf, and Ti complexes.

Scheme 3.9 Synthesis of (NNO)TiBn₂ complex **9** from (NNO)TiCl₂ complex **8**.

Scheme 3.10 Polymerization of propylene with complex **6** or **8**.

Scheme 3.11 Propylene insertion modes: 1,2-insertion (top), 2,1-insertion (middle), 3,1-insertion (bottom).

Scheme 3.12 Synthesis of *N*-benzyl-2-bromoaniline.

Scheme 3.13 Synthesis of ligand **10** from *N*-benzyl-2-bromoaniline.

Scheme 3.14 Synthesis of *N*-adamant-1-yl-2-bromoaniline via a Buchwald-Hartwig reaction.

Scheme 3.15 Synthesis of ligand **11** from *N*-adamant-1-yl-bromoaniline.

Scheme 3.16. Synthesis of 2-bromo-*N*-methoxyethylaniline via a Goldberg-modified Ullman reaction.

Scheme 3.17 Synthesis of ligand **13** from **12**.

Scheme 3.18 Synthesis of metal complexes **14-17**.

Scheme 3.19 Potential pathways for NNO catalyst modification upon activation with MAO.

Scheme 3.20 Synthesis of ligand **18** from synthon **2**.

Scheme 3.21 Synthesis of Ti complex **19**.

Scheme 3.22 Synthesis of ligand **20** via Kumada and Suzuki coupling reactions.

Scheme 3.23 Synthesis of amido(pyridine)phenoxide ligand **21**.

Scheme 3.24 Synthesis of amido(pyridine)phenoxide complexes **23-24**.

Chapter 4:

Scheme 4.1 Proposed mechanism for formation of Ti(II) from starting Ti(IV) complex upon activation with MAO. (Adapted from ref. 7).

Scheme 4.2 Proposed mechanism for selective trimerization of ethylene to 1-hexene by (FI)Ti complexes. (Adapted from ref. 7).

Scheme 4.3 Improved synthesis of phenoxy-imine ligand **3**.

Scheme 4.4 Synthesis of (FI)Ti complex **4**.

Scheme 4.5 Possible C₁₈ products from trimerization of 1-hexene.

List of Figures

Chapter 2:

Figure 2.1 Synthesized Cr Fischer carbene complexes with para-substituted aryl groups.

Figure 2.2 Average ν_{CO} against σ_{p} .

Figure 2.3 Probability ellipsoid diagram (50%) of the X-ray structure of **7**.

Figure 2.4 Probability ellipsoid diagram (50%) of the X-ray structure of **8**.

Figure 2.5 ^1H NMR and 1D NOESY spectra for **18** (a), **19** (b), and **20** (c).

Chapter 3:

Figure 3.1 Comparison of potential geometries of metal complexes with triaryl dianionic ligands and metallocene catalysts and polymer tacticity.

Figure 3.2 ^1H NMR spectra of **6** at 25 °C (top) and -30 °C (bottom) in toluene- d_8 .

Figure 3.3 Close-up of Zr-benzyl proton resonances of **6** in ^1H NMR spectra from -80 °C to 90 °C in toluene- d_8 (temperature increases up y-axis).

Figure 3.4 Probability ellipsoid diagram (50%) of the X-ray structure **8**. Selected bond lengths (Å) and angles (°): Ti(1)–O(1) = 1.8040(17), Ti(1)–N(1) = 1.879(2), Ti(1)–N(2) = 2.153(2), Ti(1)–Cl(2) = 2.3161(8), Ti(1)–Cl(3) = 2.3285(8), Ti(1)–C(1) = 2.609(2); O(1)–Ti(1)–N(1) = 110.87(8), O(1)–Ti(1)–Cl(2) = 118.49(6), N(1)–Ti(1)–Cl(2) = 127.68(7), C(1)–N(1)–Ti(1) = 104.05(15).

Figure 3.5 ^{13}C NMR spectra of PP from **6** (top) and **8** (bottom) at 120 °C in TCE- d_2 . Regions indicating 2,1-insertions are highlighted.

Figure 3.6 ^1H NMR and 2D ^1H - ^{13}C HSQC NMR spectra for PP from **6** (a) and **8** (b).

Figure 3.7 Room temperature ^1H NMR spectrum of Zr complex **14** in toluene- d_8 .

Figure 3.8 Probability ellipsoid diagram (50%) of the X-ray structure **14**. Selected bond lengths (Å) and angles (°): Zr(1)–O(1) = 1.9917(7), Zr(1)–N(1) = 2.2911(2), Zr(1)–N(2) = 2.1482(8), Zr(1)–C(21) = 2.8470(9), Zr(1)–C(40) = 2.2913(10), Zr(1)–C(39) = 2.5765(9), Zr(1)–C(32) = 2.2851(9); O(1)–Zr(1)–N(2) = 157.17(3), N(1)–Zr(1)–C(40) = 96.19(3), C(40)–Zr(1)–C(32) = 126.48(3), C(32)–Zr(1)–N(1) = 120.71(3), Zr(1)–C(40)–C(39) = 83.53(5), C(21)–N(2)–Zr(1) = 104.95(6).

Figure 3.9 Different binding modes of NNO ligands in trigonal bipyramidal metal complexes depending on the identity of the X-type ligands.

Figure 3.10 Probability ellipsoid diagram (50%) of the X-ray structure **16**. Selected bond lengths (Å) and angles (°): Ti(1)–O(1) = 1.8170(10), Ti(1)–N(1) = 2.1879(13), Ti(1)–N(2) = 1.8570(12), Ti(1)–Cl(2) = 2.3531(6), Ti(1)–Cl(1) = 2.2966(6), Ti(1)–C(1) = 2.5354(15); O(1)–Ti(1)–N(2) = 112.36(5), O(1)–Ti(1)–Cl(1) = 119.28(4), N(2)–Ti(1)–Cl(1) = 125.62(4), Cl(2)–Ti(1)–N(1) = 177.32(3), C(1)–N(2)–Ti(1) = 100.15(8).

Figure 3.11 ^{13}C NMR spectra of PP from complex **8** (top), **15** (middle), and **16** (bottom) at 120 °C in TCE- d_2 .

Chapter 3 (cont'd):

Figure 3.12 Probability ellipsoid diagram (50%) of the X-ray structure **17**. Selected bond lengths (Å) and angles (°): Ti(1)–O(1) = 1.8649(4), Ti(1)–N(1) = 2.2132(4), Ti(1)–C(5) = 2.1352(5), Ti(1)–C(22) = 2.1037(6), Ti(1)–C(6) = 2.6385(6), Ti(1)–C(25) = 2.1135(6); O(1)–Ti(1)–C(5) = 153.81(2), C(25)–Ti(1)–C(22) = 97.60(3), C(22)–Ti(1)–N(1) = 126.85(2), C(25)–Ti(1)–N(1) = 134.79(2), Ti(1)–C(22)–C(6) = 93.46(4).

Figure 3.13 ^{13}C NMR spectrum of stereoirregular regioirregular PP from complex **19** at 120 °C in TCE- d_2 .

Figure 3.14 ^{13}C NMR spectrum of stereoirregular regioirregular poly-1-hexene from complex **8**.

Figure 3.15 ^1H NMR spectrum of crude reaction between TiBn_4 and **20** in C_6D_6 after 10 min (top) and after sitting in a J. Young NMR tube at rt overnight (bottom). Toluene formed in the reaction is indicated by an asterisk.

Figure 3.17 Sticky non-solid PP produced at KFUPM (rt, 8–9 atm propylene) with precatalyst **8** (left) and nonsticky solid PP produced at Caltech (0 °C, 5 atm propylene) also with precatalyst **8** (right).

Figure 3.18 ^{13}C NMR spectra of PP from complex **8**/MAO/TIBA run at rt at KFUPM (top), PP from **8**/MMAO run at 0 °C at Caltech (middle), and PP from **8**/dry MAO run at 0 °C at Caltech (bottom). Spectra were taken at 120 °C in TCE- d_2 .

Figure 3.19 ^{13}C NMR spectrum of PP from **8**/PMAO-IP at 115 °C in TCE- d_2 . Resonances for iPP are indicated with asterisks.

Figure 3.20 ^{13}C NMR spectrum of PP from **8**/MAO at 115 °C in TCE- d_2 . Resonances for iPP are indicated with asterisks.

Figure 3.21 ^{13}C NMR spectra of PP from complex **8**/PMAO-IP (top), **8**/MAO (middle), and **8**/dry MAO/0 °C (bottom) at 115 or 120 °C in TCE- d_2 .

Chapter 4:

Figure 4.1 PNP/ $\text{CrCl}_3(\text{THF})_3$ system for selective ethylene trimerization. See ref. 5.

Figure 4.2 Trimerization of ethylene with a (FI)Ti complex at different ethylene pressures. See ref. 7.

Figure 4.3 GC trace of 1-hexene oligomerization products from **4**/MMAO with close-up of C_{18} product peaks (biphenyl is an internal standard).

List of Tables

Chapter 2:

Table 2.1 Average ν_{CO} for $(\text{CO})_5\text{Cr}\{\text{C}(\text{OMe})(p\text{-X-C}_6\text{H}_4)\}$.

Table 2.2 Crystal data and structure refinement for **7** and **8**.

Chapter 3:

Table 3.1 Conditions screened for Suzuki coupling to achieve monoarylation of 2,6-dibromopyridine.

Table 3.2 Propylene polymerization data for complexes **6**, **8**, **14-16**.

Table 3.3 Propylene polymerization data for **8**/PMAO-IP and **8**/MAO.

Table 3.4 Crystal data and structure refinement for **8**, **14**, and **16**.

Table 3.5 Crystal data and structure refinement for **7** and **24**(THF).

Chapter 4:

Table 4.1 Data for trimerization of 1-hexene with different equivalents of MMAO.

Chapter 1
General Introduction

Chapter 1

The topics covered in this dissertation focus centrally on upgrading simple carbon feedstocks into value-added products via Fischer–Tropsch type chemistry, or olefin polymerization and oligomerization. The research presented here is fundamental in nature, but intended to work toward the goal of discovering or improving homogeneous catalysts for the processes investigated, which are of central importance for our energy supply and economy: Fischer–Tropsch is an attractive alternative route to fuel,¹ while polyolefins are the highest volume commercial class of synthetic polymers with annual worldwide capacity greater than 70 billion kg.²

The first chapter focuses on investigating and developing facile methods for C–C bond formation for synthesis gas (syngas; CO + H₂) conversion. Syngas is readily available from coal, natural gas, oil shale, and biomass and represents a potential alternative feedstock for fuel and chemicals if methods for its selective transformation into higher carbon products can be discovered; syngas is currently utilized on an industrial scale in the heterogeneously-catalyzed Fischer–Tropsch process, but this process is non-selective and generates a Schultz–Flory distribution of hydrocarbons, which can be difficult and costly to separate. We are interested in developing homogeneous catalysts for syngas conversion, which may offer better opportunities for product selectivity. A fundamental step of any syngas conversion cycle is C–C bond formation; thus, we have sought to study

this process by investigating likely intermediates of Fischer–Tropsch. Chapter 2 describes our work with bis(carbene)platinum(II) complexes that may be models for carbene intermediates in Fischer–Tropsch. We report two methods to induce C–C bond formation from these complexes under very mild conditions, as well as mechanistic studies on a Pd-catalyzed carbene dimerization reaction. Ultimately, this work is promising for a multicomponent catalytic system for syngas conversion, in which a late metal catalyst such as Pd or Pt mediates C–C bond formation.

The second part of this dissertation explores polymerization and oligomerization with group 4 post-metallocene complexes. Polymerization and oligomerization both involve conversion of simple and often inexpensive feedstocks (e.g., ethylene or propylene) into more valuable products (e.g., polyethylene, polypropylene, or 1-hexene). The development of post-metallocene olefin polymerization catalysts has led to significant advances in one of the most successful and well-studied organometallic-mediated reactions;³ olefin polymerization has been extensively investigated in both industrial and academic labs since the discovery of Ziegler-Natta catalysts in the 1950s.⁴ Linear α -olefins, which are an important comonomer for many commercial polymers, including linear low density polyethylene (LLDPE), are generated industrially primarily via non-selective oligomerization of ethylene; however, non-metallocene catalysts can mediate selective olefin oligomerization and research in this area remains an important ongoing goal of both academic and industrial labs.⁵

Chapter 3 describes our continued efforts to develop post-metallocene olefin polymerization catalysts based on a triaryl dianionic (XLX) ligand framework developed in our group for supporting early metals.⁶ The ligand design takes advantage of the thermal stability of aryl–aryl bonds as well as versatile access to a wide variety of ligand scaffolds using cross-coupling chemistry. Additionally, the ligand scaffold can support various metal geometries, including C_2 and C_{2v} , which suggests the possibility of stereoselective polymerization; however, we have primarily seen stereoirregular polypropylene (PP).⁶ Our contribution to this project was to develop and study an asymmetric variant of our triaryl dianionic ligand. A modular anilide(pyridine)phenoxide (NNO) ligand was designed and synthesized that supports group 4 metals, and upon activation with methylaluminoxane (MAO), yields PP with good activity. Interestingly, these asymmetric catalysts produce a new type of stereoirregular and regioirregular PP, and we have synthesized several catalyst variants through ligand modification in an attempt to understand the origin of the unique regioselectivity of these catalysts.

The final chapter in this dissertation (Chapter 4) covers the beginning of our efforts to study selective olefin oligomerization with a Ti phenoxy-imine catalyst reported by Fujita and co-workers, which trimerizes ethylene to 1-hexene with excellent selectivity and activity.⁷ Here we report an improved synthesis of the ligand and test reactions to explore the ability of this catalyst to trimerize higher α -olefins. Importantly, initial studies indicate that the Ti catalyst will

oligomerize 1-hexene to yield C₁₈ products demonstrating the ability of this catalyst to operate with higher α -olefins.

The studies described in this dissertation together represent small steps toward increasing our knowledge of fundamental processes, namely, C–C bond formation and olefin polymerization and oligomerization. Continued research efforts in these areas by both academic and industrial labs will undoubtedly lead to improved homogeneous catalysts for a broad range of applications through rational design.

References

1. West, N. M.; Miller, A. J.; Labinger, J. A.; Bercaw, J. E. *Coord. Chem. Rev.* **2011**, 255, 881-898.
2. (a) Arriola, D. J.; Carnahan, E. M.; Hustad, P. D.; Kuhlman, R. L.; Wenzel, T. T. *Science* **2006**, 312, 714-719. (b) Hustad, P. D. *Science* **2009**, 325, 704-707.
3. Natta, G.; Pino, P.; Corradini, P.; Danusso, F.; Mantica, E.; Mazzanti, G.; Moraglio, G. *J. Am. Chem. Soc.* **1955**, 77, 1708-1710.
4. Agapie, T. *Coord. Chem. Rev.* **2011**, 255, 861-880.
5. (a) Agapie, T.; Henling, L. M.; DiPasquale, A. G.; Rheingold, A. L.; Bercaw, J. E. *Organometallics* **2008**, 27, 6245-6256. (b) Golisz, S. R.; Bercaw, J. E. *Macromolecules* **2009**, 42, 8751-8762. (c) Tonks, I. A.; Tofan, D.; Weintrob, E. C.; Agapie, T.; Bercaw, J. E. *Organometallics* **2012**, 31, 1965-1974.
6. Suzuki, Y.; Kinoshita, S.; Shibahara, A.; Ishii, S.; Kawamura, K.; Inoue, Y.; Fujita, T. *Organometallics* **2010**, 29, 2394-2396.

Chapter 2

Investigations into Pd- and Pt-promoted C–C Bond Formation Using Fischer Carbene Complexes as Stoichiometric Reagents

Adapted in part from:

Klet, R. C.; Labinger, J. A.; Bercaw, J. E. *Organometallics* **2012**, *31*, 6652–6657.

<http://dx.doi.org/10.1021/om300733h>

Copyright 2012 American Chemical Society

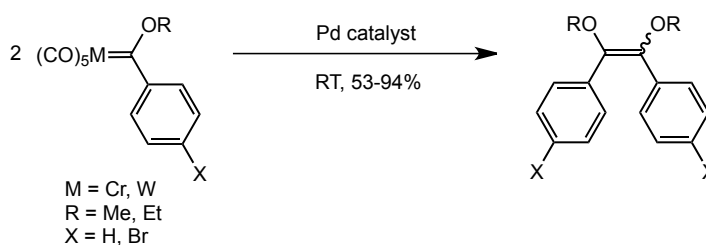
Chapter 2

Introduction

Effective utilization of alternative fuel sources promises to become increasingly important, as demand continues to rise while petroleum reserves diminish.¹ Synthesis gas (syngas; CO + H₂, readily available from coal, natural gas, oil shale, or biomass) and methane are attractive possibilities for alternative feedstocks, but currently selective transformations are known only for the C₁ product methanol. The heterogeneously catalyzed Fischer-Tropsch process converts syngas into a complex mixture of higher molecular weight hydrocarbons and oxygenates, which can be difficult and costly to separate. The discovery of homogeneous catalysts for this process may offer opportunities for better selectivity. For both approaches, C–C bond formation can be expected to be a critical step for the production of C₂₊ products. Hence, research aimed at selective and facile methods for this transformation is of considerable interest.

One attractive strategy for forming C–C bonds is carbene coupling, a process that has been observed in a number of cases, including the original Fischer carbene complexes, which exhibit thermal dimerization of carbene ligands.² Carbenes are plausible intermediates in syngas or methane conversion schemes.³ For example, we have previously shown that carbene complexes (or closely related species) of Mn and Re can be readily generated from CO and H₂ and under some conditions exhibit C–C bond formation, although a carbene

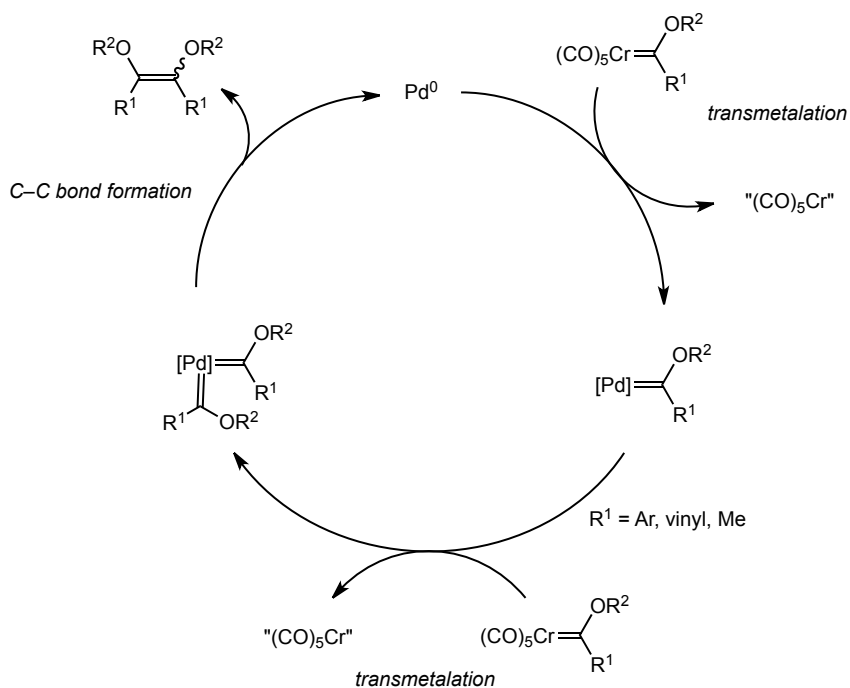
coupling mechanism was not unequivocally demonstrated.⁴ Sierra et al. have reported that a variety of Pd catalysts (including Pd(OAc)₂/Et₃N, Pd(PPh₃)₄, Pd₂dba₃·CHCl₃ (dba = dibenzylideneacetone), PdCl₂(MeCN)₂/Et₃N, PdCl₂(PPh₃)₂/Et₃N, and Pd/carbon) promote room-temperature carbene coupling in group 6 metal carbonyl (M = Cr, W) complexes, affording olefinic products in good to excellent yields (Scheme 2.1);⁵ Ni and Cu catalysts have also shown analogous activity.⁶ These findings, coupled with our work, suggest that a multicomponent catalytic system, wherein CO is reduced at a group 6 or 7 metal carbonyl complex and then transferred to a late-transition metal complex for C–C coupling, could be a viable approach. Further exploration of the catalyzed coupling reaction thus appears warranted.



Scheme 2.1 Pd-catalyzed carbene dimerization reaction.

The mechanism of Pd-catalyzed carbene coupling has not been fully elucidated. Sierra proposed sequential transmetalation from two equivalents of the group 6 carbene to the Pd(0) catalyst, giving a bis(carbene)palladium(0) intermediate, which undergoes C–C bond formation to eliminate the observed olefinic product and regenerate the Pd(0) catalyst (Scheme 2.2).^{5,7} However, no Pd–carbene intermediates were observable. Here we report attempted mechanistic investigations into the Pd(0)-catalyzed carbene dimerization

reaction; Pt(0) complexes that catalyze the same carbene coupling reaction, albeit more slowly than Pd; and, finally, stoichiometric C–C bond forming reactions from stable bis(alkoxycarbene)platinum(II) complexes, which may be relevant to the mechanism of catalytic carbene coupling.



Scheme 2.2 Proposed mechanism for Pd-catalyzed carbene dimerization reaction.

Results and Discussion

Section 2.1: Attempted Mechanistic Investigations into the Palladium-catalyzed Dimerization Reaction

Modification of the Fischer Carbene Ligand on Chromium

Transmetalation of the carbene ligand from the group 6 complex to Pd is proposed to involve nucleophilic attack by the Pd catalyst on the carbene ligand;⁶ accordingly, we hypothesized that dimerization may be inhibited for more electron-rich carbene ligands. As a first step to investigate the mechanism of the Pd-catalyzed carbene dimerization, we probed the electronic requirements of the Fischer carbene ligand originating on the group 6 metal complex. A series of Cr *para*-substituted aryl carbene complexes $(\text{CO})_5\text{Cr}\{\text{C}(\text{OMe})(p\text{-X-C}_6\text{H}_4)\}$ with both electron-withdrawing and electron-donating groups were synthesized according to literature procedures (Figure 2.1).⁸

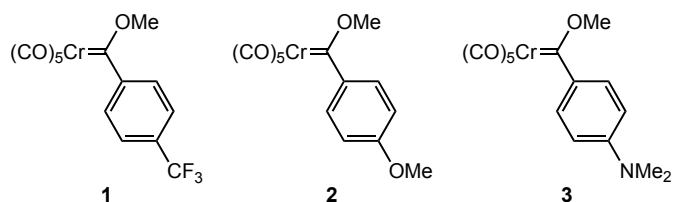
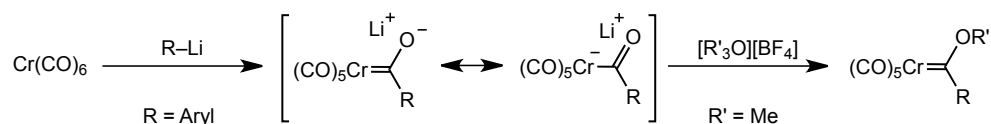


Figure 2.1 Synthesized Cr Fischer carbene complexes with *para*-substituted aryl groups.

Treatment of chromium(0) hexacarbonyl with the desired substituted aryl lithium reagent, followed by addition of Meerwein's salt yielded complexes **1-3** (Scheme 2.3).



Scheme 2.3 Synthetic route to Cr carbene complexes **1-3**.

Table 2.1 Average ν_{CO} for $(\text{CO})_5\text{Cr}\{\text{C}(\text{OMe})(p\text{-X-C}_6\text{H}_4)\}$.

X	Average ν_{CO} (cm^{-1})
CF_3	1995
Br	1992
H	1991
OMe	1984
NMe_2	1977

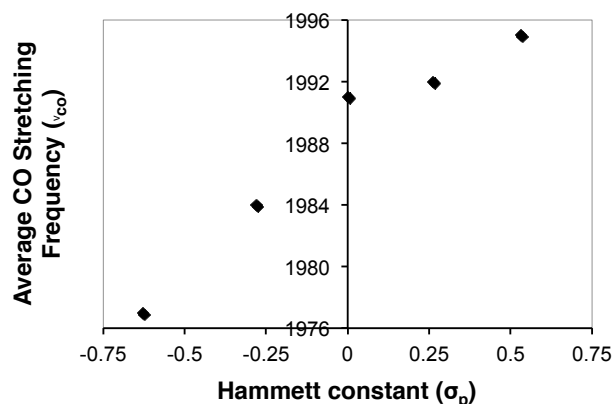
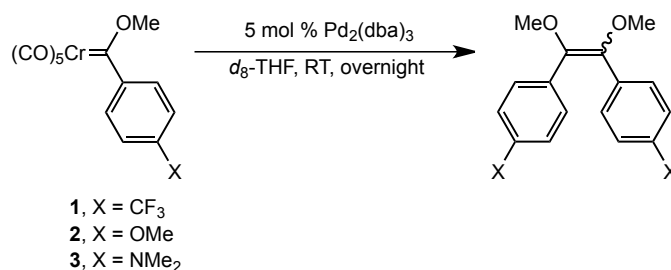


Figure 2.2 Average ν_{CO} against σ_p .

To evaluate the electronic character of the carbene complexes **1–3**, we used carbonyl stretching frequencies (ν_{CO}) reported by Fischer et al. (Table 2.1).⁸ As shown in Figure 2.2, the average ν_{CO} is directly related to the Hammett constant (σ_{Para}) or the electron-withdrawing power of the *para*-substituent.⁹

Pd-catalyzed carbene ligand dimerization was investigated by ^1H NMR spectroscopy for carbene complexes **1–3**. Reaction of **1–3** with 5 mol % $\text{Pd}_2(\text{dba})_3$ in d_8 -THF at room temperature yielded the expected *E/Z* olefinic products within 24 hours in all cases (Scheme 2.4).



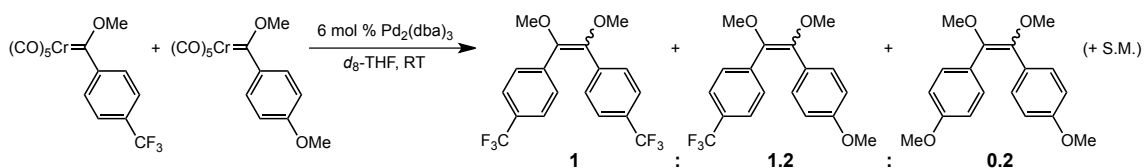
Scheme 2.4 Conversion of Cr carbenes **1–3** to *E/Z*-olefins via Pd-catalyzed carbene dimerization.

A kinetic study was envisioned to quantitatively evaluate the relative rates of dimerization for the different carbene complexes **1–3**. We expected that Cr

complexes **2** and **3** with electron-donating groups in the *para*-position of the carbene aryl group would dimerize more slowly than complex **1** with an electron-withdrawing group due to the less electrophilic nature of the carbene ligand. Unfortunately, the dimerization reactions for the complexes we investigated were not clean enough to allow for accurate kinetic measurements. For example, monitoring the Pd-catalyzed dimerization reaction of **2** by ^1H NMR spectroscopy revealed the yield of *E/Z*-olefinic products was 65-75% (by comparison to hexamethylbenzene as an internal standard); however, no other products were observed to form in the reaction, and we are unable to account for the loss of mass in the reaction. For comparison, Sierra has reported isolated yields of 80% for the dimerization reaction of $(\text{CO})_5\text{Cr}\{\text{C}(\text{OMe})(\text{C}_6\text{H}_5)\}$ with 5 mol % $\text{Pd}_2\text{dba}_3\cdot\text{CHCl}_3$ in THF, but does not describe the formation of any side products.⁵ Further complicating the reaction, precipitation of Pd black was observed in all reactions and a heterogeneously catalyzed pathway for carbene ligand dimerization cannot be excluded (*vide infra*).

Since kinetic studies were precluded for the dimerization reaction, a crossover experiment was envisioned to probe the relative rates of reaction for different carbene complexes. In a crossover experiment, the complex with the more electron-poor carbene ligand should be consumed more rapidly than the complex with the more electron-rich carbene. Additionally, a crossover experiment would elucidate whether mixed carbene dimers form (mixed carbene dimers are not ruled out by the proposed mechanism in Scheme 2.2). A

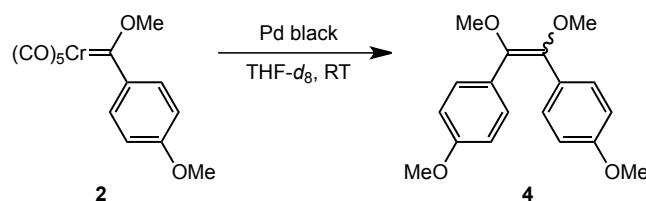
crossover experiment between the electron-poor *p*-CF₃-C₆H₄ carbene complex **1** and relatively electron-rich *p*-MeO-C₆H₄ complex **2** using 6 mol % Pd₂(dba)₃ in *d*₈-THF indeed indicated that the rate of disappearance of **1** is faster than the rate of disappearance of **2** as expected. Unsurprisingly, the experiment also revealed the formation of the mixed olefin product resulting from one carbene ligand with a CF₃ group and one with a MeO group (Scheme 2.5). Although this experiment does not provide quantitative data, it suggests that nucleophilic Pd attack is a reasonable mechanism for transmetalation since complex **1** with the more electrophilic carbene ligand was consumed more quickly than complex **2** with a less electrophilic carbene ligand.



Scheme 2.5 Ratio of *E/Z*-olefinic experiments in crossover experiment between **1** and **2**. Ratio of products is shown after approximately 6 h. The reaction took approximately 22 h to reach completion.

Since Pd black was observed to form in all dimerization reactions, the possibility of a heterogeneously catalyzed pathway was investigated. Distinguishing between an initial homogeneous reaction and a completely heterogeneous reaction, catalyzed by bulk or finely divided metal produced by decomposition of the originally homogeneous organometallic species, however, is challenging. A control reaction was performed with carbene complex **2** and commercially available Pd black (surface area 40-60 m²/g) as a catalyst. The expected dimerized olefin product (*E/Z*)-1,2-dimethoxy-1,2-bis(4-methoxyphenyl)-

ethane (**4**) was observed to form, but the reaction proceeded at a much slower rate than the reaction employing the same catalyst loading of Pd₂dba₃ (Scheme 2.6). As the surface area of any colloidal Pd produced by decomposition of Pd₂dba₃ may be different than that of commercial Pd black, the slower reaction rate does not rule out a heterogeneously catalyzed pathway. This data at least suggests that a heterogeneously catalyzed pathway is possible for carbene dimerization, but we do not have any evidence to exclude a complementary or entirely homogeneous pathway at this time.



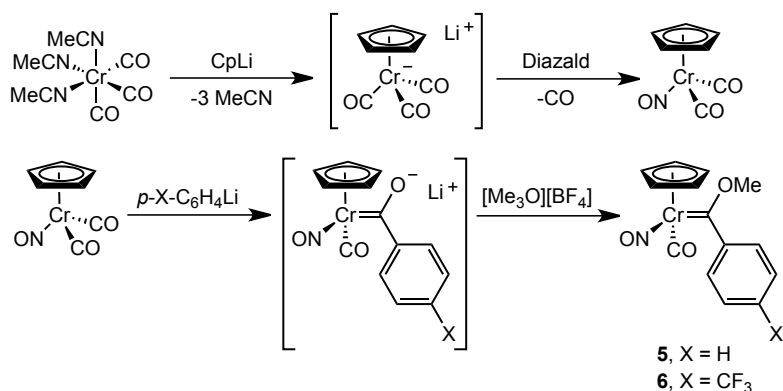
Scheme 2.6 Pd black-promoted carbene dimerization from Cr carbene complex **2** to form **4**.

Taken together, our results provide evidence that nucleophilic Pd attack on the group 6 carbene ligand is a reasonable mechanistic hypothesis for transmetalation of the carbene ligand to Pd. Additionally, this data suggests that both homogeneous and heterogeneous pathways involving Pd may operate to effect dimerization.

Modifications of the non-Carbene Ligands on Chromium

A useful late metal catalyst for inducing C–C bond formation in a syngas conversion cycle should be able to couple formyl or hydroxy carbene ligands, which are probable intermediates in Fischer-Tropsch processes. We were

therefore interested in investigating the scope of the Pd-catalyzed dimerization reaction; and in particular, testing carbene dimerization from group 6 complexes with ligands other than CO, since different ligand sets may be required to stabilize formyl or hydroxy carbene ligands. We thought that Cr carbene complexes with cyclopentadienyl (Cp) ligands would be useful substrates to investigate the scope of the Pd-catalyzed dimerization reaction because these complexes allow access to substituted aryl methoxy carbene ligands, which would facilitate comparison to group 6 pentacarbonyl carbene complexes, and group 6 Cp formyl complexes are known.¹⁰ We targeted Cp(CO)(NO)Cr{carbene} complexes with NO ligands in order to modulate the added electron-richness from the Cp ligand (compared to pentacarbonyl complexes), in light of our results that more electron-poor carbene complexes react more quickly than electron-rich carbene complexes. The complex Cp(CO)(NO)Cr{C(OMe)(C₆H₅)} **5** was synthesized following a literature procedure.¹¹ Treatment of tris(acetonitrile)tricarbonylchromium(0) with CpLi followed by addition of *N*-methyl-*N*-nitroso-*p*-toluene sulfonamide (Diazald) following the procedure of Stryker et al., led to the intermediate complex CpCr(NO)(CO)₂.¹² Treatment of CpCr(NO)(CO)₂ with PhLi followed by addition of Meerwein's salt yielded complex **5**. The related previously unknown complex Cp(CO)(NO)Cr{C(OMe)(*p*-CF₃-C₆H₄)} **6** was also synthesized using a similar procedure (Scheme 2.7).



Scheme 2.7 Synthesis of Cp(CO)(NO)Cr(carbene) complexes **5** and **6**.

The carbonyl stretching frequency data for complexes **5** and **6** suggest that the amount of backbonding to the carbonyl ligand from Cr is similar to the (average) amount of backbonding in the pentacarbonyl Cr carbene complexes (**5**¹¹ $\nu_{\text{CO}} = 1978 \text{ cm}^{-1}$, **6** $\nu_{\text{CO}} = 1983 \text{ cm}^{-1}$; see Table 2.1 for pentacarbonyl values); however, whether the electrophilicity of the carbene ligand tracks with ν_{CO} for these Cr carbene complexes with different ancillary ligands is not known.

Treatment of carbene complexes **5** and **6** with 5 mol % Pd₂dba₃ in *d*₈-THF did not lead to any product formation, even upon increasing the temperature of the reaction (ca. 100-150 °C). Although carbonyl stretching frequency data for **5** and **6** suggests that these complexes may be electronically similar to the pentacarbonyl carbene complexes, these results indicate that ν_{CO} may be too simple of a predictor for reactivity. Sierra has reported that the aminocarbene complexes (CO)₅Cr{C(NMe₂)(C₆H₅)} and (CO)₅Cr{C(NMe₂)(*p*-Br-C₆H₄)}, which are electronically similar to the carbene complexes **1–3** and **5–6** based on ν_{CO} data ($\nu_{\text{CO}} = 1977$ and 1973 cm^{-1} , respectively), also do not dimerize.⁵ The lack of

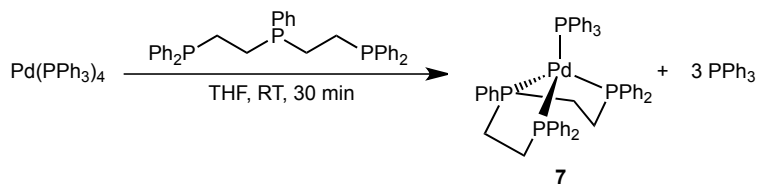
reactivity of **5** and **6** toward Pd-catalyzed carbene dimerization may also point to a steric requirement: complexes **5** and **6** are more sterically hindered than the pentacarbonyl Cr carbene complexes **1–3**, suggesting that perhaps both an electrophilic carbene ligand and a sterically accessible metal center are prerequisites for facile carbene dimerization reactions.

Synthesis of New Palladium Catalysts

Since kinetic studies on the Pd-catalyzed carbene dimerization reaction were precluded by the instability of the Pd(0) catalyst (as well as the unaccounted loss of mass), we sought to synthesize a more stable Pd catalyst. It was anticipated that the tridentate polyphosphine ligand bis(2-diphenylphosphinoethyl)phenylphosphine (triphos) would stabilize a Pd complex through the chelate effect, and would allow for both tetrahedral and square planar geometries, thereby supporting both Pd(0) and Pd(II) complexes (although the proposed catalytic cycle for carbene dimerization does not involve an oxidation state change from Pd(0)). We also hypothesized that the triphos ligand may allow for isolation of a palladium(0) intermediate because the bulky chelating triphos ligand could potentially inhibit transmetalation of a second carbene ligand to Pd, thereby preventing carbene dimerization and possibly allowing for isolation of Pd–carbene intermediates (see Scheme 2.2). Although the syntheses of several palladium(II) carbene complexes have been reported, generally via transfer of a carbene ligand from a group 6 carbene complex to a Pd(II) species,¹³ analogous

palladium(0) carbene complexes (synthesized through either carbene transfer or other methods) are not known, which may reflect the highly reactive nature of Pd(0) carbene complexes. Isolating a Pd(0) carbene intermediate would therefore not only be an interesting synthetic target, but may also provide further evidence for the proposed mechanism of carbene dimerization shown in Scheme 2.2.

The complex (triphos)(PPh₃)Pd(0) **7** was synthesized by reacting triphos with Pd(PPh₃)₄ in a THF solution (Scheme 2.8). A crystal suitable for X-Ray diffraction was grown by slow vapor diffusion of petroleum ether into a concentrated THF solution of **7** (Figure 2.3). As expected, the coordination around the Pd(0) center is distorted tetrahedral due to the chelating ligand. The bond angles and bond distances observed for **7** are similar to those observed for other P₄Pd(0) complexes with chelating phosphine ligands.¹⁴



Scheme 2.8 Synthesis of (triphos)(PPh₃)Pd **7**.

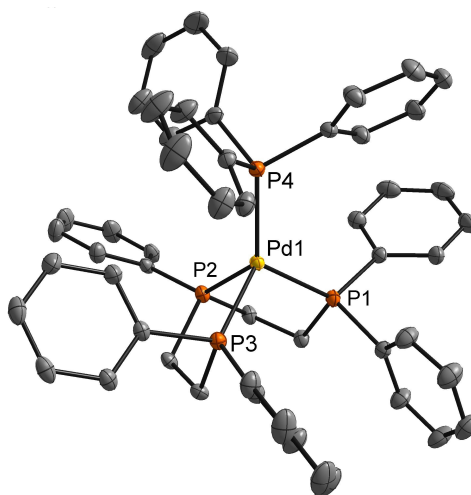


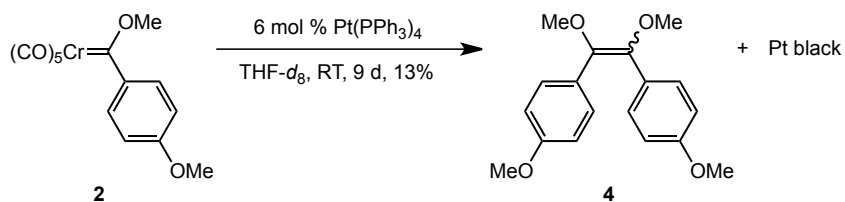
Figure 2.3 Probability ellipsoid diagram (50%) of the X-ray structure of **7**. Selected bond lengths (Å) and angles (°): Pd(1)–P(1) = 2.3219(3), Pd(1)–P(2) = 2.3231(3), Pd(1)–P(3) = 2.3382(3), Pd(1)–P(4) = 2.3121(3); P(4)–Pd(1)–P(1) = 122.862(10), P(4)–Pd(1)–P(2) = 127.370(10), P(1)–Pd(1)–P(2) = 87.350(10), P(4)–Pd(1)–P(3) = 116.876(10), P(1)–Pd(1)–P(3) = 106.987(10), P(2)–Pd(1)–P(3) = 87.550(9).

Reaction of carbene complex **2** with 5 mol % **7** in THF-*d*₈ led to the formation of the expected *E/Z*-olefinic products **4**, without any observable intermediates. Unfortunately, the chelating phosphine ligand did not appear to increase the stability of the Pd(0) catalysts as decomposition of the catalyst to Pd black was still observed over the course of the reaction, suggesting that the triphos ligand (or at least phosphine arms of the ligand) may be labile under the reaction conditions.

Carbene Dimerization Reactions with Platinum(0) Catalysts

Platinum complexes often promote similar reactivities as their palladium congeners, while being more robust with respect to decomposition; switching from Pd(0) to Pt(0) might afford more stable intermediates and thus facilitate

mechanistic study. We were therefore interested in investigating the potential for platinum-catalyzed carbene dimerization. Addition of 6 mol % $\text{Pt}(\text{PPh}_3)_4$ to a solution of **2** in $\text{THF-}d_8$ resulted in very slow conversion to the expected dimerization products **4** as an *E/Z*-isomeric mixture (Scheme 2.9). The reaction was only 13% complete after 9 days at room temperature, with catalyst decomposition evidenced by the formation of a Pt mirror on the NMR tube. Heating the reaction mixture to 50 °C resulted in significant decomposition without further product formation. As with dimerization reactions catalyzed by $\text{Pd}(0)$, no observable intermediates were generated.



Scheme 2.9 Pt-catalyzed carbene dimerization of Cr complex **2** to **4** and Pt black.

We again employed the chelating phosphine ligand triphos in an attempt to synthesize a more robust $\text{Pt}(0)$ catalyst. $(\text{Triphos})(\text{PPh}_3)\text{Pt}(0)$ **8** was synthesized by reacting triphos and $\text{Pt}(\text{PPh}_3)_4$ in a THF solution. A crystal suitable for X-Ray diffraction was grown by slow vapor diffusion of petroleum ether and diethyl ether into a concentrated THF solution of **8** (Figure 2.4). The crystal structure of **8** reveals nearly the identical geometry (distorted tetrahedral) and bond angles as the Pd analog **7**. Select bond length and bond angle data are shown in Figure 2.4.

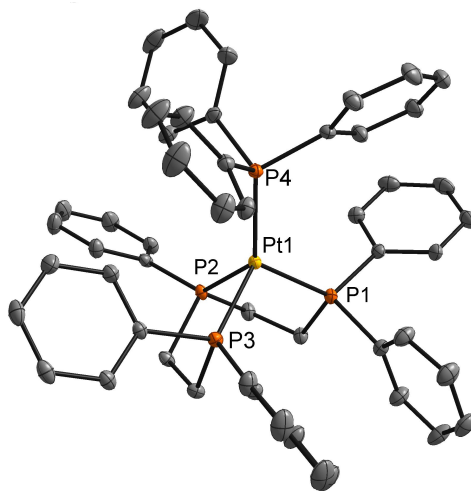


Figure 2.4 Probability ellipsoid diagram (50%) of the X-ray structure of **8**. Selected bond lengths (Å) and angles (°): Pt(1)–P(1) = 2.2878(3), Pt(1)–P(2) = 2.2910(2), Pt(1)–P(3) = 2.2994(3), Pt(1)–P(4) = 2.2739(3); P(4)–Pt(1)–P(1) = 121.954(10), P(4)–Pt(1)–P(2) = 128.339(10), P(1)–Pt(1)–P(2) = 87.539(9), P(4)–Pt(1)–P(3) = 116.282(9), P(1)–Pt(1)–P(3) = 107.833(10), P(2)–Pt(1)–P(3) = 87.598(9).

Addition of 5 mol % **8** to a solution of **2** in THF- d_8 resulted in very slow conversion to the expected carbene dimerization products **4**. Complex **8** appears to be slightly more stable than Pt(PPh₃)₄, as evidenced by slower formation of a platinum mirror on the NMR tube, but **8**, like Pt(PPh₃)₄, ultimately decomposes before complex **2** is completely consumed at room temperature.

These results demonstrate that although platinum(0) complexes are able to promote room-temperature carbene coupling in Cr metal carbonyl complexes, platinum(0) catalysts, like Pd(0) catalysts, decompose under the reaction conditions. Furthermore, platinum(0) catalysts did not allow for observable intermediates in the dimerization reaction and, in fact, the slower reaction rate and instability of the Pt(0) catalysts investigated prevented carbene dimerization

reactions from running to completion. These experiments, together with Sierra's work, demonstrate that all group 10 metals are able to catalyze the carbene dimerization reaction to form C–C bonds;⁵ however, Pd(0) complexes appear to be the most efficient catalysts of the triad with the largest substrate scope. Importantly, these results suggest that there are many potential late metal candidates to induce C–C bond formation in a syngas conversion cycle by carbene dimerization.

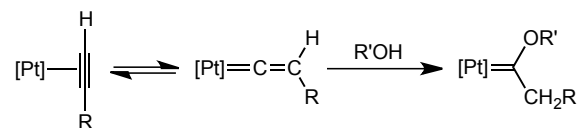
Section 2.2: Investigations into C–C Bond Formation from Bis(carbene)platinum(II) Complexes: Implications for the Pd-catalyzed Carbene Dimerization Reaction

Synthesis of Platinum(II) Bis(alkoxycarbene) Complexes

Platinum(II) bis(alkoxycarbene) complexes were first reported by Struchkov et al., in 1979 and were followed up in 2006 by Steinborn and co-workers.^{15,16} Since we have demonstrated that Pt(0) complexes react with Cr carbene complexes to effect carbene coupling, presumably through a platinum(0) bis(carbene) intermediate, platinum(II) bis(carbene) complexes seemed like excellent model substrates to use for probing the proposed mechanism for the dimerization reaction.

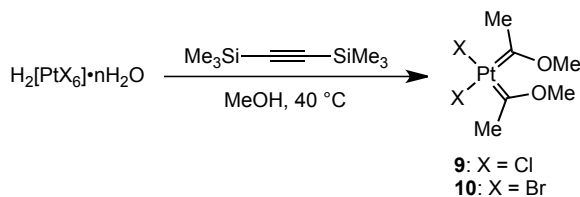
Platinum(II) bis(alkoxycarbene) complexes are synthesized from platinum(IV) hexahalide salts and an appropriate alkyne in dry alcohol solvents.

The reaction is proposed to involve intermediate formation of a metal–vinylidene complex, followed by nucleophilic attack by the alcohol (Scheme 2.10).¹⁷

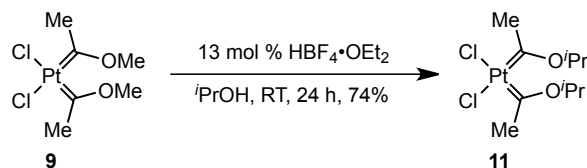


Scheme 2.10 Proposed mechanism for carbene formation on Pt complexes from alkynes and alcohols.

Bis(methoxycarbene)platinum complexes **9** and **10** were obtained by the published procedure, treating bis(trimethyl)silylacetylene with hexachloroplatinic acid and hexabromoplatinic acid, respectively, in dry methanol (Scheme 2.11).¹⁶ (Platina- β -diketones are obtained instead if the alcohol is not dry.¹⁸) We were unable to reproduce the reported analogous synthesis of the bis(isopropoxycarbene)platinum complex **11**;¹⁵ however, we were able to obtain **11** via an alternate route: addition of HBF_4 in diethyl ether to **9** in dry isopropanol (Scheme 2.12).¹⁶



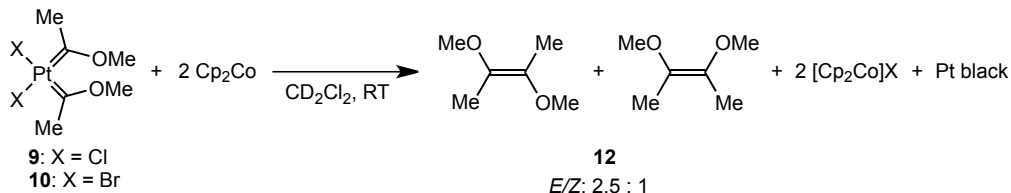
Scheme 2.11 Synthesis of bis(carbene)platinum complexes **9** and **10**.



Scheme 2.12 Synthesis of bis(carbene)platinum complex **11** from **9**.

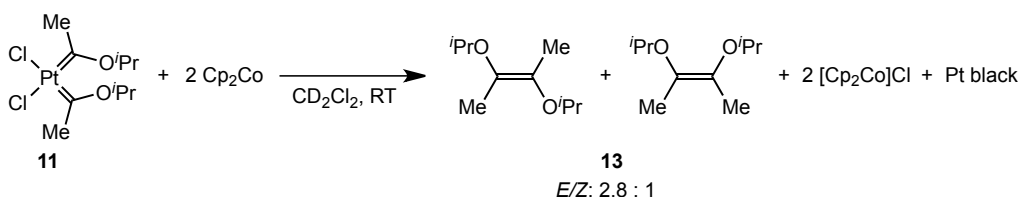
Reduction of Platinum(II) Bis(alkoxycarbene) Complexes

As the proposed active species for the carbene dimerization reaction is Pd(0), and therefore by analogy Pt(0), reducing the isolated platinum(II) bis(carbene) complexes seemed like a logical first step. Notably, Sierra and co-workers have reported a Pd(II) bis(carbene) complex that was stable to thermal decomposition, oxidation, iodine, bases, and addition of PMe₃; attempted reduction of this species to Pd(0) was not reported and apparently not investigated.^{13d} Gratifyingly, we found that reduction of chloro methoxycarbene complex **9** with two equivalents of cobaltocene in dichloromethane resulted in immediate conversion of **9** into (*E/Z*)-2,3-dimethoxybut-2-ene (**12**) in 64% yield (by ¹H NMR), along with Pt black and cobaltocenium chloride. The bromo analog **10** behaved similarly, giving **12** in 49% yield (Scheme 2.13). **12** was isolated by vacuum transfer, and its identity confirmed by comparison of the ¹H NMR and GC-MS data to literature data.¹⁹ The *E/Z* ratio was determined by ¹H NMR spectroscopy to be 2.5:1. Addition of only one equivalent of cobaltocene led to only 50% conversion of **9** to **12**.



Scheme 2.13 Reduction of carbene complexes **9** and **10** with cobaltocene to yield *E/Z*-olefinic products **12**.

The reaction of chloro isopropoxycarbene complex **11** with two equivalents of cobaltocene was noticeably less clean than the reduction of **9** and **10**; unfortunately, the minor side products in this reaction could not be characterized. The major product of the reduction of **11** was the carbene coupling product (*E/Z*)-2,3-diisopropoxybut-2-ene (**13**) in 42% yield (Scheme 2.14). **13** decomposed into multiple species on attempted vacuum transfer, and was therefore characterized by ^1H and ^{13}C NMR spectroscopy of the crude reaction mixture; the *E/Z* ratio was determined to be 2.8:1.



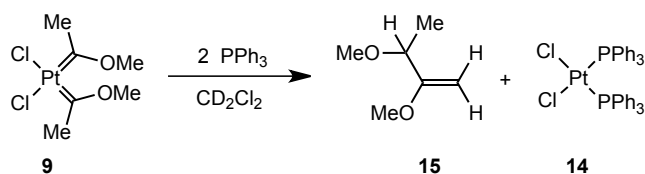
Scheme 2.14 Reduction of carbene complex **11** with cobaltocene to yield *E/Z*-olefinic products **13**.

These results are consistent with the proposed mechanism for carbene dimerization via a bis(carbene)palladium(0) intermediate shown in Scheme 2.2: reduction of complexes **9–11** with cobaltocene leads to (unobservable) bis(carbene)platinum(0) intermediates that instantaneously eliminate but-2-ene products via carbene coupling.

Reaction of Platinum(II) Bis(alkoxycarbene) Complexes with L-type Ligands

Although reduction of bis(carbene)platinum(II) complexes **9–11** led to the desired carbene dimerization reaction, we were interested in exploring other approaches to induce C–C bond formation from complexes **9–11**. One strategy we found particularly attractive was to add L-type ligands to isolated bis(carbene)platinum(II) complexes in order to displace carbene ligands and potentially induce carbene coupling.

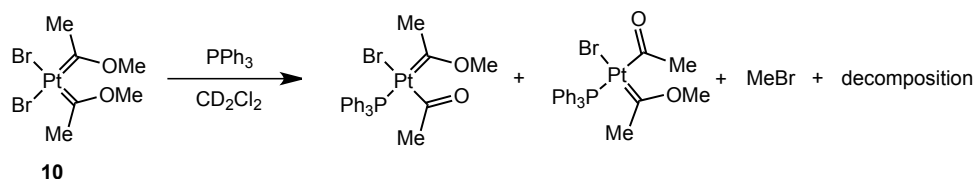
Indeed, treatment of **9** with two equivalents of PPh₃ in dichloromethane at room temperature resulted in rapid and nearly quantitative conversion to *cis*-dichlorobis(triphenylphosphine)platinum(II) (**14**) and a new organic product resulting from C–C bond formation, identified by ¹H NMR, ¹³C NMR, and HRMS as 2,3-dimethoxybut-1-ene (**15**; Scheme 2.15). Notably, **15** is a *constitutional isomer* of **12**, the product from reduction of **9** or **10** with cobaltocene. Addition of only one equivalent of PPh₃ to **9** led to conversion of only half of the starting material to products.



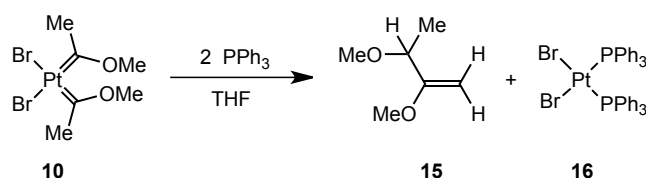
Scheme 2.15 Addition of PPh₃ to **9** to form **14** and **15**.

Unexpectedly, addition of two equivalents of PPh₃ to the analogous bromide carbene complex **10** in dichloromethane did *not* give **15**; instead, ¹H and ³¹P NMR spectroscopy revealed the formation of two new acetyl platinum complexes, tentatively assigned as *cis*- and *trans*-

$\text{Br}(\text{PPh}_3)\text{Pt}(\text{COMe})\{\text{C}(\text{OMe})(\text{Me})\}$, along with bromomethane and some unidentified byproducts (Scheme 2.16). However, reaction of **10** with two equivalents of PPh_3 in THF (in which it is only sparingly soluble) at $50\text{ }^\circ\text{C}$ did give **15** and *cis*-dibromobis(triphenylphosphine)platinum(II) (**16**) (Scheme 2.17).

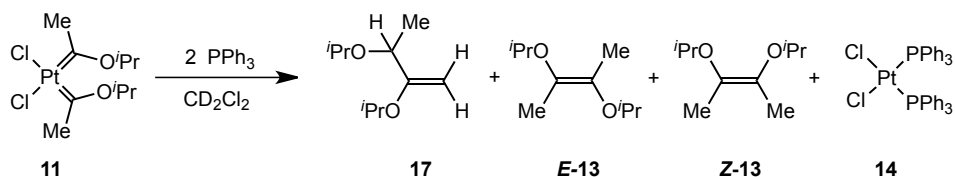


Scheme 2.16 Addition of PPh_3 to **10** in CD_2Cl_2 led to the formation of *cis*- and *trans*- $\text{Br}(\text{PPh}_3)\text{Pt}(\text{COMe})\{\text{C}(\text{OMe})(\text{Me})\}$, MeBr , and unidentified decomposition.



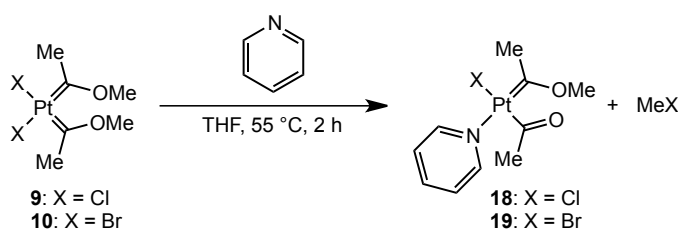
Scheme 2.17 Addition of PPh_3 to **10** in THF to form **15** and **16**.

Reaction of chloro isopropoxycarbene complex **11** with two equivalents of PPh_3 in dichloromethane yielded a *mixture* of 2,3-diisopropoxybut-1-ene (**17**), characterized by ^1H NMR, ^{13}C NMR, and HRMS, along with **13** and **14** (Scheme 2.18). The *E/Z* ratio of **13** was 9:1, substantially different from that observed in the reduction of **11** with cobaltocene; the ratio of *E*-**13** to **17** was 1:1.7.

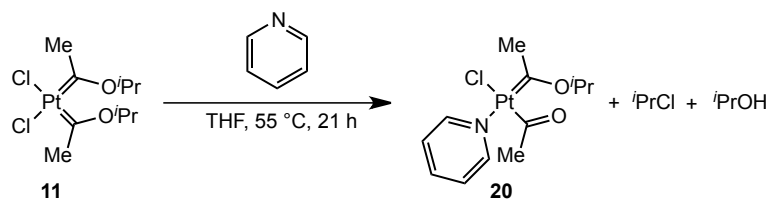


Scheme 2.18 Addition of PPh_3 to **11** to form *E/Z*-**13**, **14**, and **17**.

In addition to the L-type ligand PPh_3 , we explored the reactivity of **9–11** with pyridine. Interestingly, reaction of **9** with one equivalent of pyridine in THF at $55\text{ }^\circ\text{C}$ resulted, after about 2 h, in nearly quantitative conversion to the acetyl methoxycarbene complex **18**,²⁰ accompanied by liberation of chloromethane, which was identified by ^1H NMR (Scheme 2.19). No organic products resulting from C–C bond formation were observed to form. The assignment of **18** is based on the ^{13}C NMR spectrum, which exhibits downfield singlets at δ 283.0 ($^1J_{\text{PtC}} = 1428\text{ Hz}$) and δ 212.8 ($^1J_{\text{PtC}} = 1126\text{ Hz}$), characteristic of carbene and acyl resonances, respectively, along with IR spectroscopy (acyl $\nu_{\text{C=O}} = 1639\text{ cm}^{-1}$) and ^1H NMR. Reaction of **10** with pyridine similarly gave **19** and bromomethane. The chloro isopropoxycarbene complex **11** also reacted with pyridine, but the reaction was significantly slower under the same conditions, requiring about 21 h to give **20**, which exhibited spectroscopic features similar to those of **18** and **19**, along with isopropyl chloride and isopropanol (Scheme 2.20).



Scheme 2.19 Addition of pyridine to **9** and **10** to yield acetyl methoxycarbene complexes **18** and **19**.



Scheme 2.20 Addition of pyridine to **11** to yield acetyl methoxycarbene complex **20**.

The stereochemistry of **18–20** was assigned on the basis of 1D NOESY experiments, which show interaction between the methyl group on the acetyl ligand and the ortho protons on the pyridine ring, indicating those two ligands are cis to one another. Only a single isomer was observed in each case. NOESY and ^1H NMR spectra for complexes **18–20** are shown in Figure 2.5.

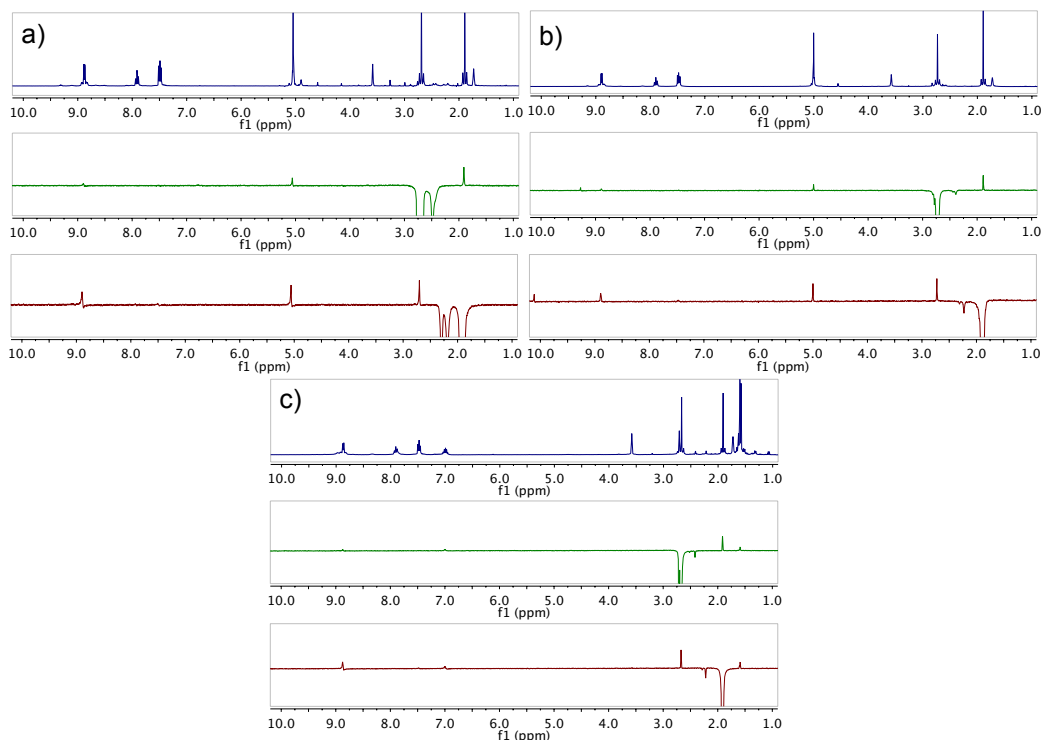
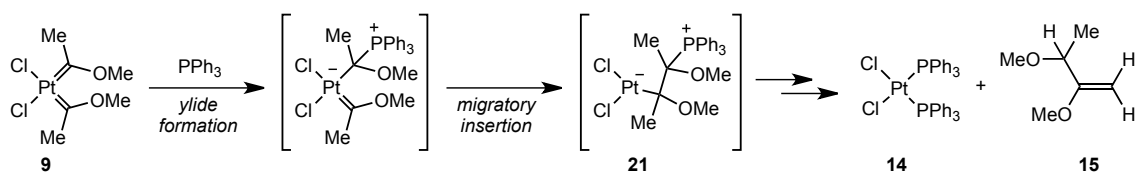
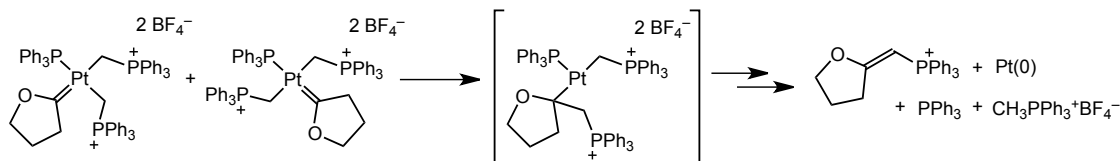


Figure 2.5 ^1H NMR and 1D NOESY spectra for **18** (a), **19** (b), and **20** (c). Blue: ^1H NMR; green: NOESY, irradiation of CCH_3 ; red: NOESY, irradiation of COCH_3 . Positive peaks indicate interactions.

These experiments demonstrate an interesting dichotomy between different L-type ligands: while addition of PPh₃ (and other phosphine ligands) can lead to C–C bond formation from bis(carbene)platinum(II) complexes *without* reducing the Pt(II) complexes, pyridine – in contrast – leads to new pyridine acyl Pt(II) metal complexes and no coupled organic products. Remarkably, different olefinic products are obtained from the addition of PPh₃ than from reduction: phosphine leads to the alkoxy-substituted but-1-enes **15** and **17**, while reduction leads to the but-2-enes **12** and **13**. This product switch, along with the failure of pyridine to induce similar coupling, suggests a mechanism involving phosphine attack at one carbene ligand to give an alkyl complex, perhaps better described as a stabilized ylide, which undergoes migratory insertion with the other carbene ligand to form the C–C bond (Scheme 2.21). Both steps have precedents: formation of phosphonium ylide complexes by phosphine attack at Fischer carbene ligands is well-known,^{2b, 21} and a closely related example of phosphonium ylide migration to a carbene ligand has been reported for a platinum(II) complex (Scheme 2.22).²² The precise mechanism by which the but-2-yl species **21** would eliminate **15** is not clear, but a sequence in which β -hydride elimination is followed by hydride transfer to carbon along with (or after) phosphine dissociation seems plausible.



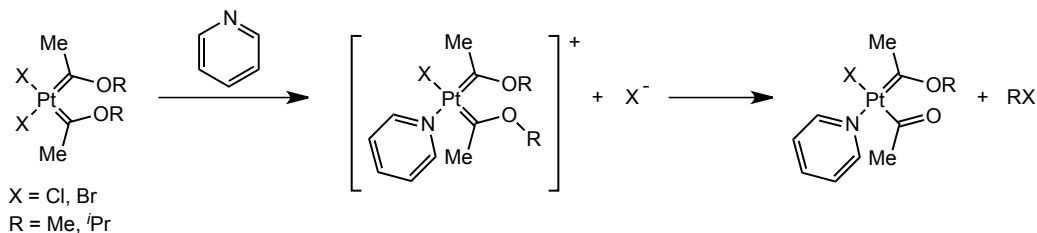
Scheme 2.21 Proposed mechanism for C–C bond formation from bis(carbene)platinum(II) complexes upon addition of PPh₃.



Scheme 2.22 Proposed mechanism for phosphonium ylide migration to a carbene ligand on a Pt(II) complex. (Adapted from ref. 22).

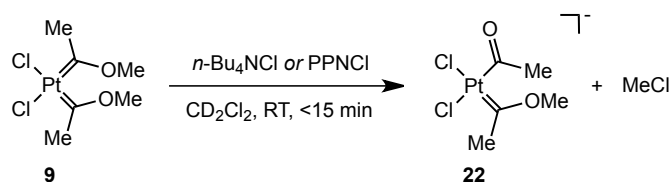
Addition of pyridine to bis(carbene) complexes **9–11**, on the other hand, does *not* bring about coupling,²³ but instead generates pyridine acyl platinum(II) complexes with concomitant elimination of alkyl halide. Although some metal-bound pyridinium ylides are known,²⁴ they are not common and we have not found any reports of such derivatives for heteroatom-substituted carbenes, suggesting that reaction of pyridine according to Scheme 2.21 might be expected to be unfavorable. Instead, displacement of halide by pyridine, followed by S_N2 attack of the free halide on the alkoxy substituent of the carbene ligand, presumably leads to formation of alkyl halide and an acyl ligand (Scheme 2.23). In support of the S_N2 mechanism, the methoxycarbene complexes **9** and **10** undergo this transformation considerably more rapidly than does isopropoxycarbene complex **11**; these involve halide attack at 1° and 2°

positions, respectively. (Attempts to synthesize a *tert*-butoxycarbene complex, which would not be expected to exhibit such reactivity at all, were unsuccessful.)



Scheme 2.23 Proposed mechanistic pathway for reaction of pyridine with **9–11**.

To further probe the $\text{S}_{\text{N}}2$ mechanism, we investigated the addition of chloride salts to complex **9**. Treatment of **9** with one equivalent of either bis(triphenylphosphine)iminium (PPN) chloride or tetra-*n*-butylammonium chloride in dichloromethane resulted in immediate formation of the anionic (acetyl)(methoxycarbene)platinum complex **22** and chloromethane, consistent with the proposed mechanism (Scheme 2.24). **22** was identified by the characteristic ^{13}C carbene and acyl resonances at δ 277.4 ($^1J_{\text{PtC}} = 1575$ Hz) and δ 213.2, respectively, along with the $\nu_{\text{C}=\text{O}}$ stretch at 1637 cm^{-1} . Attempts to convert **22** back to **9** by addition of one equivalent of methyl triflate led to decomposition.



Scheme 2.24 Addition of chloride salts to **9** to form acyl Pt(II) complex **22**.

Conclusions

Our experiments with Cr and Pt complexes provide strong support for the mechanism proposed by Sierra and co-workers for transition metal-catalyzed carbene dimerization shown in Scheme 2.2. Experiments with *para*-substituted aryl Cr carbene complexes **1–3** provide evidence that nucleophilic Pd attack leads to carbene transmetalation, since complexes with more electrophilic carbene ligands reacted more quickly than those with more electron-rich carbene ligands. We have also demonstrated that Pt(0) complexes are able to catalyze the carbene dimerization reaction; however, Pt(0) catalysts are less stable and less efficient compared to their Pd(0) congeners leading to incomplete reactions. Importantly, reduction of isolated bis(carbene)platinum(II) complexes **9–11** led to the expected *E/Z*-olefinic products, which we believe provides strong evidence for a bis(carbene)palladium(0) intermediate as proposed by Sierra.⁵

Additionally, we have demonstrated that steric factors may be important for carbene dimerization, as Cp-substituted Cr carbene complexes **5–6** did not dimerize, despite having seemingly similar electronics to related pentacarbonyl Cr carbene complexes **1–3**, which undergo dimerization under very mild conditions. We have also shown that heterogeneously-catalyzed pathways appear to be accessible for the carbene dimerization reaction; however, whether the primary pathway for dimerization is homogeneous or heterogeneous has not been determined. Finally, we have also discovered a new pathway to form C–C bonds from bis(carbene)platinum(II) complexes under mild conditions by the

simple addition of phosphine ligands. Taken together, these results represent encouraging steps of progress toward our goal of developing of a multicomponent homogeneous catalytic system, that incorporates a late transition metal catalysts for C–C bond formation, to ultimately generate value-added higher hydrocarbons from simple feedstocks such as syngas.

Experimental Section

General Considerations

All air- and moisture-sensitive compounds were manipulated using standard vacuum line or Schlenk techniques or in a glovebox under a nitrogen atmosphere. The solvents for air- and moisture-sensitive reactions were dried by the method of Grubbs et al. or by distillation from sodium.²⁵ All NMR solvents were purchased from Cambridge Isotopes Laboratories, Inc. Dichloromethane- d_2 was dried by passage through activated alumina. Tetrahydrofuran- d_8 was purchased in a sealed ampule and dried by passage through activated alumina. Unless otherwise noted, materials were used as received. Dihydrogen hexachloroplatinate(IV) hexahydrate and dihydrogen hexabromoplatinate(IV) nonahydrate were purchased from Alfa Aesar. We found that the source of the platinum salt greatly affected the yields of bis(carbene)platinum(II) complexes; we achieved the best and most consistent yields with materials from Alfa Aesar. *n*-Butyllithium (2.2M in hexane) and tert-butyllithium (nominally 1.5M in *n*-pentane) were purchased from Alfa Aesar. Pd₂dba₃ and

Tetrakis(triphenylphosphine)platinum(0) was purchased from Strem Chemicals, Inc. Bis(trimethyl)silylacetylene was purchased from Acros Organics. Methanol was purchased from Sigma Aldrich and was distilled from Mg and then dried over sequential 4 Å molecular sieves prior to use. Isopropanol was purchased from Sigma Aldrich dried over 4 Å molecular sieves prior to use. Triphenylphosphine Cr(CO)₆, triphos, bis(trimethylsilyl)acetylene, 4-bromobenzotrifluoride, 4-bromoanisole, 4-bromoaniline, trimethyloxonium tetrafluoroborate and Pd black was purchased from Sigma Aldrich. (CO)₅Cr{C(OMe)(*p*-CF₃-C₆H₄)} (**1**), (CO)₅Cr{C(OMe)(*p*-MeO-C₆H₄)} (**2**), and (CO)₅Cr{C(OMe)(*p*-NMe₂-C₆H₄)} (**3**),⁸ Br₂Pt{C(OMe)(Me)}₂ (**10**), and Cl₂Pt{C(O^{*i*}Pr)(Me)}₂ (**11**) were synthesized according to literature procedures.¹⁶ Cp(NO)(CO)Cr{C(OMe)(C₆H₅)} **5** was synthesized by a literature procedure;¹¹ however, the precursor (Cp)(CO)₂(NO)Cr was synthesized according to the improved procedure by Stryker et al.¹² ¹H, ³¹P, ¹³C, and ¹⁹⁵Pt NMR spectra were recorded on Varian Mercury 300, Varian INOVA-500, and Varian INOVA-600 spectrometers at room temperature. Chemical shifts are reported with respect to residual internal protio solvent for ¹H and ¹³C{¹H} spectra. Other nuclei were referenced to an external standard: H₃PO₄ (³¹P), H₂PtCl₆·6H₂O in 30% v/v D₂O/1 M HCl (¹⁹⁵Pt), all at 0 ppm. Infrared spectra were recorded on a Thermo Scientific Nicolet 6700 series spectrometer. GC-MS analyses were performed on an HP model 6890N chromatograph equipped with a 30 m × 25 mm × 0.40 μm HP5-1 column and equipped with an HP 5973 mass-selective EI detector. High-resolution mass spectra (HRMS) were

obtained at the California Institute of Technology Mass Spectral Facility. Elemental analyses were performed by Midwest Microlab LLC, Indianapolis, IN 46250. X-ray quality crystals were grown as indicated in the experimental procedures for each complex. The crystals were mounted on a glass fiber with Paratone-N oil. Data collection was carried out on a Bruker KAPPA APEX II diffractometer with a 0.71073 Å MoK α source. Structures were determined using direct methods with standard Fourier techniques using the Bruker AXS software package. In some cases, Patterson maps were used in place of the direct methods procedure. Some details regarding crystal data and structure refinement are available in Tables 2.2. Selected bond lengths and angles are supplied in the corresponding figures.

General Procedure for Pd-Catalyzed Carbene Dimerization Reaction of *para*-substituted Aryl (CO)₅Cr{C(OMe)(Ar)} 1-3. To a J-Young NMR tube was added 0.040 mmol of the carbene complex, 5 mol % of Pd₂dba₃ and THF-*d*₈. The tube was sealed and the reaction was monitored by ¹H NMR spectroscopy until no starting material remained. The formation of Pd black was evident in all reaction mixtures after a few hours. Complete conversion of starting material to olefinic products occurred within 24 hours. In some cases, hexamethylbenzene or ferrocene was used as an internal standard to calculate product yields. Dimerization was also observed when Pd(PPh₃)₄ (5 mol %) was employed as the catalyst. For **1**: (Product ratio: 1:2.8) Major isomer: ¹H NMR (300 MHz, THF-*d*₈) δ

7.52 (d, $J = 8.3$, 4H), 7.35 (d, $J = 8.2$, 4H), 3.64 (s, 6H). Minor isomer: ^1H NMR (300 MHz, THF- d_8) δ 7.91 (d, $J = 8.4$, 4H), 7.73 (d, $J = 8.3$, 4H), 3.37 (s, 6H). For **2**: (Product ratio: 1:1.5) Major isomer: ^1H NMR (300 MHz, THF- d_8) δ 7.06 (d, $J = 8.9$, 4H), 6.70 (d, $J = 8.8$, 4H), 3.71 (s, 6H), 3.51 (s, 6H). Minor isomer: ^1H NMR (300 MHz, THF- d_8) δ 7.64 (d, $J = 9.0$, 4H), 6.91 (d, $J = 8.9$, 4H), 3.79 (s, 6H), 3.28 (s, 6H). For **3**: ^1H NMR (300 MHz, THF- d_8) δ 7.57 (d, $J = 9.0$), 7.47 (d, $J = 9.0$), 7.01 (d, $J = 8.9$), 6.73 (d, $J = 9.0$), 6.71 (d, $J = 9.0$), 6.51 (d, $J = 8.9$), 6.28 (d, $J = 7.5$), 5.07 (d, $J = 7.6$), 3.47 (s), 3.39 (s), 3.34 (s), 3.28 (s), 2.98 (s), 2.96 (s), 2.91 (s), 2.88 (s). Notably, **3** led to the formation of other side products beyond the *E/Z*-olefinic products, but these products were not characterized.

Crossover Experiment between $(\text{CO})_5\text{Cr}\{\text{C}(\text{OMe})(p\text{-CF}_3\text{-C}_6\text{H}_4)\}$ **1 and $(\text{CO})_5\text{Cr}\{\text{C}(\text{OMe})(p\text{-MeO-C}_6\text{H}_4)\}$ **2**.** To a J-Young NMR tube was added 9.5 mg (0.025 mmol) of **1**, 9.7 mg (0.028 mmol) of **2**, 2.8 mg of Pd₂dba₃ (6 mol %) and THF- d_8 . The tube was sealed and the reaction was monitored by ^1H NMR spectroscopy for 24 hours. The expected *E/Z*-dimerization products were observed for **1** and **2**, as well as new *E/Z*-olefinic product for the mixed species. For mixed olefinic species: (Product ratio: 1:2.2) ^1H NMR (300 MHz, THF- d_8) δ 7.93 (d, $J = 8.6$), 7.67 (d, $J = 11.2$), 7.42 (d, $J = 8.4$), 7.29 (d, $J = 8.3$), 7.11 (d, $J = 8.8$), 6.96 (d, $J = 8.9$), 6.79 (d, $J = 8.7$), 3.82 (s), 3.74 (s), 3.62 (s), 3.54 (s), 3.52 (s), 3.36 (s), 3.31 (s).

Carbene Dimerization Reaction of $(\text{CO})_5\text{Cr}\{\text{C}(\text{OMe})(p\text{-MeO-C}_6\text{H}_4)\}$ **2 and Pd black.** To a J-Young NMR tube was added 14.5 mg of **2**, 0.2 mg of Pd black (4 mol %) and THF- d_8 . The tube was sealed and the reaction was monitored by ^1H NMR spectroscopy. Formation of the expected *E/Z*-olefinic products for **2** were observed. The reaction was monitored for two weeks and complete conversion was not observed.

$\text{Cp}(\text{NO})(\text{CO})\text{Cr}\{\text{C}(\text{OMe})(p\text{-CF}_3\text{-C}_6\text{H}_4)\}$ (6**).** To a 250 mL Schlenk flask charged with a stir bar was added 1.40 g of $\text{Cp}(\text{CO})_2(\text{NO})\text{Cr}$. A 50 mL portion of diethyl ether was transferred via cannula into the flask and the resulting reaction mixture was cooled to 0 °C. To a separate Schlenk flask charged with a stir bar was added 0.97 mL of 4-bromobenzotrifluoride and a 25 mL of diethyl ether was added via cannula transfer. The solution was cooled to -78 °C before a 4.3 mL portion of *n*-butyllithium was added via syringe very slowly. The resulting solution was stirred for 30 min before being cannula transferred onto the ether solution of $\text{Cp}(\text{CO})_2(\text{NO})\text{Cr}$. The reaction mixture was allowed to stir for 1 hr then was warmed to room temperature. Solvent was removed *in vacuo* and the resulting residue was redissolved in degassed water under Ar. A 1.39 g portion of trimethyloxonium tetrafluoroborate was added under air and the resulting solution was filtered through celite. The aqueous layer was extracted with diethyl ether until no orange color was seen in the organic layer. The organic layers were combined and dried over magnesium sulfate and filtered. The solvent was

removed by rotary evaporation and the crude material was purified by flash chromatography using 1:4 dichloromethane/hexanes as the eluent, and nitrogen to provide pressure to afford 1.09 g (42%) of an orange powder. ^1H NMR (300 MHz, CDCl_3) δ 7.54 (d, $J = 8.0$, 2H), 7.06 (d, $J = 8.0$, 2H), 4.97 (s, 5H), 4.64 (s, 3H). IR (petroleum ether): 1983 (s), 1678 (s), 1324 (m) cm^{-1} .

Procedure for Pd-Catalyzed Carbene Dimerization Reaction with $\text{Cp}(\text{NO})(\text{CO})\text{Cr}\{\text{C}(\text{OMe})(\text{C}_6\text{H}_5)\}$ 5 and $\text{Cp}(\text{NO})(\text{CO})\text{Cr}\{\text{C}(\text{OMe})(p\text{-CF}_3\text{-C}_6\text{H}_4)\}$ 6.

The same procedure as that for carbene dimerization of *para*-substituted aryl complexes $(\text{CO})_5\text{Cr}\{\text{C}(\text{OMe})(\text{Ar})\}$ 1-3 was used; however, no products were observed. Heating the reaction mixture at 100 °C overnight resulted in the formation of Pd black, but no olefinic products were observed.

(triphos)(PPh_3)Pd (7). To a 20 mL vial was added 51.0 mg of $\text{Pd}(\text{PPh}_3)_4$, 24.5 mg of triphos and ~2 mL of THF. The reaction mixture was allowed to stir for 30 minutes before the solvent was removed *in vacuo* to afford a yellow oil. The product was recrystallized by slow vapor diffusion from THF/petroleum ether to remove free PPh_3 . ^1H NMR (300 MHz, $\text{THF-}d_8$) δ 7.58 – 6.78 (m), 2.48 – 1.76 (m). ^{31}P NMR (121 MHz, $\text{THF-}d_8$) δ 33.93 (m), 30.73 (dq, $J = 57.0, 32.5$), 26.16 (ddd, $J = 61.3, 25.7, 3.6$).

Coupling of $(\text{CO})_5\text{Cr}\{\text{C}(\text{OMe})(p\text{-MeOC}_6\text{H}_4)\}$ **2 with $\text{Pt}(\text{PPh}_3)_4$.** To a J. Young NMR tube was added a solution of 32.1 mg (0.094 mmol) of Cr(carbene) **2** and 7.4 mg (0.0059 mmol) of $\text{Pt}(\text{PPh}_3)_4$ in $\text{THF-}d_8$. Conversion to 13% of dimerization product (by ^1H NMR integration) took place over 9 days; the formation of a Pt mirror was observed to form on the NMR tube over time. Subsequent heating at 50 °C in an oil bath for 16 hours did not result in any further conversion of **2** to products. The *E/Z*-olefinic products have been reported in the literature,²⁶ but we were unable to find suitable spectral data for the compound; therefore, we synthesized the products independently by reacting 18.5 mg (0.054 mmol) of Cr(carbene) **2** with 10 mol % Pd_2dba_3 in dichloromethane- d_2 . During stirring for 48 h at ambient temperature the solution changed from bright red to dark brown with visible Pd black precipitation. The solvent was removed from the reaction mixture, and the resulting dark brown residue was dissolved in diethyl ether and filtered through a plug of silica gel. Removal of solvent from the filtrate gave the olefinic products as a pale yellow powder. Yield: 74%. Data for (*E/Z*)-1,2-dimethoxy-1,2-bis(4-methoxyphenyl)ethane are as follows: ^1H NMR (300 MHz, $\text{THF-}d_8$): δ 7.64 (d, $J = 8.3$ Hz, 2H, *ArH*), 7.06 (d, $J = 8.3$ Hz, 2H, *ArH*), 6.91 (d, $J = 8.4$ Hz, 2H, *ArH*), 6.70 (d, $J = 8.2$ Hz, 2H, *ArH*), 3.80 (s, 3H, OCH_3), 3.71 (s, 3H, OCH_3), 3.51 (s, 3H, OCH_3), 3.28 (s, 3H, OCH_3). ^{13}C NMR (126 MHz, $\text{THF-}d_8$): δ 160.16, 160.10, 145.29, 143.57, 131.65, 130.29, 128.63, 127.70, 114.14, 114.11, 58.24, 55.40, 55.30. HRMS (FAB): m/z calcd for $\text{C}_{18}\text{H}_{20}\text{O}_4$ $[\text{M}]^+$ 300.1362; found 300.1359.

(triphos)(PPh₃)Pt (8). To a 20 mL vial was added 51.0 mg of Pt(PPh₃)₄, 23.0 mg of triphos and ~2 mL of THF. The reaction mixture was allowed to stir for 30 minutes before being filtered through glass microfiber filter paper. The solvent was removed *in vacuo* to afford an orange oil. The product was recrystallized by slow vapor diffusion from THF/petroleum ether/diethyl ether to remove free PPh₃. ¹H NMR (300 MHz, THF-*d*₈) δ 7.74 – 6.66 (m), 2.65 – 1.82 (m). ³¹P NMR (121 MHz, THF-*d*₈) δ 46.80 (m, ¹J_{Pt,P} = 3023), 26.82 (m, ¹J_{Pt,P} = 3667), 8.29 (m).

Procedure for Carbene Dimerization Reaction of (CO)₅Cr{C(OMe)(*p*-MeO-C₆H₄)} 2 and Pd(PPh₃)(triphos) 7 or Pt(PPh₃)(triphos) 8. The same procedure as that for carbene dimerization of *para*-substituted aryl complexes (CO)₅Cr{C(OMe)(Ar)} 1-3 was used employing either 5 mol % of 7 or 8. The tube was sealed and the reaction was monitored by ¹H NMR spectroscopy until no starting material remained.

Cl₂Pt{C(OMe)(Me)}₂ (9). Complex 9 was prepared by a modified literature procedure. A 2.00 g (3.86 mmol) amount of hexachloroplatinic acid was dissolved in 12 mL of dry MeOH, and 5.3 mL (23.4 mmol) of bis(trimethylsilyl)acetylene was added via syringe. The orange solution was stirred at 49 °C; after 3 h, the solution turned yellow and white solids formed. Approximately two-thirds of the solvent was removed *in vacuo*, and the white solid was filtered and washed three

times with 3 mL portions of MeOH. In some preparations a yellow solid was obtained, which could be further purified by dissolving in dichloromethane and filtering through a glass frit; removal of solvent from the filtrate resulted in a white powder. The identity of the compound was confirmed by comparison with the reported spectroscopic data.

General Procedure for Reduction of Bis(carbene)platinum(II) Complexes 9-

11. To a J. Young NMR tube was added 20.2 mg (0.053 mmol) of bis(carbene) **9** in dichloromethane- d_2 , followed by 19.9 mg (0.11 mmol) of CoCp₂ in dichloromethane- d_2 , resulting in an immediate color change of the solution from nearly colorless to dark brown and the formation of a Pt mirror on the NMR tube. (*E/Z*)-2,3-dimethoxybut-2-ene (**12**) was the only product observed by ¹H NMR spectroscopy. **12** was isolated by vacuum transfer to a clean J-Young tube. Yield: 64%. Data for **12** (product ratio: 1:2.36) are as follows. Major isomer (*E*)-2,3-dimethoxybut-2-ene: ¹H NMR (300 MHz, CD₂Cl₂) δ 3.43, 1.77; ¹³C NMR (75 MHz, CD₂Cl₂) δ 140.9, 56.79, 10.81. Minor isomer (*Z*)-2,3-dimethoxybut-2-ene: ¹H NMR (300 MHz, CD₂Cl₂) δ 3.50, 1.71; ¹³C NMR (75 MHz, CD₂Cl₂) δ 137.1, 57.12, 13.95. (*E/Z*)-2,3-dimethoxybut-2-ene: GC–MS *m/z* (% relative intensity, ion): 116 (43, M), 101 (73, M – Me), 73 (62), 43 (100).

The analogous reaction of **10** with CoCp₂ gave **12** in 49% yield. In the analogous reaction of **11**, attempts to isolate **13** by vacuum transfer resulted in decomposition to unidentified products. **13** was therefore characterized in the

presence of [CoCp₂]Cl in the crude reaction mixture; side products in the reaction could not be identified. Yield: 41%. Major isomer (*E*)-2,3-diisopropoxybut-2-ene: ¹H NMR (500 MHz, CD₂Cl₂) δ 3.96 (m, 2H), 1.72 (s, 6H), 1.11 (d, *J* = 6.1 Hz, 12H); ¹³C NMR (126 MHz, CD₂Cl₂) δ 138.80, 69.45, 22.51, 12.52. Minor isomer (*Z*)-2,3-diisopropoxybut-2-ene: ¹H NMR (500 MHz, CD₂Cl₂) δ 4.15 (m, 2H), 1.67 (s, 6H), 1.12 (d, *J* = 6.0 Hz, 12H); ¹³C NMR (126 MHz, CD₂Cl₂) δ 135.47, 79.51, 22.91, 12.52. (*E/Z*)-2,3-diisopropoxybut-2-ene: HRMS (EI) *m/z* calcd for C₁₀H₂₀O₂ [M]⁺ 172.1463, found 172.1493.

General Procedure for Reaction of Bis(carbene)platinum(II) Complexes

with PPh₃. To a J. Young NMR tube was added 21.5 mg (0.056 mmol) of **9** in dichloromethane-*d*₂. Addition of 28.3 mg (0.11 mmol) of PPh₃ as a solution in dichloromethane-*d*₂ to the NMR tube resulted in an immediate color change of the solution from nearly colorless to yellow. The formation of Cl₂Pt(PPh₃)₂ (**14**) was confirmed by comparison of ¹H and ¹³P NMR data to literature values.²⁷ 2,3-Dimethoxybut-1-ene (**15**) was also formed and was isolated by vacuum transfer to a clean J. Young tube. 2,3-Dimethoxybut-1-ene: quantitative yield; ¹H NMR (300 MHz, CD₂Cl₂): δ 4.09 (d, *J* = 2.1 Hz, 1H), 4.01 (d, *J* = 2.1 Hz, 1H), 3.64 (q, *J* = 6.5 Hz, 1H), 3.55 (s, 3H), 3.24 (s, 3H), 1.24 (d, *J* = 6.5 Hz, 3H); ¹³C NMR (75 MHz, CD₂Cl₂): δ 163.5, 81.43, 78.24, 56.24, 54.94, 19.75; HRMS (EI) *m/z* calcd for C₆H₁₂O₂ [M]⁺ 116.0837, found 116.0798.

Similar addition of PPh₃ to **10** in dichloromethane-*d*₂ did not result in formation of **15**, but addition of 14.0 mg (0.053 mmol) of PPh₃ as a solution in THF-*d*₈ to a J. Young NMR tube containing 12.2 mg (0.026 mmol) of **10** in THF-*d*₈ gave a heterogeneous mixture containing sparingly soluble **10** as a white solid, which when heated in a 50 °C oil bath overnight resulted in a homogeneous solution containing Br₂Pt(PPh₃)₂ (**16**) and **15**, as confirmed by ¹H, ¹³C, and ³¹P NMR spectroscopy.

Similar reaction of **11** with PPh₃ in dichloromethane gave a mixture of **17** and (*E/Z*)-**13**. 2,3-Diisopropoxybut-1-ene (**17**): 51% yield, ¹H NMR (500 MHz, CD₂Cl₂) δ 4.25 (m, 1H), 4.14 (d, *J* = 1.8 Hz, 1H), 3.91 (dd, *J* = 1.8, 0.6 Hz, 1H), 3.78 (q, *J* = 6.5 Hz, 1H), 3.63 (hept, *J* = 6.1 Hz, 1H), 1.22 (d, *J* = 5.9 Hz, 3H), 1.21 (d, *J* = 6.0 Hz, 3H), 1.20 (d, *J* = 6.5 Hz, 3H), 1.10 (d, *J* = 6.2 Hz, 3H), 1.09 (d, *J* = 6.1 Hz, 3H); ¹³C NMR (126 MHz, CD₂Cl₂): δ 162.82, 81.24, 74.29, 69.39, 69.04, 23.57, 21.87, 21.66, 21.14, 18.39. (*E*)-2,3-diisopropoxybut-2-ene (*E*-**13**): 37% yield; ¹H NMR (500 MHz, CD₂Cl₂): δ 3.99 (hept, *J* = 6.1 Hz, 2H), 1.74 (s, 6H), 1.14 (d, *J* = 6.1 Hz, 12H); ¹³C NMR (126 MHz, CD₂Cl₂) δ 138.99, 69.63, 22.68, 12.67. (*Z*)-2,3-diisopropoxybut-2-ene (*Z*-**13**): 4.5% yield; ¹H NMR (500 MHz, CD₂Cl₂): δ 4.17 (m, 2H), 1.70 (s, 6H), 1.16 (d, *J* = 6.1 Hz, 12H). Because of the small percentage of (*Z*)-2,3-diisopropoxybut-2-ene formed in the reaction, peaks were not identified for this compound in the ¹³C NMR of the organics. We were able to identify the ¹³C NMR peaks when *Z*-**13** was formed by reduction of

11 with CoCp_2 (*vide supra*). 2,3-Diisopropoxybutenes: HRGC (EI) m/z calcd for $\text{C}_{10}\text{H}_{20}\text{O}_2$ $[\text{M}]^+$ 172.1463, found 172.1481.

General Procedure for Reaction of Bis(carbene)platinum(II) Complexes

with Pyridine. In a J. Young NMR tube was added 0.040 g (0.10 mmol) of bis(carbene) **9** as a solution in $\text{THF-}d_8$, and 8.5 μL (0.11 mmol) of pyridine was added via microsyringe. The NMR tube was sealed and heated in an oil bath at 55 °C for 2 h, during which time the reaction mixture changed from colorless to a dichroic green/red solution. The reaction mixture was filtered through Celite and solvent was removed from the filtrate, resulting in isolation of a dark green oil. Despite repeated attempts to purify the product, analytically pure material could not be obtained.

Cl(py)Pt(COMe){C(OMe)(Me)} (18). Dark green oil. Yield: 93%. ^1H NMR (300 MHz, $\text{THF-}d_8$): δ 8.88 (m, 2H, *o*-CH), 7.91 (t, $J = 7.7$, 1H, *p*-CH), 7.49 (t, $J = 7.0$, 2H, *m*-CH), 5.04 (s, 3H, $^4J_{\text{Pt,H}} = 7.9$ Hz, OCH_3), 2.69 (s, 3H, $^3J_{\text{Pt,H}} = 22.3$ Hz, CCH_3), 1.89 (s, 3H, $^3J_{\text{Pt,H}} = 21.7$ Hz, COCH_3). ^{13}C NMR (126 MHz, $\text{THF-}d_8$): δ 283.0 (s, $^1J_{\text{Pt,C}} = 1428$ Hz, Pt=C), 212.8 (s, $^1J_{\text{Pt,C}} = 1130$ Hz, Pt-COMe), 152.9 (s, $^3J_{\text{Pt,C}} = 16$ Hz, *o*-CH), 139.7 (s, *p*-CH), 126.1 (s, $^4J_{\text{Pt,C}} = 24$ Hz, *m*-CH), 70.47 (s, $^3J_{\text{Pt,C}} = 116$ Hz, OCH_3), 44.68 (s, $^2J_{\text{Pt,C}} = 355$ Hz, COCH_3), 42.52 (s, $^2J_{\text{Pt,C}} = 170$ Hz, CCH_3). ^{195}Pt NMR (107 MHz, CD_2Cl_2) δ -2431. IR (THF): ν_{CO} 1639 cm^{-1} . This compound is air and moisture sensitive and despite repeated attempts the molecular ion peak calcd for: $\text{C}_{10}\text{H}_{14}\text{ClNO}_2\text{Pt}$ $[\text{M} + \text{H}]^+$ 410.0361 could not be

detected. The ion fragment $[M - \text{Me}]$ was detected in sample of **18**. HRMS (FAB): m/z calcd for: $\text{C}_9\text{H}_{11}\text{ClNO}_2\text{Pt}$ $[M - \text{Me}]$ 396.0116, found 396.0113.

Br(py)Pt(COMe){C(OMe)(Me)} (**19**). This compound was obtained similarly as a yellow oil. Yield: 98%. ^1H NMR (300 MHz, THF- d_8): δ 8.90 (m, 2H, *o*-CH), 7.90 (m, 1H, *p*-CH), 7.48 (dd, $J = 7.1, 5.8$, 2H, *m*-CH), 5.01 (s, 3H, $^4J_{\text{Pt,H}} = 7.4$ Hz, OCH_3), 2.74 (s, 3H, $^3J_{\text{Pt,H}} = 22.7$ Hz, CCH_3), 1.90 (s, 3H, $^3J_{\text{Pt,H}} = 22.0$ Hz, COCH_3). ^{13}C NMR (126 MHz, THF- d_8): δ 282.9 (s, $^1J_{\text{Pt,C}} = 1408$ Hz, Pt=C), 212.7 (s, $^1J_{\text{Pt,C}} = 1138$ Hz, Pt-COMe), 153.2 (s, $^3J_{\text{Pt,C}} = 17$ Hz, *o*-CH), 139.5 (s, *p*-CH), 126.0 (s, $^4J_{\text{Pt,C}} = 24$ Hz, *m*-CH), 70.36 (s, $^3J_{\text{Pt,C}} = 116$ Hz, OCH_3), 43.53 (s, $^2J_{\text{Pt,C}} = 370$ Hz, COCH_3), 42.39 (s, $^2J_{\text{Pt,C}} = 169$ Hz, CCH_3). IR (THF): ν_{CO} 1642 cm^{-1} . HRMS (FAB): m/z calcd for $\text{C}_{10}\text{H}_{15}\text{BrNO}_2\text{Pt}$ $[M + \text{H}]^+$ 454.9914, found 455.9917.

Cl(py)Pt(COMe){C(OⁱPr)(Me)} (**20**): The reaction of **11** with pyridine was slower than those of **9** and **10**; the sealed J. Young NMR tube containing the reaction mixture was heated for 21 h at 55 °C, and similar workup gave **20** as an orange oil. Yield: 98%. ^1H NMR (300 MHz, THF- d_8): δ 8.87 (m, 2H, *o*-CH), 7.90 (m, 1H, *p*-CH), 7.47 (ddd, $J = 7.7, 5.0, 1.5$, 2H, *m*-CH), 7.00 (sp, 1H, OCH), 2.67 (s, 3H, $^3J_{\text{Pt,H}} = 23.0$ Hz, CCH_3), 1.91 (s, 3H, $^3J_{\text{Pt,H}} = 20.3$ Hz, COCH_3), 1.59 (d, $J = 6.3$, 6H, $\text{CH}(\text{CH}_3)_2$). ^{13}C NMR (126 MHz, THF- d_8): δ 276.9 (s, $^1J_{\text{Pt,C}} = 1421$ Hz, Pt=C), 213.5 (s, $^1J_{\text{Pt,C}} = 1125$ Hz, Pt-COMe), 153.0 (s, $^3J_{\text{Pt,C}} = 17$ Hz, *o*-CH), 139.6 (s, *p*-CH), 126.1 (s, $^4J_{\text{Pt,C}} = 25$ Hz, *m*-CH), 91.58 (s, $^3J_{\text{Pt,C}} = 107$ Hz, OCH), 44.46 (s, $^2J_{\text{Pt,C}} = 351$ Hz, COCH_3), 42.72 (s, $^2J_{\text{Pt,C}} = 164$ Hz, CCH_3), 21.94

(CH(CH₃)₂). IR (THF): ν_{CO} , 1638 cm⁻¹. HRMS (FAB): m/z calcd for C₁₂H₁₈NO₂ClPt [M + H]⁺ 438.0674, found 438.0649.

[Cl₂Pt(COMe){C(OMe)(Me)}]nBu₄N (22): To a J. Young NMR tube was added 30.0 mg (0.078 mmol) of **9** in dichloromethane-*d*₂. Addition of 21.8 mg (0.078 mmol) of *n*Bu₄NCl as a solution in dichloromethane-*d*₂ to the NMR tube resulted in an immediate color change of the solution from nearly colorless to bright yellow. **22** was the only product observed to form by ¹H NMR spectroscopy. Removal of solvent from the reaction mixture followed by trituration with pentane resulted in isolation of a pale yellow powder. Yellow crystals of **22** were obtained by carefully layering pentane onto a concentrated THF solution of **22** at ambient temperature. Yield: 87% (44.5 mg). ¹H NMR (300 MHz, CD₂Cl₂): δ 4.89 (s, 3H, ⁴*J*_{Pt,H} = 8.7 Hz, OCH₃), 3.23 (m, 8H, NCH₂CH₂CH₂CH₃), 2.44 (s, 3H, ³*J*_{Pt,H} = 23.2 Hz, CCH₃), 2.23 (s, 3H, ³*J*_{Pt,H} = 14.3 Hz, COCH₃), 1.65 (m, 8H, NCH₂CH₂CH₂CH₃), 1.45 (m, 8H, NCH₂CH₂CH₂CH₃), 1.01 (t, *J* = 7.3 Hz, 12H, NCH₂CH₂CH₂CH₃). ¹³C NMR (75 MHz, CD₂Cl₂): δ 277.38 (s, ¹*J*_{Pt,C} = 1575 Hz, Pt=C), 213.23 (s, Pt-COMe), 68.86 (s, ³*J*_{Pt,C} = 120 Hz, OCH₃), 59.40 (s, NCH₂CH₂CH₂CH₃), 44.63 (s, ²*J*_{Pt,C} = 310 Hz, COCH₃), 41.99 (s, ²*J*_{Pt,C} = 182 Hz, CCH₃), 24.52 (s, NCH₂CH₂CH₂CH₃), 20.25 (s, NCH₂CH₂CH₂CH₃), 13.97 (s, NCH₂CH₂CH₂CH₃). IR (THF): ν_{CO} , 1637 cm⁻¹. Anal. Calcd for C₂₄H₅₂Cl₂NO₂Pt: C, 44.17; H, 8.03; N, 2.15. Found: C, 41.28; H, 7.25; N, 2.14. This compound is air

and moisture sensitive, and satisfactory combustion analysis could not be obtained.

Table 2.2 Crystal data and structure refinement for **7** and **8**.

	7	8
CCDC Number	702931	703009
Empirical formula	C ₅₂ H ₄₈ P ₄ Pd	C ₅₂ H ₄₈ P ₄ Pt
Formula weight	903.18	991.87
T (K)	100(2)	100(2)
a, Å	11.3578(5)	11.2917(5)
b, Å	30.6439(12)	30.7052(12)
c, Å	13.6011(6)	13.6118(6)
α, deg	-	-
β, deg	112.582(2)	112.646(2)
γ, deg	-	-
Volume, Å ³	4370.9(3)	4355.5(3)
Z	4	4
Crystal system	Monoclinic	Monoclinic
Space group	P2 ₁ /c	P2 ₁ /c
<i>d</i> _{calc} , g/cm ³	1.373	1.513
θ range, deg	1.75 to 38.09	1.75 to 40.79
Abs. coefficient, mm ⁻¹	0.607	3.404
Abs. correction	None	Semi Emp.
GOF	2.659	2.12
<i>R</i> ₁ , <i>wR</i> ₂ [<i>I</i> > 2σ(<i>I</i>)]	0.0323, 0.0537	0.0240, 0.0387

References

1. *Annual Energy Outlook 2009*, Department of Energy, 2009.
2. (a) Fischer, E. O.; Heckl, B.; Dötz, K. H.; Müller, J.; Werner, H. J. *Organomet. Chem.* **1969**, *16*, P29. (b) Dötz, K. H.; Fischer, H.; Hofmann, P.; Kreissl, F. R.; Schubert, U.; Weiss, K. *Transition Metal Carbene Complexes*; Verlag Chemic: Deerfield Beach, FL, 1983.
3. Herrmann, W. A. *Angew. Chem. Int. Ed.* **1982**, *21*, 117-130.
4. (a) Miller, A. J. M.; Labinger, J. A.; Bercaw, J. E. *J. Am. Chem. Soc.* **2008**, *130*, 11874. (b) Elowe, P. R.; West, N. M.; Labinger, J. A.; Bercaw, J. E. *Organometallics* **2009**, *28*, 6218. (c) Miller, A. J. M.; Labinger, J. A.; Bercaw, J. E. *J. Am. Chem. Soc.* **2010**, *132*, 3301. (d) West, N. M.; Labinger, J. A.; Bercaw, J. E. *Organometallics* **2011**, *30*, 2690. (e) Hazari, A.; Labinger, J. A.; Bercaw, J. E. *Angew. Chem. Int. Ed.* **2012**, *51*, 8268-8271.
5. (a) Sierra, M. A.; Mancheño, M. J.; Sáez, E.; del Amo, J. C. *J. Am. Chem. Soc.* **1998**, *120*, 6812. (b) Sierra, M. A.; del Amo, J. C.; Mancheño, M. J.; Gómez-Gallego, M. *J. Am. Chem. Soc.* **2001**, *123*, 851. (c) Gómez-Gallego, M.; Mancheño, M. J.; Sierra, M. A. *Acc. Chem. Res.* **2005**, *38*, 44.
6. del Amo, J. C.; Mancheño, M. J.; Gómez-Gallego, M.; Sierra, M. A. *Organometallics* **2004**, *23*, 5021.
7. Fernández, I.; Mancheño, M. J.; Vicente, R.; López, L. A.; Sierra, M. A. *Chem. Eur. J.* **2008**, *14*, 11222.
8. Fischer, E. O.; Kreiter, C. G.; Kollmeier, H. J.; Muller, J.; Fischer, R. D. *J. Organomet. Chem.* **1971**, *28*, 237.
9. Ritchie, C. D.; Sager, W. *Progr. Phys. Org. Chem* **1964**, *2*, 323-400.
10. (a) Leoni, P.; Landi, A.; Pasquali, M. *J. Organomet. Chem.* **1987**, *321*, 365-369. (b) Asdar, A.; Lapinte, C.; Toupet, L. *Organometallics* **1989**, *8*, 2708-2717.
11. Fischer, E. O.; Beck, H. J. *Chem. Ber.* **1971**, *104*, 3101-3107.
12. Norman, D. W.; Ferguson, M. J.; McDonald, R.; Stryker, J. M. *Organometallics* **2006**, *25*, 2705-2708.

13. (a) Albéniz, A. C.; Espinet, P.; Manrique, R.; Pérez-Mateo, A. *Angew. Chem. Int. Ed.* **2002**, *41*, 2363-2366. (b) Albeniz, A. C.; Espinet, P.; Manrique, R.; Pérez-Mateo, A. *Chem. Eur. J.* **2005**, *11*, 1565-1573. (c) Albéniz, A. C.; Espinet, P.; Pérez-Mateo, A.; Nova, A.; Ujaque, G. *Organometallics* **2006**, *25*, 1293-1297. (d) López-Alberca, M. P.; Mancheño, M. J.; Fernández, I.; Gómez-Gallego, M.; Sierra, M. A.; Torres, R. *Org. Lett.* **2007**, *9*, 1757-1759. (e) Meana, I.; Albéniz, A. C.; Espinet, P. *Organometallics* **2008**, *27*, 4193-4198. (f) Meana, I.; Toledo, A.; Albéniz, A. C.; Espinet, P. *Chem. Eur. J.* **2012**, *18*, 7658-7661.
14. (a) Portnoy, M.; Milstein, D. *Organometallics* **1993**, *12*, 1655-1664. (b) Moncarz, J. R.; Brunker, T. J.; Jewett, J. C.; Orchowski, M.; Glueck, D. S.; Sommer, R. D.; Lam, K.-C.; Incarvito, C. D.; Concolino, T. E.; Ceccarelli, C. *Organometallics* **2003**, *22*, 3205-3221. (c) Broadwood-Strong, G. T.; Chaloner, P. A.; Hitchcock, P. B. *Polyhedron* **1993**, *12*, 721-729.
15. Struchkov, Y. T.; Aleksandrov, G. G.; Pukhnarevich, V. B.; Sushchinskaya, S. P.; Voronkov, M. G. *J. Organomet. Chem.* **1979**, *172*, 269-272.
16. Werner, M.; Lis, T.; Bruhn, C.; Lindner, R.; Steinborn, D. *Organometallics* **2006**, *25*, 5946-5954.
17. (a) Anderson, G. K.; Cross, R. J.; Manojlović-Muir, L.; Muir, K. W.; Wales, R. A. *J. Chem. Soc., Dalton Trans.* **1979**, 684-689. (b) Clark, H.; Jain, V.; Rao, G. *J. Organomet. Chem.* **1983**, *259*, 275-282.
18. (a) Steinborn, D.; Gerisch, M.; Merzweiler, K.; Schenzel, K.; Pelz, K.; Bogel, H.; Magull, J. *Organometallics* **1996**, *15*, 2454. (b) Nordhoff, K.; Steinborn, D. *Organometallics* **2001**, *20*, 1408.
19. Schubert, U.; Fischer, E. O. *Chem. Ber.* **1973**, *106*, 1062.
20. A related pyridine(acyl)carbene platinum complex has been reported: Gosavi, T.; Wagner, C.; Merzweiler, K.; Schmidt, H.; Steinborn, D. *Organometallics* **2005**, *24*, 533.
21. ¹ (a) Werner, H.; Rascher, H. *Helv. Chim. Acta* **1968**, *51*, 1765. (b) Kreissl, F. R.; Kreiter, C. G.; Fischer, E. O. *Angew. Chem. Int. Ed.* **1972**, *11*, 643. (c) Kreissl, F. R.; Fischer, E. O.; Kreiter, C. G.; Fischer, H. *Chem. Ber.* **1973**, *106*, 1262. (d) Fischer, H. *J. Organomet. Chem.* **1979**, *170*, 309
22. Hoover, J. F.; Stryker, J. M. *J. Am. Chem. Soc.* **1990**, *112*, 464.
23. Espinet et al. have recently reported acyl-carbene coupling via migratory insertion on palladium complexes: Meana, I.; Albéniz, A. C.; Espinet, P. *Organometallics* **2012**, *31*, 5494-5499.

24. Rudler, H.; Audouin, M.; Parlier, A.; Martin-Vaca, B.; Goumont, R.; Durand-Réville, T.; Vaissermann, J. *J. Am. Chem. Soc.* **1996**, *118*, 12045.
25. Pangborn, A. B.; Giardello, M. A.; Grubbs, R. H.; Rosen, R. K.; Timmers, F. J. *Organometallics* **1996**, *15*, 1518-1520.
26. (a) Connor, J. A.; Day, J. P.; Turner, R. M. *J. Chem. Soc., Dalton Trans.* **1976**, 283. (b) Merz, A.; Tomahogh, R., *J. Chem. Res., Synop.* **1977**, *11*, 273.
27. MacDougall, J. J.; Nelson, J. H.; Mathey, F. *Inorg. Chem.* **1982**, *21*, 2145.

Chapter 3

Synthesis and Polymerization Behavior of Asymmetric Group 4 Post-Metallocene Catalysts

Adapted in part from:

Klet, R. C.; VanderVelde, D. G.; Labinger, J. A.; Bercaw, J. E. *Chem. Commun.*, **2012**, *48*, 6657–6659.

<http://dx.doi.org/10.1039/c2cc32806b>

© The Royal Society of Chemistry 2012

Chapter 3

Introduction

Polyolefins constitute one of the most important classes of commercial synthetic polymers, with annual worldwide capacity greater than 70 billion kg.¹ Since the discovery of Ziegler-Natta catalysts in the 1950s,² α -olefin polymerization has been one of the most widely studied catalytic organometallic reactions. The past three decades have seen the development of soluble single-site olefin polymerization catalysts that span the transition metal series and allow access to previously unrealized polymer architectures.³ The development of metallocene catalysts in the 1980s led to significant advances in our understanding of how catalyst structure affects the polymer microstructure.⁴ Groundbreaking studies by Brintzinger, Bercaw and others revealed a direct correlation between metallocene catalyst symmetry and polymer tacticity; in general, C_2 - and C_1 -symmetric complexes produce isotactic polymers, C_s -symmetric catalysts lead to syndiotactic polymers, and C_{2v} -symmetric catalysts yield stereoirregular polymers.⁴ More recently, “post-metallocene” olefin polymerization catalysts have emerged and have led to significant innovations in living polymerization⁵ and the preparation of olefin block copolymers.⁶ Our ability to develop new catalysts that produce specific polymer architectures will rely on continuing research efforts to understand and progress post-metallocene polymerization catalysts.

Our group has recently developed olefin polymerization catalysts based on early transition metals supported by symmetric, triaryl, dianionic (XLX) ligands as part of a program for developing new post-metallocene catalysts for olefin polymerization. The ligand design includes thermally robust aryl–aryl linkages, as well as versatile access to a wide variety of ligand scaffolds using cross-coupling chemistry. Additionally, these ligands can adopt various geometries when coordinated to a metal, including C_2 and C_{2v} , which suggested the possibility of stereoselective polymerization, based on precedents with metallocene polymerization catalysts (Figure 3.1).

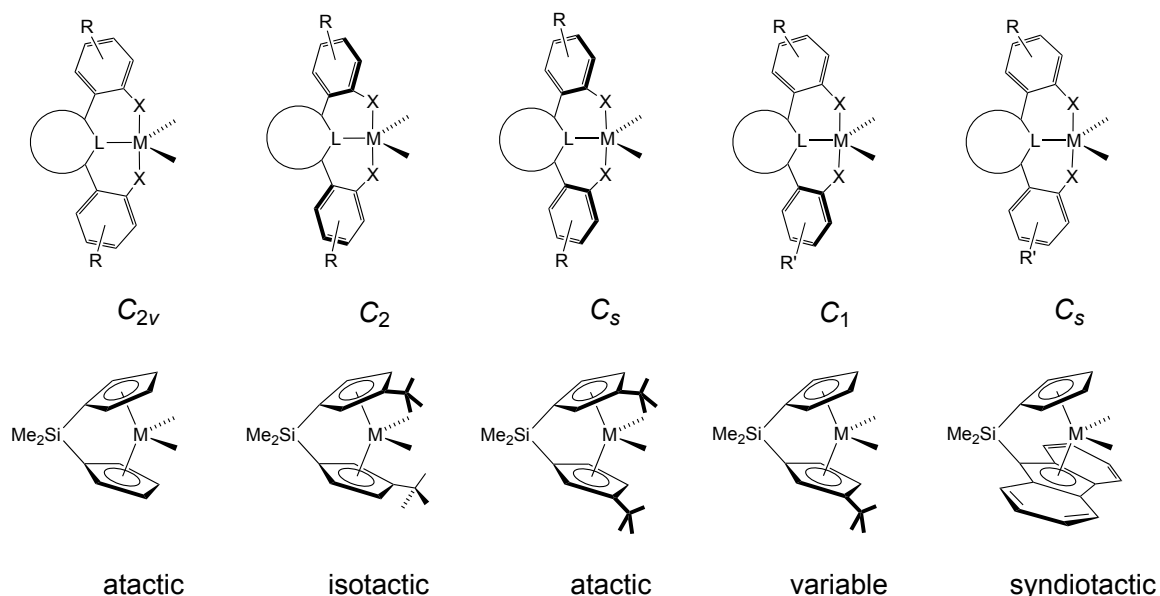
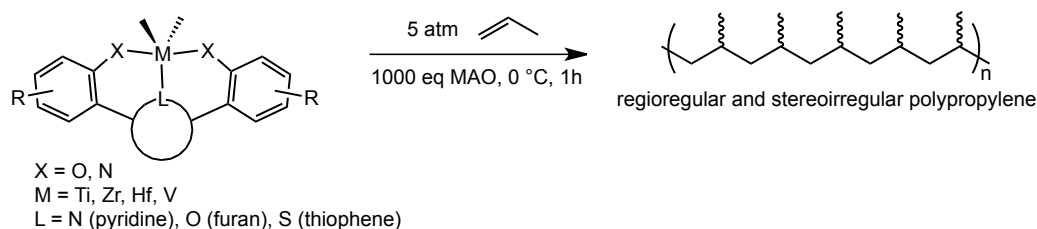


Figure 3.1 Comparison of potential geometries of metal complexes with triaryl dianionic ligands and metallocene catalysts and polymer tacticity.

We have reported a series of heterocycle-linked bis(phenolate) ligands, where the heterocycle is pyridine (ONO), furan (OOO), or thiophene (OSO), which upon complexation with titanium, zirconium, hafnium, and vanadium can give propylene polymerization precatalysts that exhibit good to excellent activities

upon activation with methylaluminoxane (MAO).⁷ (We have also reported bis(anilide)pyridyl ligands (NNN),⁸ but their group 4 metal complexes exhibit poor activity for polymerization.) Despite the promising polymerization activity of these catalysts, we have thus far observed disappointing stereocontrol; we have generally produced stereoirregular polypropylene (Scheme 3.1).



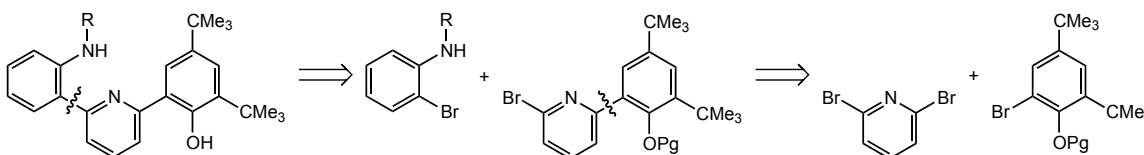
Scheme 3.1 Propylene polymerization with post-metallocene complexes of triaryl dianionic ligands.

Results and Discussion

NNO Ligand: Design and Synthesis

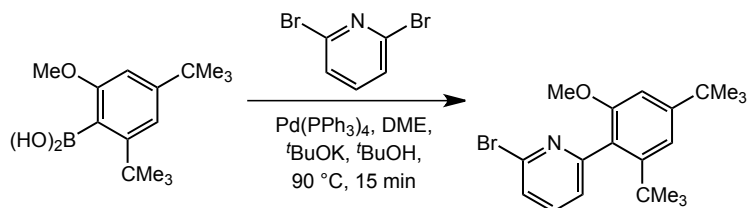
In order to further our understanding of the fundamental processes governing stereocontrol in these post-metallocene complexes, we decided to examine the effect of an asymmetric ligand. As a first target, we designed an anilide(pyridine)phenoxide (NNO) ligand. The modular design of the NNO ligand allows for facile variation of substituents using cross-coupling reactions, including access to enantiopure catalysts (which can be difficult to access with metallocene frameworks) for potential asymmetric applications by incorporation of a chiral group into the ligand. For our first asymmetric NNO ligand, we selected a ligand containing a chiral (1-phenylethyl)amine group.

The synthesis of the ligand was envisioned through a series of cross coupling reactions (Scheme 3.2). We planned for a common intermediate (pyridine-phenoxide) in the ligand design that we could couple with different anilines to give access to various frameworks through systematic changes.



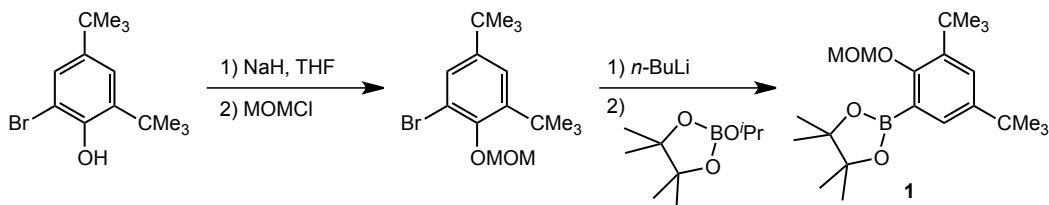
Scheme 3.2 Retrosynthetic scheme for anilide(pyridine)phenoxide ligands.

The first obstacle in our synthesis was to find a methodology for selective monoarylation of 2,6-dibromopyridine. Although the asymmetrically substituted 2-bromo-6-iodopyridine is commercially available, it is prohibitively expensive, especially compared to 2,6-dibromopyridine: Alfa Aesar lists 2-bromo-6-iodopyridine at \$544/5g (~\$109/1g),⁹ while 2,6-dibromopyridine is \$50/25g (\$2/1g).¹⁰ 2-bromo-6-chloropyridine, a less desirable substrate for cross coupling, is even more costly: \$278/1g.¹¹ The synthesis of 2-bromo-6-iodopyridine is also non trivial, with most reported syntheses suffering from low yield and poor regioselectivity.¹² We were encouraged, however, by a report from Chan and co-workers that described monoarylation of 2,6-dibromopyridine with a protected phenol substrate using a Suzuki coupling (Scheme 3.3).¹³ Based on this report, we predicted that conditions to achieve monoarylation of 2,6-dibromopyridine with our substrate could be discovered.



Scheme 3.3 Literature precedent for monoarylation of 2,6-dibromopyridine using a Suzuki coupling. (Adapted from ref. 14).

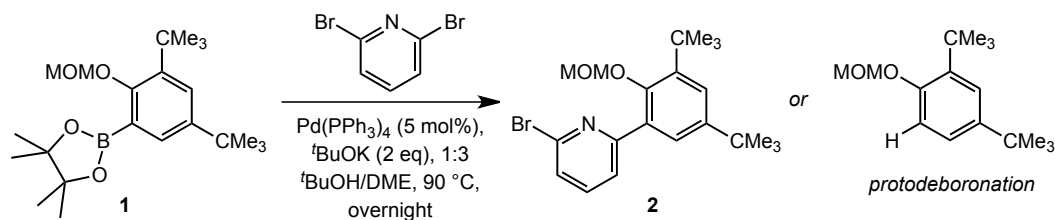
As a first step, we needed to synthesize the boronic ester coupling partner of 2,6-dibromopyridine: (3,5-di-*t*-butyl-2-(methoxymethoxy)phenyl)pinacolborane. Deprotonation of commercially available 2-bromo-4,6-di-*t*-butylphenol with NaH, followed by treatment with chloromethyl methyl ether (MOMCl) led to the MOM-protected bromo-phenol intermediate.¹⁴ Lithium halogen exchange of this intermediate with *n*-butyl lithium, followed by reaction with 2-isopropoxy-4,4,5,5-tetramethyl-1,3,2-dioxaborolane yielded the desired boronic ester **1** in good yield after recrystallization from hot methanol (Scheme 3.4).



Scheme 3.4 Synthesis of boronic ester **1**.

Initial small-scale reactions of **1** with 2,6-dibromopyridine following the Suzuki coupling reaction conditions employed by Chan et al. (cat.: 5 mol % Pd(PPh₃)₄, base: 2 equiv KO^{*t*}Bu, solvent: DME/^{*t*}BuOH 3:1; DME = dimethoxymethane)¹³ yielded the desired monoarylated pyridine intermediate **2** in acceptable yields. Repeated reactions and attempts to scale the coupling reaction up, however, revealed very inconsistent and unpredictable yields, with

some reactions resulting in exclusive formation of the protodeboronated product of the boronic ester **1** and no pyridine-phenoxide coupled product **2** (Scheme 3.5).



Scheme 3.5 Suzuki coupling **1** and 2,6-dibromopyridine led to inconsistent product formation with complete conversion of **1** to the protodeboronated product without any formation of **2** occurring in many instances.

Despite careful investigation of each component of the reaction, we were ultimately unable to determine what led to protodeboronation over C–C bond formation (Table 3.1). One potential culprit could be the solvent DME, as DME is prone to develop peroxides over time, which could react unfavorably with the Pd(0) catalyst; however, we still observed significant protodeboronation when using a brand new bottle of DME, DME passed through alumina prior to use (to remove peroxide impurities), and DME collected from drying columns and kept 100% air-free. We also considered that water or protic solvents, although commonly employed in Suzuki reactions, could facilitate protodeboronation. Ultimately, after screening many reaction conditions, we found that non-aqueous conditions with Pd(PPh₃)₄, K₃PO₄, and toluene gave consistent yields for the coupled product **2** with no protodeboronated product observed to form in the reaction (Table 3.1). The bis-arylated pyridine product **3** was observed to form in small quantities under these reaction conditions; however, it could mostly be separated from the monoarylated product **2** via column chromatography.

Alternatively, we later discovered that this minor impurity could be carried on and easily separated in later synthetic steps without affecting product yields. Finally, achieving monoarylation under our optimized conditions requires long reaction times of nearly 7 d; employing a more efficient catalyst, such as Pd₂(dba)₃/SPhos (dba = dibenzylideneacetone, SPhos = 2-dicyclohexylphosphino-2',6'-dimethoxybiphenyl), results in faster reaction times, but exclusive formation of the bis-arylated product **3** without formation of any monoarylated product **2**.

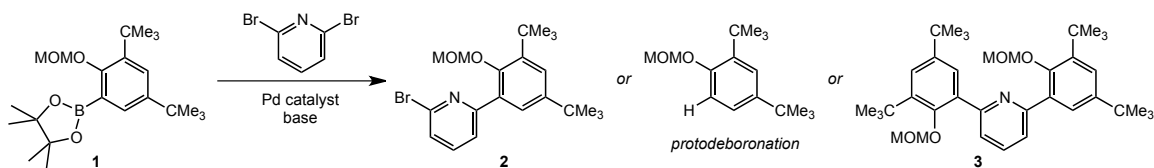
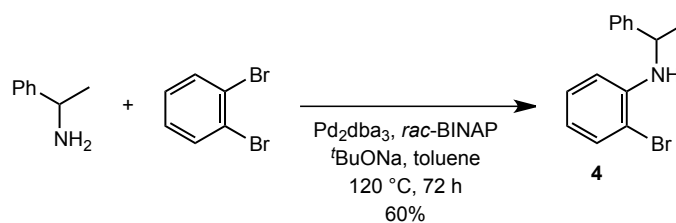


Table 3.1 Conditions screened for Suzuki coupling to achieve monoarylation of 2,6-dibromopyridine.

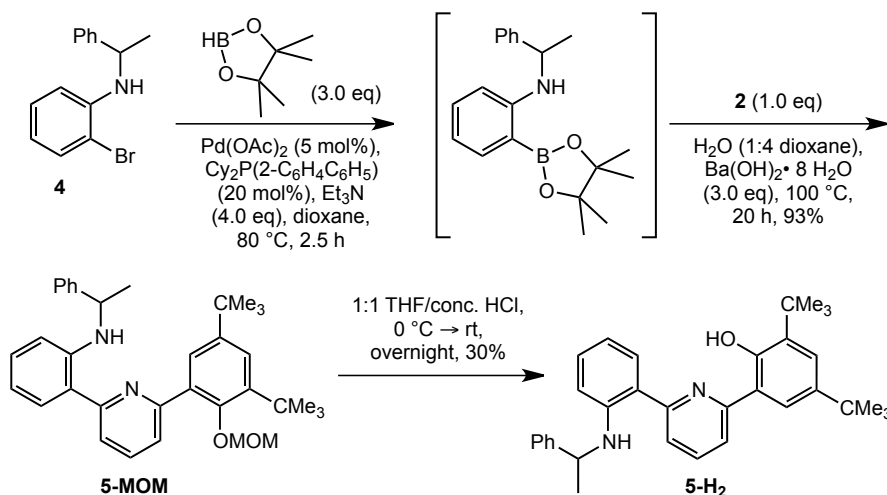
Catalyst	Base	Solvent	% Yield of 2	% Yield of proto-deboronated	% Yield of 3	Scale	Comments
Pd(PPh ₃) ₄	KO ^t Bu	DME/BuOH (3:1)	57	43	0	0.500 g	
Pd(PPh ₃) ₄	KO ^t Bu	DME/BuOH (3:1)	0	100	0	1.5 g	
Pd(PPh ₃) ₄	KO ^t Bu	DME/BuOH (3:1)	0	100	0	100 mg	
Pd(PPh ₃) ₄	KO ^t Bu	DME/BuOH (3:1)	40	13	47	100 mg	DME through alumina to remove peroxides
Pd(PPh ₃) ₄	KO ^t Bu	DME/BuOH (3:1)	0	100	0	2 g	DME through alumina to remove peroxides
Pd(PPh ₃) ₄	KO ^t Bu	DME/BuOH (3:1)	0	100	0	200 mg	DME from columns
Pd(PPh ₃) ₄	KO ^t Bu	dioxane/BuOH (3:1)	69	6	25	50 mg	Dioxane dried over mol sieves
Pd(PPh ₃) ₄	KO ^t Bu	dioxane/BuOH (3:1)	0	100	0	250 mg	
Pd(PPh ₃) ₄	KO ^t Bu	toluene/BuOH (3:1)	68	21	11	50 mg	Toluene from columns
Pd(PPh ₃) ₄	KO ^t Bu	toluene/BuOH (3:1)	0	100	0	250 mg	
Pd(OAc) ₂ /SPhos	K ₃ PO ₄	toluene	0	69	31	50 mg	SPhos added
Pd ₂ (dba) ₃ /SPhos	K ₃ PO ₄	toluene	0	0	100	50 mg	
Pd(PPh ₃) ₄	K ₃ PO ₄	toluene	84	0	16	50 mg	Very slow (5 d v. overnight)

Synthesis of the anilide portion of the ligand was significantly more straightforward than monoarylation of 2,6-dibromopyridine. Chiral 2-bromo-N-(1-phenylethyl)aniline **4** was prepared according to a reported synthesis utilizing a Buchwald-Hartwig coupling (Scheme 3.6).¹⁵ **4** was then coupled to **2** with a Suzuki coupling using a modified literature procedure reported for coupling pyridines and anilines.¹⁶ Finally, deprotection with acidic THF afforded the

desired asymmetric NNO ligand **5** (Scheme 3.7).



Scheme 3.6 Buchwald-Hartwig coupling to yield 2-bromo-N-(1-phenylethyl)aniline **4**.

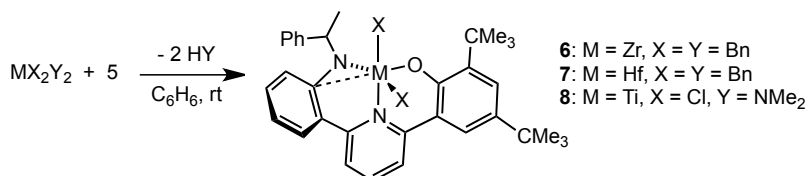


Scheme 3.7 Synthesis of ligand **5** from coupling **4** and **2**.

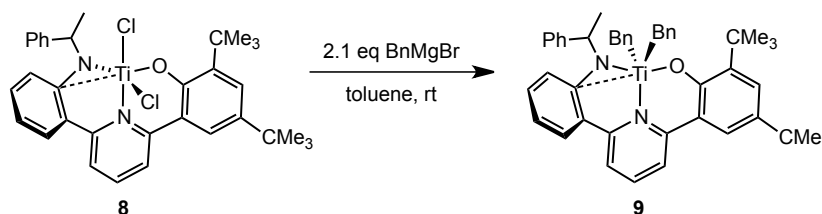
NNO Ligand: Metalation

Metalation of NNO ligand **5** was achieved by protonolysis of suitable group **4** starting materials. Reaction of **5** with tetrabenzylzirconium and tetrabenzylhafnium gave (NNO)ZrBn₂ **6** and (NNO)HfBn₂ **7**, respectively. The analogous reaction of **5** with tetrabenzyltitanium led to an inseparable mixture; however, reaction of **2** with TiCl₂(NMe₂)₂ yielded a related titanium complex, (NNO)TiCl₂ **8** (Scheme 3.8). **8** could be converted into (NNO)TiBn₂ **9** by treating **8** with 2.1 equiv of BnMgCl; however, we found that working with (NNO)TiCl₂ was sufficient

for our purposes, and, in fact, easier to purify compared to the highly soluble dibenzyl species (Scheme 3.9).



Scheme 3.8 Synthesis of anilide(pyridine)phenoxide Zr, Hf, and Ti complexes.



Scheme 3.9 Synthesis of (NNO)TiBn₂ complex **9** from (NNO)TiCl₂ complex **8**.

The ¹H NMR spectrum of the Ti complex **8** gives sharp signals at room temperature; in contrast, the resonances of the Zr complex **6** are broad at room temperature, suggestive of fluxional behavior on the NMR time scale. Upon lowering the temperature to −30 °C, the resonances for **6** were observed to sharpen and give the expected number of peaks for the complex **6** (Figure 3.2). As expected, increasing the temperature above room temperature led to further broadening of the resonances for **6**. Surprisingly, the benzylic protons (4 doublets integrating to 1H each for the C₁ symmetric complex **6**) broadened at different rates; in particular, one benzylic proton remained a sharp doublet, while the three other benzylic protons broadened. This behavior is especially unexpected for protons on the same carbon, which would be predicted to have the same temperature dependent fluxionality. Additionally, the temperature dependence of the chemical shifts of the two sets of benzylic protons is different, with the more

downfield set of benzylic protons shifting approximately 0.5 ppm over a 130 degree temperature range, while the more upfield protons shift only about 0.25 ppm over the same temperature range (Figure 3.3). Unfortunately, we do not have a good explanation for this observed fluxionality at this time, but notably, a large temperature dependence on Zr benzylic protons has been observed previously.¹⁷

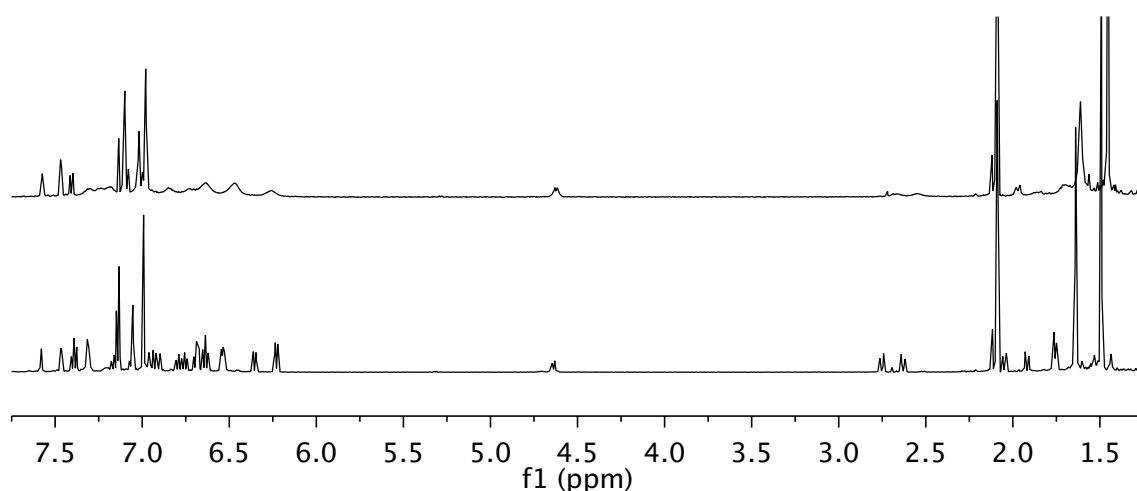


Figure 3.2 ^1H NMR spectra of **6** at 25 °C (top) and -30 °C (bottom) in toluene- d_8 .

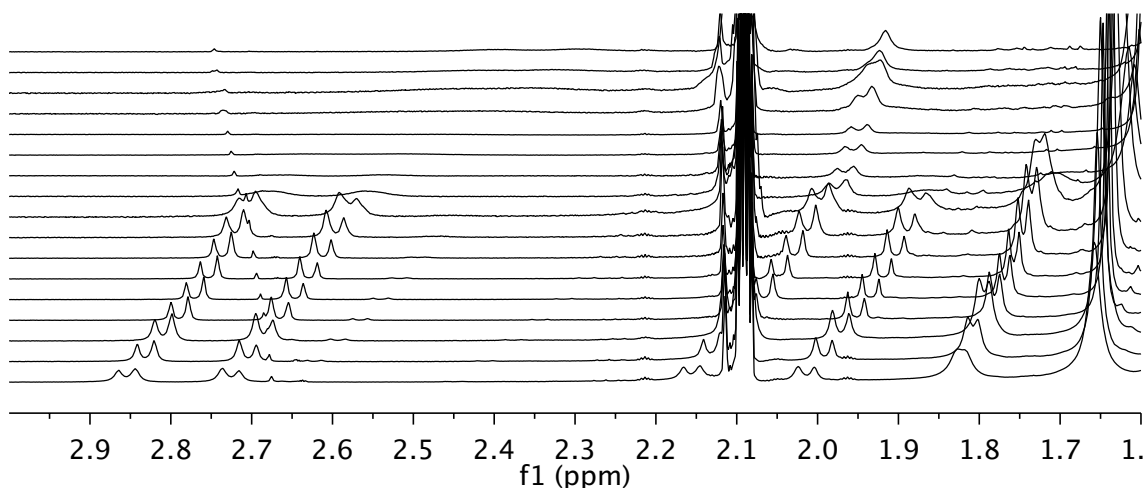


Figure 3.3 Close-up of Zr-benzylic proton resonances of **6** in ^1H NMR spectra from -80 °C to 90 °C in toluene- d_8 (temperature increases up y-axis).

Crystals of **8** suitable for X-ray diffraction were grown by slow vapor diffusion of pentane into a concentrated ether/dichloromethane solution; the X-ray structure reveals distorted trigonal bipyramidal geometry about titanium (Fig 3.4). The bond lengths and angles for **8** are similar to other five-coordinate Ti(IV) complexes.^{7a,18} Notably, the Ti(1)–C(1)_{ipso} distance is quite contracted at 2.61 Å, with a Ti(1)–N(1)–C(1)_{ipso} angle of 104.05°, suggestive of an *ipso* interaction, which may help stabilize the highly electrophilic Ti center. We have observed a similar *ipso* interaction in a related anilide-containing metal complex (NNN)TiCl₂.⁸

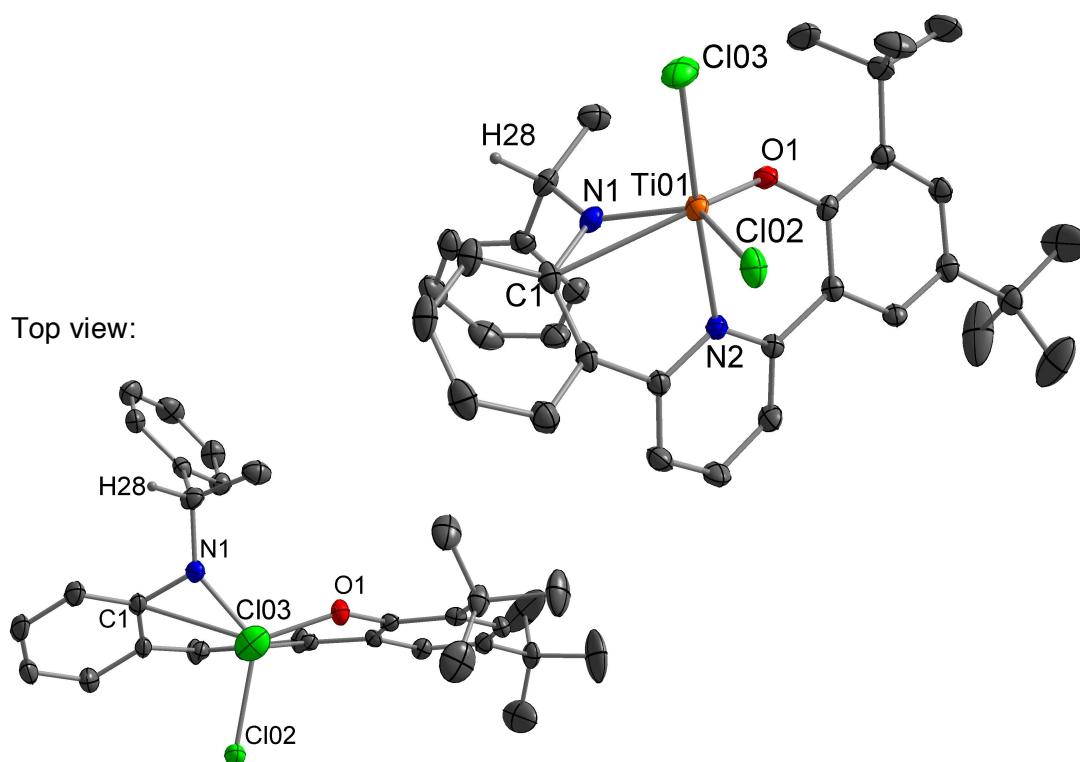
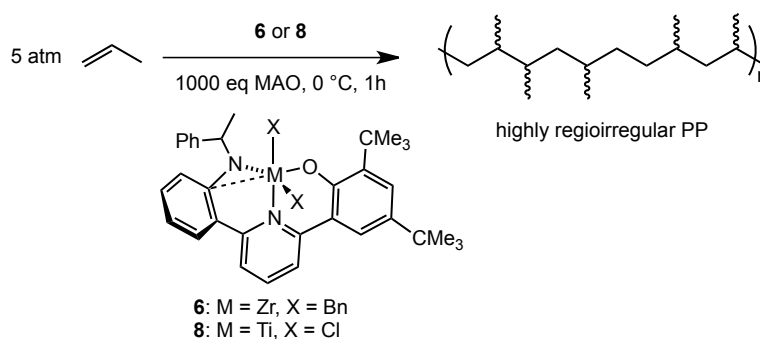


Figure 3.4 Probability ellipsoid diagram (50%) of the X-ray structure **8**. Selected bond lengths (Å) and angles (°): Ti(1)–O(1) = 1.8040(17), Ti(1)–N(1) = 1.879(2), Ti(1)–N(2) = 2.153(2), Ti(1)–Cl(2) = 2.3161(8), Ti(1)–Cl(3) = 2.3285(8), Ti(1)–C(1) = 2.609(2); O(1)–Ti(1)–N(1) = 110.87(8), O(1)–Ti(1)–Cl(2) = 118.49(6), N(1)–Ti(1)–Cl(2) = 127.68(7), Cl(3)–Ti(1)–N(2) = 175.84(6), C(1)–N(1)–Ti(1) = 104.05(15).

NNO Complexes: Polymerization Behavior

Activation of complexes **6** and **8** in toluene or chlorobenzene solution, respectively, resulted in formation of polypropylene (PP) under 5 atm propylene at 0 °C (Scheme 3.10). Somewhat surprisingly, the Hf analogue **7** showed no activity under these conditions; Hf is the most active group 4 metal for some types of post-metallocene catalysts.¹⁹ The PP obtained from both **6** and **8** was a solid, nonsticky, elastomeric polymer.



Scheme 3.10 Polymerization of propylene with complex **6** or **8**.

The activity of **6** was 1.7×10^4 g PP (mol cat)⁻¹ h⁻¹, while the Ti complex **8** was approximately an order of magnitude more active, at 1.5×10^5 g PP (mol cat)⁻¹ h⁻¹. The activity of **8** remains the same after 3 h as after 30 min at 0 °C, suggesting that the active species is relatively stable under polymerization conditions.

Gel permeation chromatograms (GPC) on the polymers obtained from **6** and **8** show narrow molecular weight distributions, with M_w/M_n of 1.8 and 1.5, respectively, suggesting catalysis occurs at a single site. The M_n values are higher for **8** than **6**: 147,000 and 26,000 g/mol, respectively. Thus with this ligand framework, Ti gives a better polymerization catalyst than Zr, in terms of activity

and polymer molecular weight (Table 3.2, below). The polymers from **6** and **8** were not observed to have melting points (T_m), but the glass transition temperatures (T_g) of the polymers were determined to be -8.8 °C and -14.4 °C, respectively, which is approximately the expected T_g of stereoirregular PP.²⁰

^{13}C NMR spectroscopy was carried out to determine whether these C_1 -symmetric precatalysts led to any degree of stereocontrol. Unexpectedly, we instead found that these catalysts make PP with low regio- and stereocontrol. The ^{13}C NMR spectra of polypropylene obtained from **6** and **8** reveal a large number of 2,1-insertions; as many as *30-40% of insertions may be inverted* (Figure 3.5). In contrast, primarily regioregular (and stereoirregular) polypropylene was obtained using the related bis(phenoxide)pyridyl (ONO) and bis(anilide)pyridyl (NNN) complexes previously reported by our group.^{7,8}

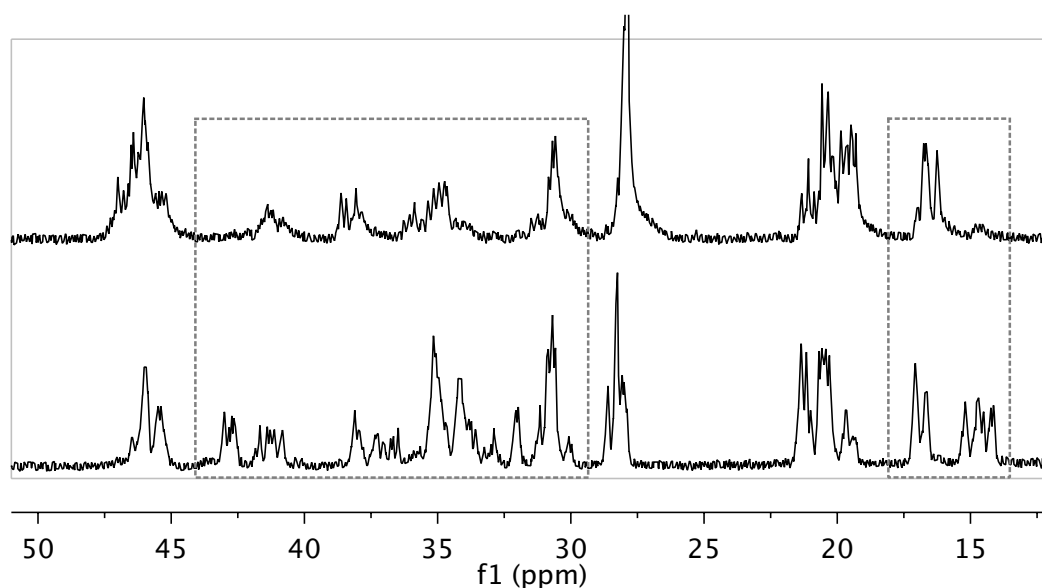
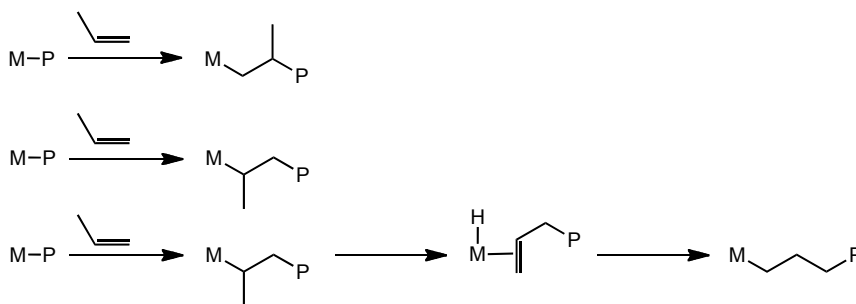


Figure 3.5 ^{13}C NMR spectra of PP from **6** (top) and **8** (bottom) at 120 °C in $\text{TCE-}d_2$. Regions indicating 2,1-insertions are highlighted.

We also sought to determine the presence of “3,1-insertions” — $-(CH_2)_3-$ groupings — which can result from β -hydride elimination and re-insertion in the opposite sense following a 2,1-insertion (Scheme 3.11). Such a process would result in an excess of methylene groups; in its absence the ratio of $CH:CH_2:CH_3$ groups would be 1:1:1. ^{13}C NMR spectroscopy alone is not able to determine the ratio, as the regions containing the signals for methine and methylene carbons are known to overlap; the methyl carbons are well separated and upfield of both methine and methylene carbons (see Appendix B for detailed ^{13}C NMR assignments of PP).²¹ We performed 2D 1H - ^{13}C HSQC NMR spectroscopy on the PP obtained from **6** and **8**; such experiments determine the proton connectivity of each ^{13}C signal, as well as the 1H chemical shift of the associated protons. Although the methine and methylene signals do indeed overlap in the ^{13}C NMR spectra, all three types (CH , CH_2 and CH_3) are sufficiently separated in the 1H NMR spectra to allow their relative abundance to be determined by integration. In fact, we observe a 1:1:1 ratio for $CH:CH_2:CH_3$, which suggests that there is little or no 3,1-insertion, only 1,2- and 2,1-, during propylene polymerization (Figure 3.6).



Scheme 3.11 Propylene insertion modes: 1,2-insertion (top), 2,1-insertion (middle), 3,1-insertion (bottom).

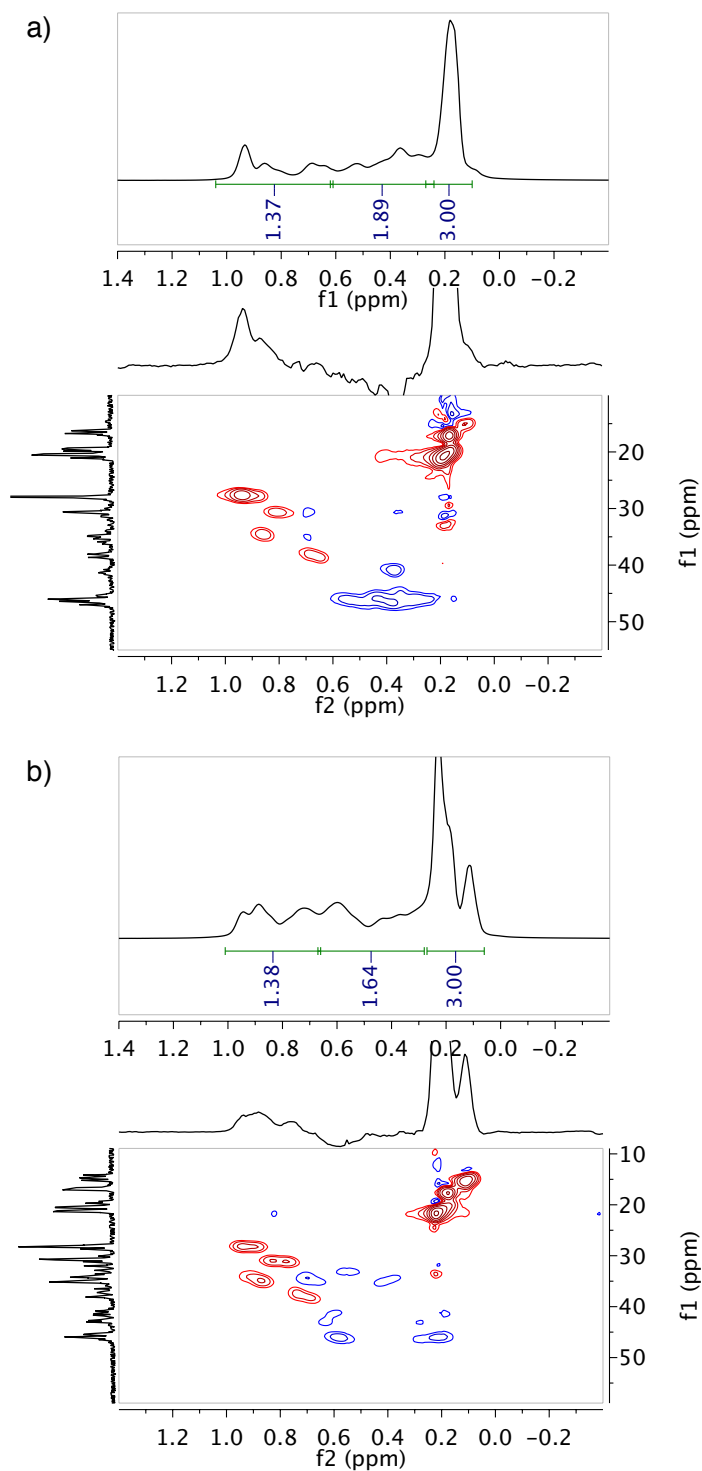


Figure 3.6 ^1H NMR and 2D ^1H - ^{13}C HSQC NMR spectra for PP from **6** (a) and **8** (b). Red or positive peaks indicate odd numbers of protons on carbon, and blue or negative peaks indicate even numbers of protons on carbon.

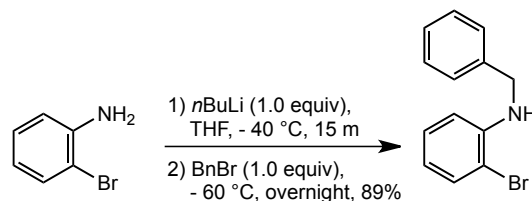
For early transition metal metallocene catalysts 1,2-insertion is typically

avored by both electronic and steric factors; competing 2,1-insertion is usually quite rare, on the order of <1 mol%.²² There are examples of post-metallocene catalysts that appear to propagate exclusively via a 2,1-insertion mechanism,²³ but to the best of our knowledge, this is the only early metal catalyst that shows so little apparent preference for 1,2- vs. 2,1-insertions;²⁴ such low regiocontrol is more commonly observed with late metal polymerization catalysts that can undergo “chain running” and incorporate 3,1-insertions.²⁵ A half-metallocene system has been reported that incorporates 2,1-insertions on the order of 10% at 25 °C, but the percentage decreased at lower temperatures – our polymerizations are run at 0 °C. The relative steric openness of the half-metallocene system was offered as a possible explanation for the higher frequency of inversion relative to metallocene polymerization catalysts.²⁶ In our case, the (NNO) catalysts **6** and **8** are sterically very similar to their symmetric (ONO) and (NNN) analogues, which exhibit no such regioirregularity,^{7,8} suggesting that some factor other than simple sterics may control regioselectivity in these post-metallocene polymerization catalysts.

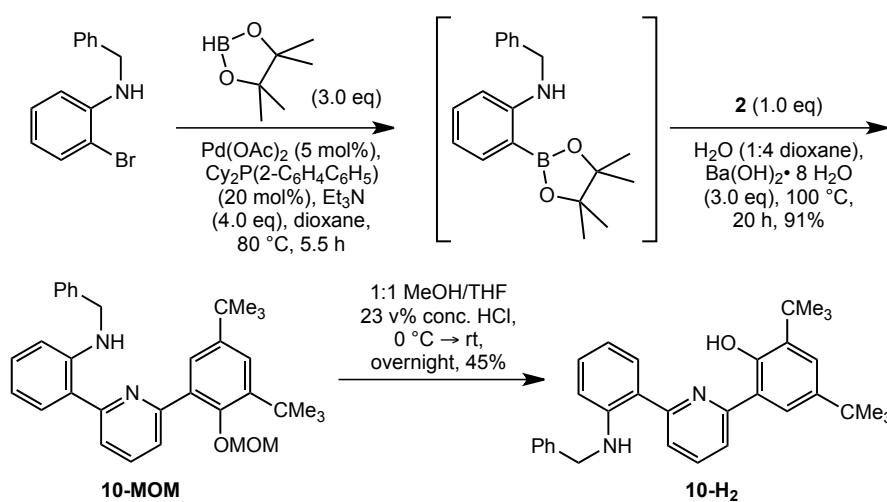
Modification of the Amine R-group: ^RNNO Ligand Synthesis

The initial ligand design **5** included a chiral 1-phenylethyl group on the anilide arm resulting in a C_1 -symmetric ligand and precatalyst. The NNO ligand was designed to be easily variable at the anilide R-group, and given the proximity of this group to the metal center, it was expected to have some influence on

incoming monomers. We reasoned one potential source of regioerrors could be the chiral group on the ligand arm. To probe the effect of this group on regiocontrol, we sought to make C_s -symmetric ligands. Ligands **10** and **11**, with benzyl and adamantyl groups, respectively, were synthesized using synthetic procedures similar to that reported for the synthesis of **5**. *N*-benzyl-2-bromoaniline was synthesized following the procedure of Glorius et al., by treating 2-bromoaniline with *n*-butyl lithium then benzyl bromide (Scheme 3.12).²⁷ This aniline could then be coupled to **2** with a Suzuki coupling using the same procedures employed for the synthesis of **5**. Deprotection with an acidic THF/MeOH solution led to the benzyl-substituted NNO ligand **10** (Scheme 3.13).

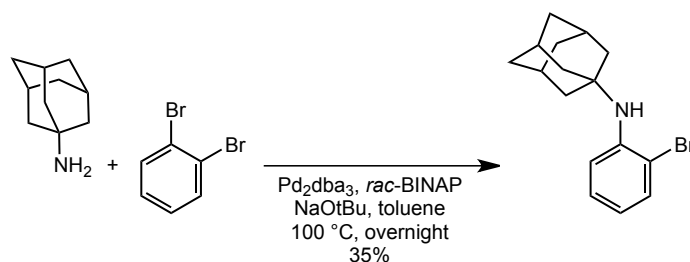


Scheme 3.12 Synthesis of *N*-benzyl-2-bromoaniline.

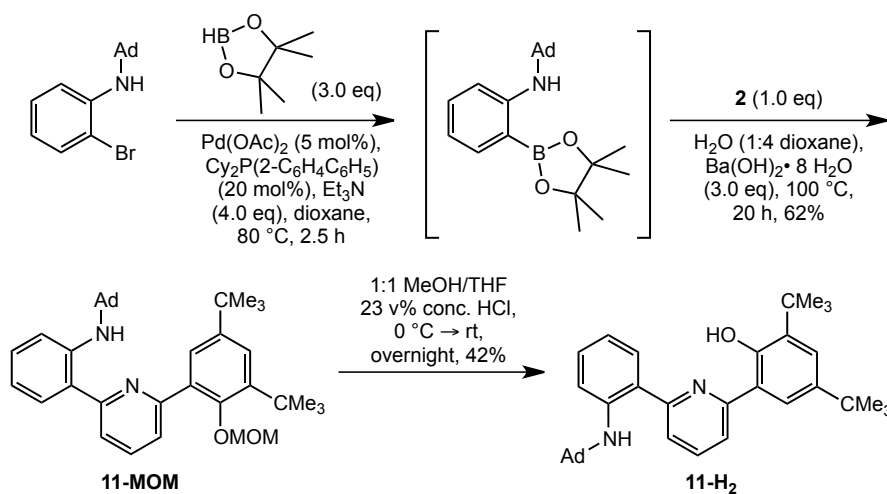


Scheme 3.13 Synthesis of ligand **10** from *N*-benzyl-2-bromoaniline.

A Buchwald-Hartwig coupling was used to access *N*-adamant-1-yl-2-bromoaniline from 1-adamantylamine and 1,2-dibromobenzene (Scheme 3.14).²⁸ Coupling this aniline with **2** via a Suzuki reaction, followed by deprotection of the MOM group with an acidic THF/MeOH solution led to the adamantyl-substituted NNO ligand **11** (Scheme 3.15).



Scheme 3.14 Synthesis of *N*-adamant-1-yl-2-bromoaniline via a Buchwald-Hartwig reaction.

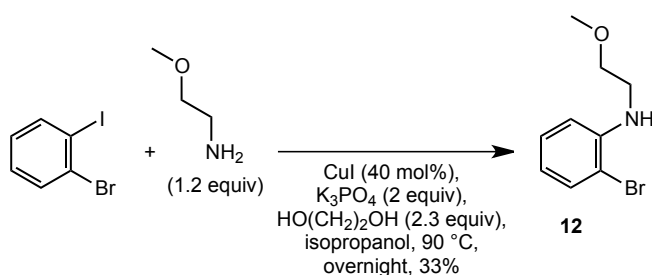


Scheme 3.15 Synthesis of ligand **11** from *N*-adamant-1-yl-2-bromoaniline.

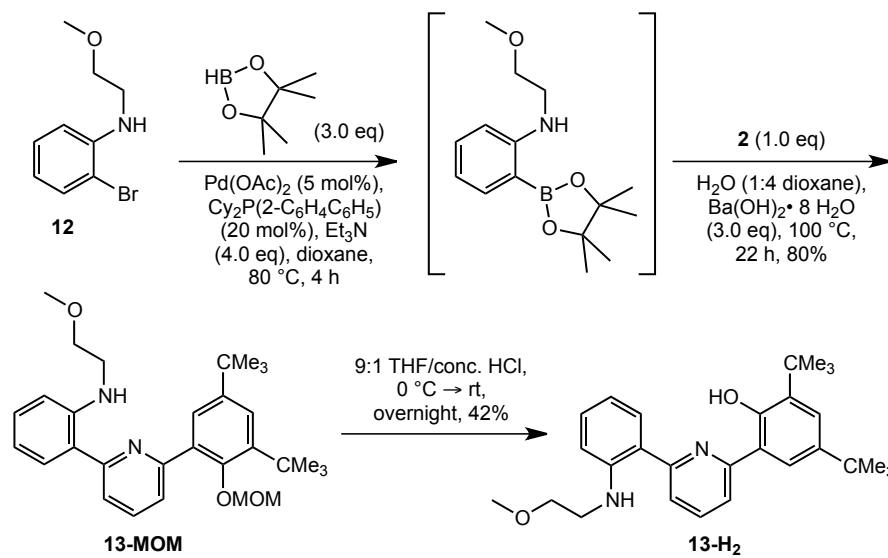
In addition to ligands **10** and **11**, we sought to make a new L_2X_2 ligand based on the success of polymerization catalysts pioneered by Mosche Kol and co-workers. Kol has developed post-metallocene polymerization catalysts based on Ti and Zr supported by amine bis(phenolate) and diamine bis(phenolate) ligands. These precatalysts, upon activation with $\text{B}(\text{C}_6\text{F}_5)_3$, polymerize 1-hexene

with excellent activities²⁹ and can produce high molecular weight stereocontrolled poly-1-hexene.³⁰ For some catalysts, living polymerization was achieved.³¹ In any case, all of the ligands employed were tetradentate L_2X_2 . This led us to hypothesize that perhaps increasing the coordination number of our ligands (from XLX to L_2X_2) would lead to more stable and more active polymerization catalysts. We saw an opportunity to test this hypothesis with the NNO ligands since this ligand could be easily modified to include a pendant L-donor on the anilide arm.

Our target for an L_2X_2 ligand was methoxyethyl-NNO with a pendant methoxy group. The substituted aniline precursor 2-bromo-*N*-methoxyethylaniline **12** was synthesized using a Cu-catalyzed Goldberg-modified Ullman reaction to couple 1-bromo-2-iodobenzene and 2-methoxyethylamine by adapting a procedure reported by Buchwald et al. (Scheme 3.16).³² Suzuki coupling with **2** and deprotection following our standard conditions led to the methoxyethyl-NNO ligand **13** (Scheme 3.17).



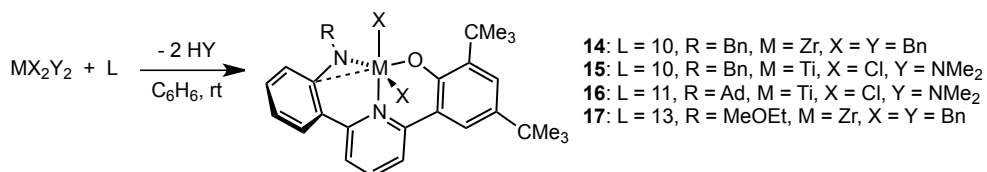
Scheme 3.16. Synthesis of 2-bromo-*N*-methoxyethylaniline via a Goldberg-modified Ullman reaction.



Scheme 3.17 Synthesis of ligand **13** from **12**.

*R*NNO Ligands: Metalation

Metalation of the NNO variant ligands **10**, **11** and **13** was achieved through either protonolysis with tetrabenzylzirconium or reaction with $\text{TiCl}_2(\text{NMe}_2)_2$ to yield $(\mathbf{10})\text{ZrBn}_2$ **14**, $(\mathbf{10})\text{TiCl}_2$ **15**, $(\mathbf{11})\text{TiCl}_2$ **16** and $(\mathbf{13})\text{ZrBn}_2$ **17** (Scheme 3.18). As Hf complexes did not produce polymer in our initial report, we did not pursue any Hf complexes for the new ligands.



Scheme 3.18 Synthesis of metal complexes **14-17**.

Notably, unlike the Zr dibenzyl complex with the 1-phenylethyl NNO ligand **5** (**6**), the Zr dibenzyl complex with the benzyl ligand **10** (**14**) has sharp resonances in the ^1H NMR spectrum at room temperature (Figure 3.7).

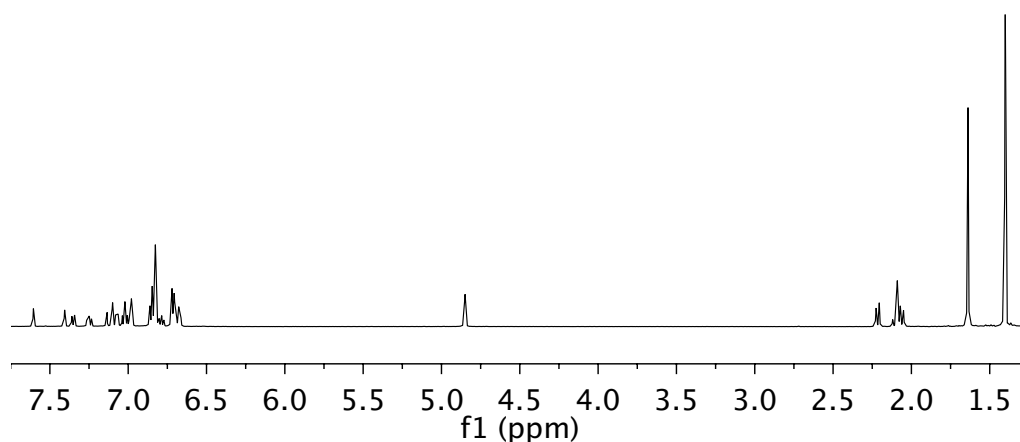


Figure 3.7 Room temperature ^1H NMR spectrum of Zr complex **14** in toluene- d_8 .

Crystals of **14** suitable for X-Ray diffraction were grown from a concentrated pentane solution at 35 °C (Figure 3.8). The crystal structure of **14** is similar to the structure of (5)TiCl₂ **8**. Both complexes have distorted trigonal bipyramidal geometry and the anilide arm is noticeably distorted out of the O–N(pyridine)–M plane. In the case of **8**, the anilide and phenoxide arms of the meridional ligand **5** coordinate in the equatorial plane to put the most π -donating ligand (Cl) in the axial position to maximize the potential for π -donation. In contrast, **14** has the anilide and phenoxide arms in axial positions, since the other ancillary ligands (benzyl groups) cannot participate in π -bonding (Figure 3.9).

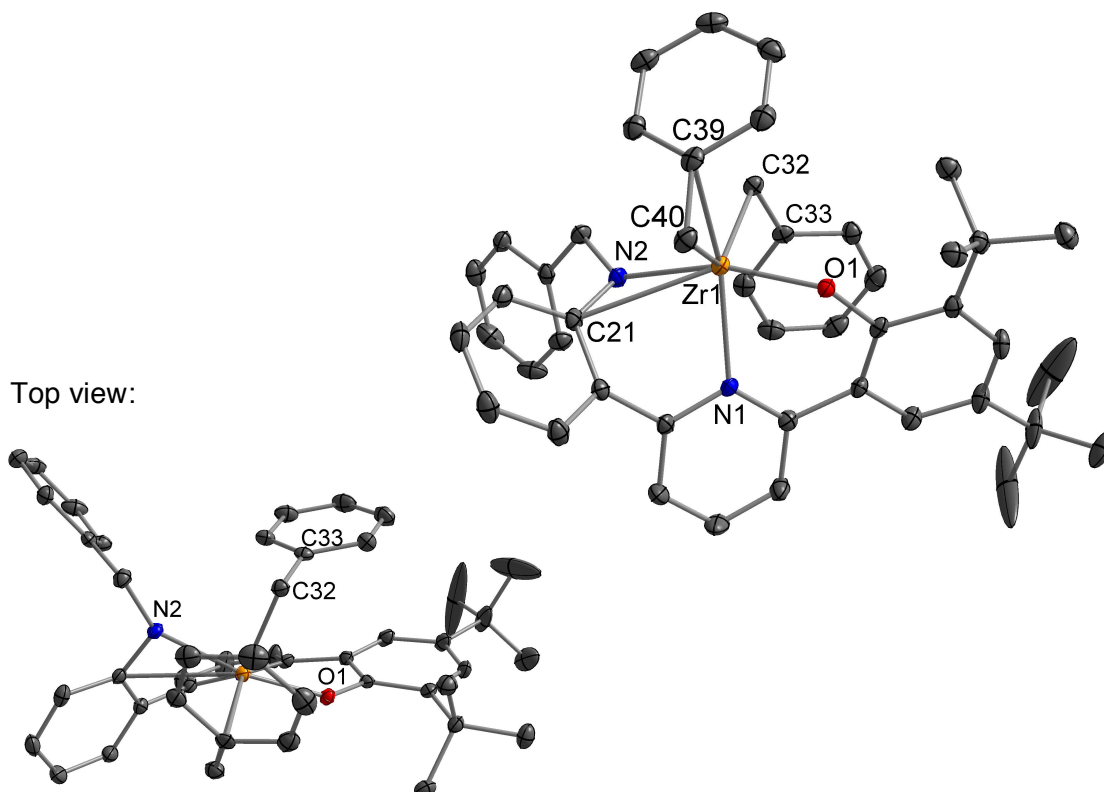


Figure 3.8 Probability ellipsoid diagram (50%) of the X-ray structure **14**. Selected bond lengths (Å) and angles (°): Zr(1)–O(1) = 1.9917(7), Zr(1)–N(1) = 2.2911(2), Zr(1)–N(2) = 2.1482(8), Zr(1)–C(21) = 2.8470(9), Zr(1)–C(40) = 2.2913(10), Zr(1)–C(39) = 2.5765(9), Zr(1)–C(32) = 2.2851(9); O(1)–Zr(1)–N(2) = 157.17(3), N(1)–Zr(1)–C(40) = 96.19(3), C(40)–Zr(1)–C(32) = 126.48(3), C(32)–Zr(1)–N(1) = 120.71(3), Zr(1)–C(40)–C(39) = 83.53(5), C(21)–N(2)–Zr(1) = 104.95(6).

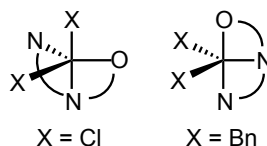


Figure 3.9 Different binding modes of NNO ligands in trigonal bipyramidal metal complexes depending on the identity of the X-type ligands.

As has been observed for other early metal dibenzyl complexes,^{7a,29a,33,34}

one of the benzyl groups in **14** strongly interacts with Zr and is significantly bent toward the metal center to give a Zr–C–C_{ipso} angle of 83.5° and a short Zr–C_{ipso} distance of 2.58 Å.

The molecular structure of **16** was also determined by single crystal X-Ray diffraction of crystals grown from slow vapor diffusion of pentane into a concentrated dichloromethane solution of **16** (Figure 3.10). The structure of **16** is very similar to that obtained for **8** with distorted trigonal bipyramidal geometry about titanium, and very similar bond lengths and angles. Similar to **8**, **16** appears to have an *ipso* interaction with a short Ti(1)–C(1)_{*ipso*} distance of 2.54 Å, and a Ti(1)–N(2)–C(1)_{*ipso*} angle of 100.2°.

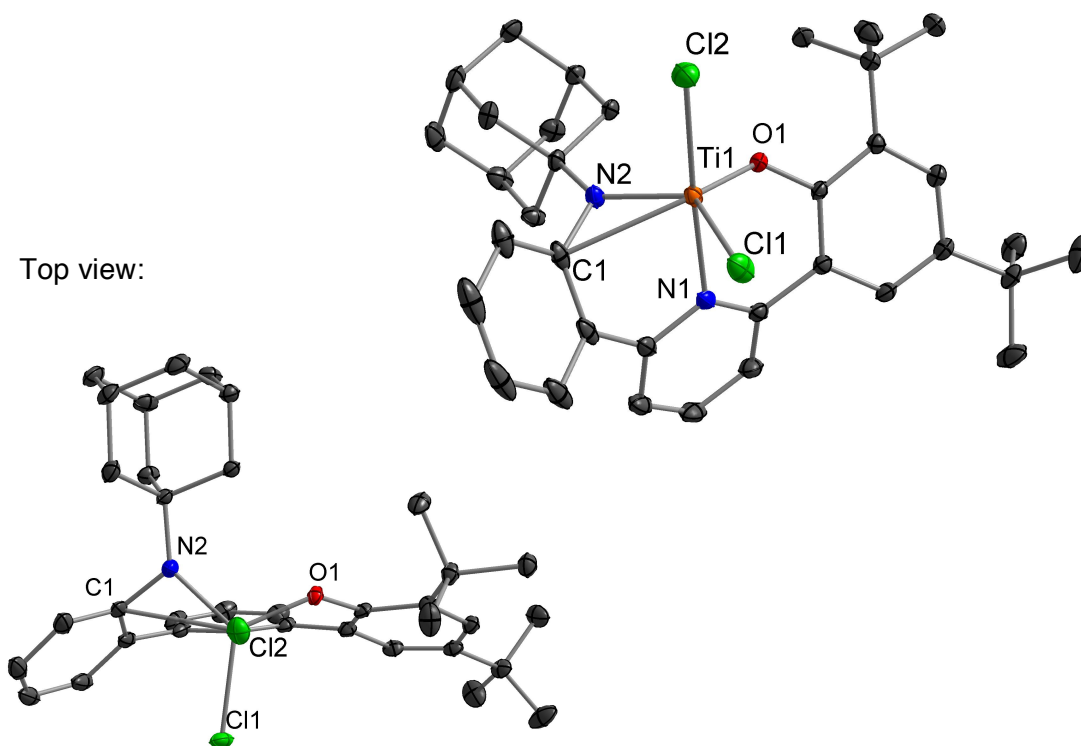


Figure 3.10 Probability ellipsoid diagram (50%) of the X-ray structure **16**. Selected bond lengths (Å) and angles (°): Ti(1)–O(1) = 1.8170(10), Ti(1)–N(1) = 2.1879(13), Ti(1)–N(2) = 1.8570(12), Ti(1)–Cl(2) = 2.3531(6), Ti(1)–Cl(1) = 2.2966(6), Ti(1)–C(1) = 2.5354(15); O(1)–Ti(1)–N(2) = 112.36(5), O(1)–Ti(1)–Cl(1) = 119.28(4), N(2)–Ti(1)–Cl(1) = 125.62(4), Cl(2)–Ti(1)–N(1) = 177.32(3), C(1)–N(2)–Ti(1) = 100.15(8).

*R*NNO Ligands: Polymerization Behavior

Activation of complexes **14–16** with MAO in toluene or chlorobenzene resulted in formation of PP under 5 atm of propylene at 0 °C; complex **17** was not active for polymerization. The activity, molecular weight, and polydispersity index (PDI) (when available) are shown in Table 3.2. Data for **6** and **8** is included for comparison. As was observed previously for complexes supported by ligand **5**, Ti complexes are more active than their Zr congeners for the NNO ligand system. In comparing the Ti catalysts with three different amine R-groups (1-phenylethyl (**8**), benzyl (**15**), and adamantyl (**16**)), **8** was observed to be the most active catalyst and gave the highest molecular weight polymer; overall, however, the activities are not significantly different. Additionally, no obvious trend between R-group and molecular weight is apparent for this small data set. Notably, all of the polymers obtained have narrow PDIs (M_w/M_n) suggesting single-site catalysis. The PP from complexes **15** and **16** had no melting points, as expected for stereoirregular PP, and had similar T_g values to those measured for the PP from complexes **6** and **8**.

Table 3.2 Propylene polymerization data for complexes **6**, **8**, **14–16**.

Precatalyst	Precatalyst (mmol)	Time (h)	Yield PP (mg) ^a	Activity (g PP (mol cat) ⁻¹ h ⁻¹)	T_g (°C)	M_w (g/mol)	M_w/M_n
6	0.0076	1	130.8	1.6×10^4	-8.77	26000	1.8
8	0.0092	0.5	553.7	1.2×10^5	-15.25	93190	1.50
8	0.0096	1	2412	2.5×10^5	-14.40	147000	1.5
8	0.0091	3	3963	1.5×10^5	-12.76	400810	1.99
14	0.0081	1	609.8	3.8×10^4			
15	0.0093	0.5	384.2	8.3×10^4	-13.66	80192	1.47
15	0.0098	1	839.3	8.6×10^4	-13.54	133384	1.55
15	0.0100	3	2504	8.4×10^4	-13.22	196942	2.38
16	0.0102	1	589.3	5.8×10^4	-15.36	91529	1.35

^aPolymerizations were carried out in 30 mL liquid propylene with 1000 eq dry MAO in 3 mL of toluene or PhCl at 0 °C for the time indicated.

^{13}C NMR spectroscopy was carried out on the polymers obtained from complexes **15–16**. We were particularly interested in comparing the microstructure of the PP for the Ti catalysts with three different amine R-groups (**8**, **15** and **16**). Surprisingly, we observed nearly no difference between the polymer microstructures as determined by ^{13}C NMR spectroscopy (Figure 3.11).

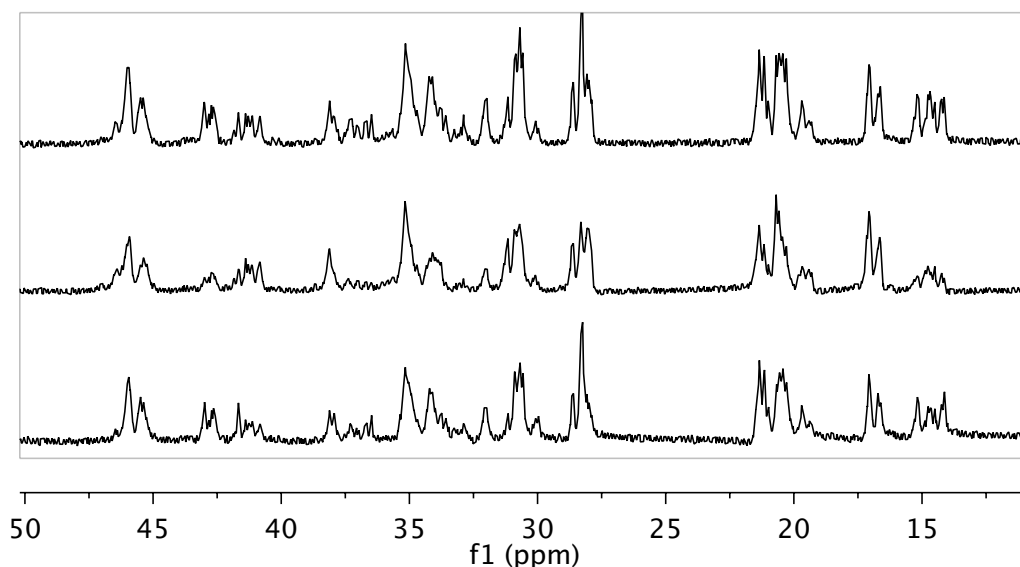


Figure 3.11 ^{13}C NMR spectra of PP from complex **8** (top), **15** (middle), and **16** (bottom) at 120 °C in $\text{TCE-}d_2$.

These results suggest that – contrary to our original hypothesis – the amine R-group does not seem to affect the stereo- or regiocontrol of the active polymerization catalyst. Although it is possible that the R-group is just an observer to the polymerization reaction in terms of monomer selectivity, we also considered catalyst modification pathways to explain the identical regioselectivity for different precatalysts, especially considering how unusual this type of PP is for an early metal polymerization catalyst. In fact, no other early metal

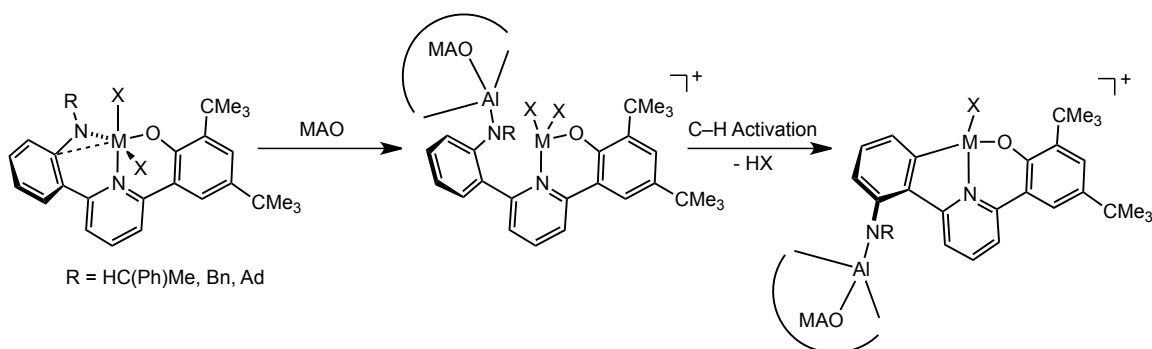
polymerization catalysts are known that make the same type of regioirregular PP as the Ti and Zr NNO-type catalysts described here.

One hypothesis for catalyst modification that may explain the identical regioselectivity for the Ti catalysts **8**, **15** and **16** is anilide arm dissociation under polymerization conditions, which would perhaps prevent the amine R-group from having any influence on the catalyst stereo- or regioselectivity. Notably, bis(anilide)pyridyl polymerization catalysts reported by our group, have very large PDIs for propylene polymerization (4.9-31.2),⁸ which may indicate the instability of the Ti–(anilide)N linkages under polymerization conditions; if the Ti–N bonds are susceptible to cleavage, multiple active species may be obtained leading to a broad molecular weight distribution and large PDIs. In contrast, the NNO polymerization catalysts reported here exhibit narrow PDIs indicative of primarily one active species (Table 3.2); thus, even if the Ti–(anilide)N bonds of the NNO ligand are unstable, the active polymerization catalysts appear to be stabilized by having a phenoxide moiety in the ligand framework.

CNO Ligand: Design and Synthesis

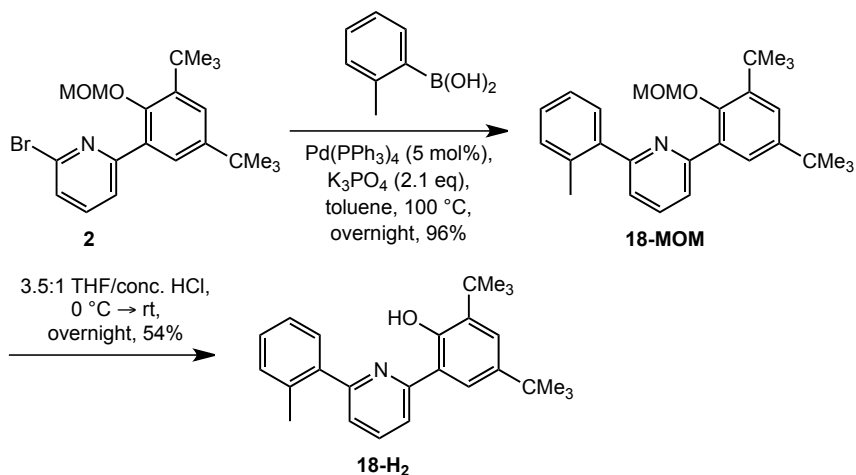
In considering the possibility of anilide arm dissociation – perhaps facilitated by MAO – we postulated that the arm could remain uncoordinated, or could rotate along the C_{aryl}–C_{aryl} bond and possibly C–H activate *meta* to the C_{aryl}–N_{anilide} bond (Scheme 3.19). Since studying the active catalyst in solution was not feasible, we sought to synthesize model complexes that upon activation

with MAO would be analogous to either a (perhaps) fluxional dissociated anilide arm or a C–H-activated anilide arm. Group 4 orthometalated aryl(pyridine)phenoxide (CNO) complexes are well known and, in fact, have been used in polymerizations with ethylene as well as ethylene/propylene copolymerizations, thus a CNO-ligated group 4 complex was our first target.³⁵



Scheme 3.19 Potential pathways for NNO catalyst modification upon activation with MAO.

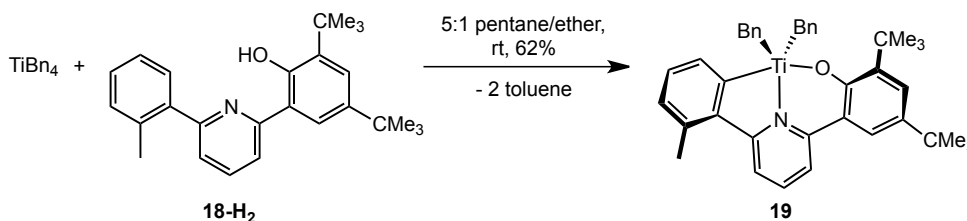
Ligand **18** was synthesized as shown in Scheme 3.20. The 2-bromo-6-(3,5-di-*t*-butyl-2-(methoxymethoxy)phenyl)pyridine synthon **2** underwent Suzuki coupling with commercially available *o*-tolyl-boronic acid. Deprotection of this intermediate with acidic THF afforded the desired CNO ligand **18**.



Scheme 3.20 Synthesis of ligand **18** from synthon **2**.

CNO Ligand: Metalation

Metalation of **18** was achieved by reaction with tetrabenzyltitanium to yield orthometalated (**18**)TiBn₂ **19** (Scheme 3.21). An X-Ray quality crystal of **19** was grown from a 5:1 pentane/ether solution at room temperature, which shows the expected distorted trigonal bipyramidal structure and bond lengths and angles similar to those reported for crystal structures of other (CNO)TiBn₂ complexes (Figure 3.12).^{35a} Notably, the Ti–C–C_{ipso} angle for one of the benzyl groups is slightly distorted at 93.7° and has a shortened Ti–C_{ipso} distance of 2.64 Å (compare to 123.3° and 3.18 Å for the other benzyl group) suggesting a weak η²-*ipso* interaction between the benzyl group and Ti.



Scheme 3.21 Synthesis of Ti complex **19**.

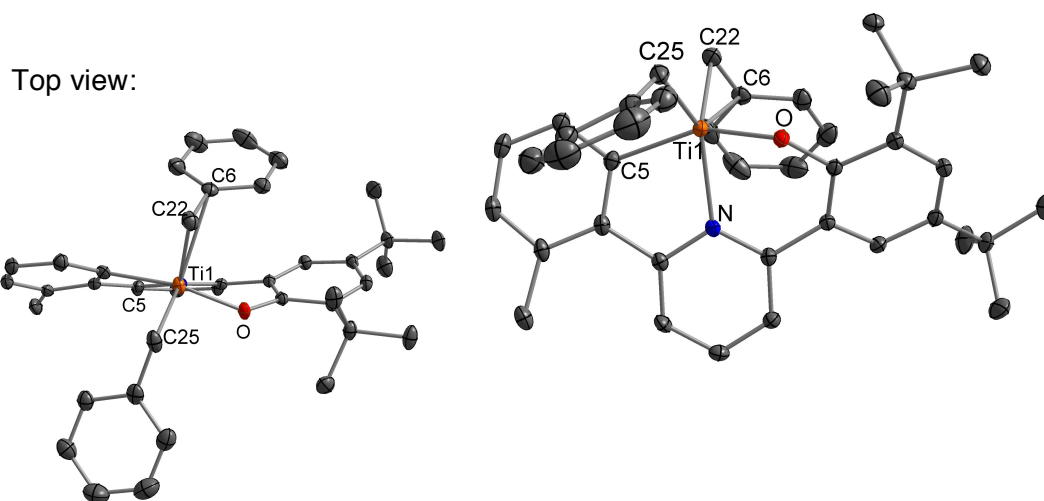


Figure 3.12 Probability ellipsoid diagram (50%) of the X-ray structure **17**. Selected bond lengths (Å) and angles (°): Ti(1)–O(1) = 1.8649(4), Ti(1)–N(1) = 2.2132(4), Ti(1)–C(5) = 2.1352(5), Ti(1)–C(22) = 2.1037(6), Ti(1)–C(6) = 2.6385(6), Ti(1)–C(25) = 2.1135(6); O(1)–Ti(1)–C(5) = 153.81(2), C(25)–Ti(1)–C(22) = 97.60(3), C(22)–Ti(1)–N(1) = 126.85(2), C(25)–Ti(1)–N(1) = 134.79(2), Ti(1)–C(22)–C(6) = 93.46(4).

CNO Ligand: Polymerization Behavior

Activation of **19** with MAO in toluene under 5 atm propylene at 0 °C yielded PP. The activity of the complex was measured to be 1.5×10^4 g PP (mol cat)⁻¹ h⁻¹, which is an order of magnitude less active than the NNO-type Ti polymerization catalysts **8**, **15**, and **16**. Importantly, investigation of the PP from **19** with ¹³C NMR spectroscopy revealed stereoirregular and regioregular PP (Figure 3.13). This result tentatively suggests that the NNO complexes do not C–H activate to form CNO polymerization catalysts.

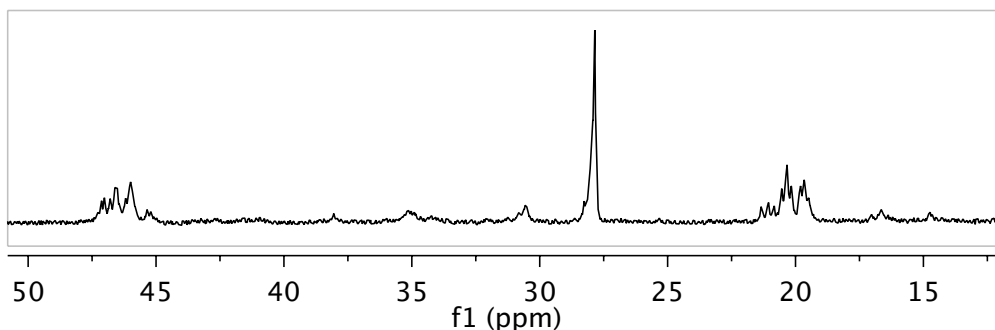


Figure 3.13 ^{13}C NMR spectrum of stereoirregular regioirregular PP from complex **19** at 120 °C in $\text{TCE-}d_2$.

To further investigate the possibility of C–H activation, a solution of **8** in chlorobenzene was activated with 50 equiv of MAO in the presence of 1-hexene; we have separately demonstrated that **8** polymerizes 1-hexene to make stereoirregular and regioirregular poly-1-hexene (Figure 3.14).³⁶

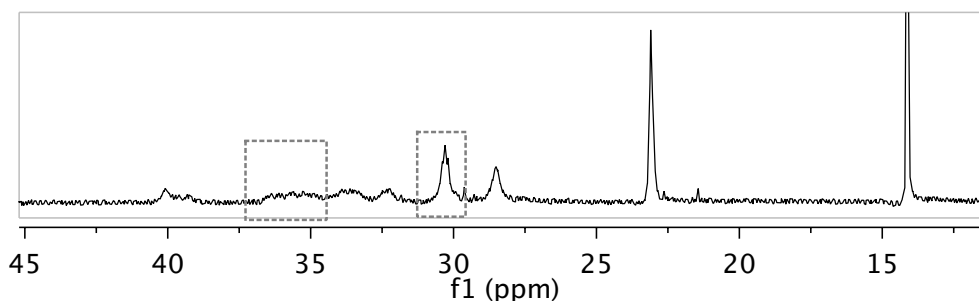
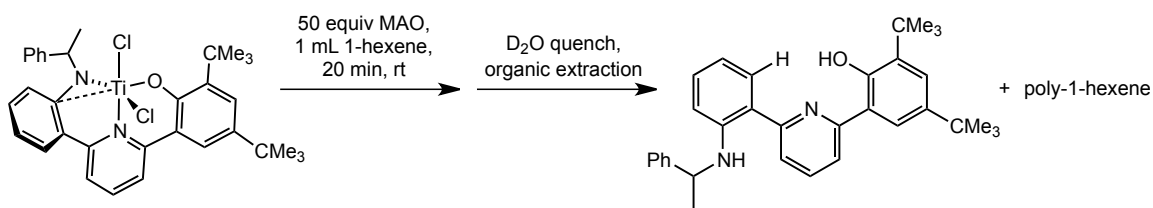


Figure 3.14 ^{13}C NMR spectrum of stereoirregular regioirregular poly-1-hexene from complex **8**. Regions indicating regioerrors are highlighted.

The solution of precatalyst **8**, MAO, and 1-hexene was stirred for 20 min and then quenched with D_2O . The organic layer was extracted and analyzed by ^1H NMR spectroscopy, which revealed the formation of poly-1-hexene and recovery of the intact ligand **5** (Scheme 3.22). If C–H activation occurred with MAO, we would expect to see deuterium incorporation into the aryl ring of the ligand; however, the ligand isolated from the reaction of **8**/MAO did not show

deuterium incorporation into the aryl ring by either HRMS or ^1H NMR spectroscopy. Additionally, the 1-phenylethyl R-group on the NNO ligand **5** was intact, ruling out N–C bond cleavage by MAO as another potential pathway for catalyst modification to make identical $\{(\text{NNO})\text{Ti}\}$ active species. Finally, monomer was not incorporated into the isolated ligand, as has been observed for Hf pyridyl–amide catalysts discovered by Dow and Symyx (these catalysts are modified by insertion of a monomer into a M–C bond, which admittedly is far more likely than insertion into M–O or M–N bonds).³⁷ Based on these experiments, we have tentatively ruled out (1) C–H activation of the anilide arm to form a $\{(\text{CNO})\text{Ti}\}$ complex (2) N–C bond cleavage of the anilide R-group and (3) monomer insertion into M–ligand bonds to explain the identical regiocontrol observed for NNO-type polymerization catalysts.

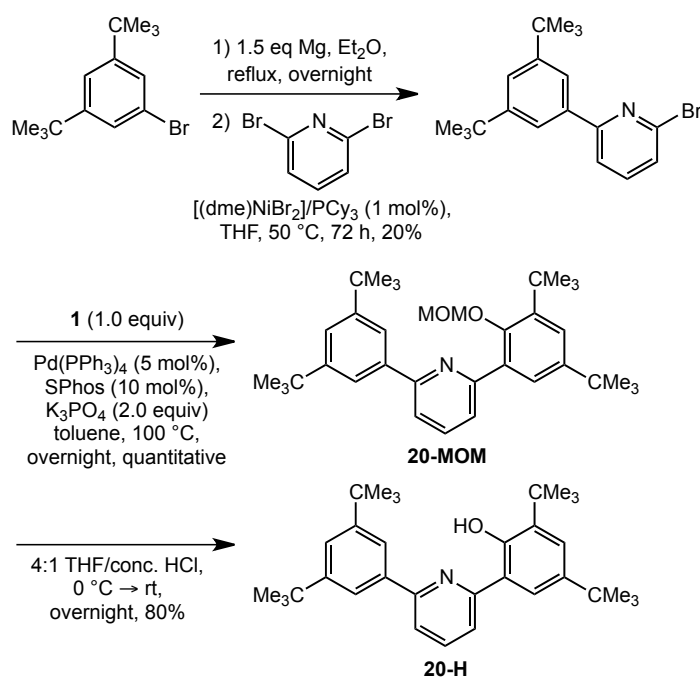


Scheme 3.22 Recovery of ligand **5** after activation and polymerization of 1-hexene with complex **8**.

ArNO Ligand: Synthesis

Synthesizing a model complex for anilide arm dissociation to make a pyridine(phenoxide) catalyst has, unfortunately, proven challenging (Scheme 3.19, middle complex). We designed a bulky aryl(pyridine)phenoxide (ArNO) ligand that we anticipated would resist aryl C–H activation, and might allow for formation of mono-ligated metal complexes (rather than homoleptic bis-ligated

complexes) despite being a bidentate coordinating ligand. Coupling 3,5-di-*t*-butylbromobenzene with 2,6-dibromopyridine via a Kumada coupling following a literature procedure led to the monoarylated pyridine intermediate 2-bromo-6-(3,5-di-*t*-butylphenyl)pyridine.³⁸ A Suzuki coupling reaction between 2-bromo-6-(3,5-di-*t*-butylphenyl)pyridine and the boronic ester **1**, followed by deprotection with acidic THF led to the target ArNO ligand **20** (Scheme 3.22).



Scheme 3.22 Synthesis of ligand **20** via Kumada and Suzuki coupling reactions.

ArNO Ligand: Metalation

Although we were able to synthesize the desired ligand, we were unable to obtain clean Ti complexes to test for polymerization, possibly because the pyridine(phenoxy) ligand **20** leads to metal complexes that are too electron poor to be stable.

Reaction of **20** with $\text{TiCl}_2(\text{NMe}_2)_2$ led to a species we have tentatively assigned as $(\mathbf{20})\text{TiCl}_2(\text{NMe}_2)$, however, clean isolation of this species was complicated by residual HNMe_2 in the reaction mixture. Alternatively, reaction of **20** with TiBn_4 initially yielded the complex $(\mathbf{20})\text{TiBn}_3$ with concomitant formation of 1 equiv of toluene; however, over time or upon removal of solvent this species was observed to decompose to a new unidentifiable – albeit clean – product perhaps resulting from dimerization of Ti species (Figure 3.15). Synthesis of $(\mathbf{20})\text{TiCl}_3$ was also attempted by reaction of **20** with TiCl_4 , but formation of HCl was unobserved and the product of the reaction appears to be $(\mathbf{20-H})\text{TiCl}_4$ with a diagnostic downfield resonance at 12.31 ppm indicative of an O–H group. Although other metal starting materials or synthetic routes might have yielded an appropriate Ti complex, we ultimately decided to not pursue this ligand framework for polymerization studies.

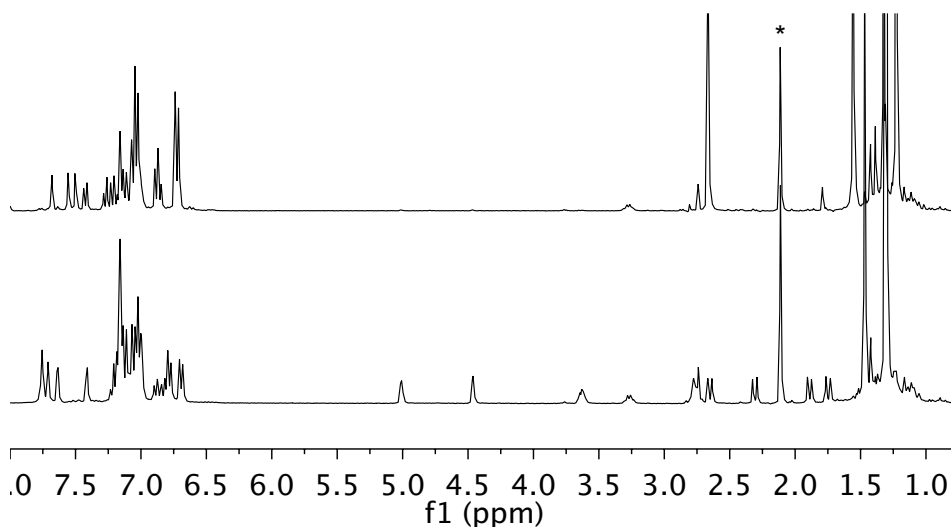


Figure 3.15 ^1H NMR spectrum of crude reaction between TiBn_4 and **20** in C_6D_6 after 10 min (top) and after sitting in a J. Young NMR tube at rt overnight (bottom). Toluene formed in the reaction is indicated by an asterisk.

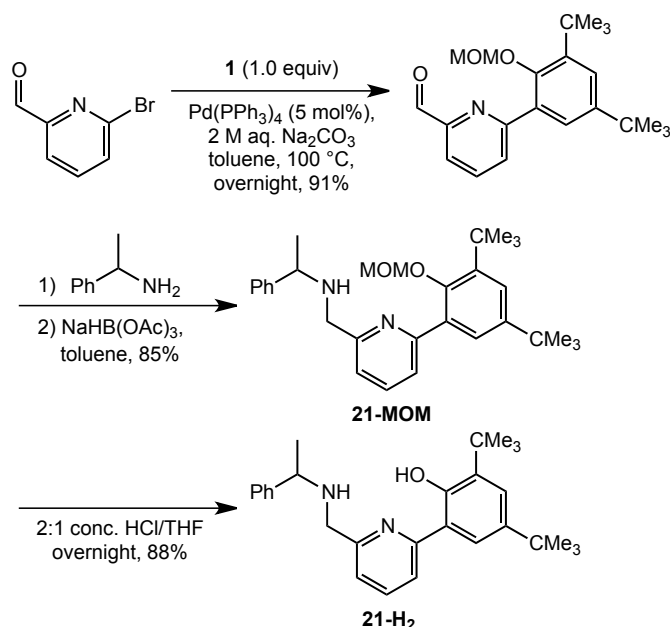
Nonetheless, our studies up to this point with the CNO–Ti complex **19**, as well as our activation study with the NNO–Ti complex **8** in the presence of monomer seem to disfavor a catalyst modification hypothesis and, in fact, provide no evidence for anilide arm dissociation under polymerization conditions. Despite the proximity of the R-group on the anilide arm to the metal center (Figures 3.4, 3.8, and 3.10), it appears to have no (or at a minimum very little) influence on monomer selectivity. Thus, while an explanation for the unique regioselectivity of NNO-type polymerization catalysts remains, as yet, out of reach, based on the data presented here, we suspect that the active species involves the intact anilide(pyridine)phenoxide ligand bound to the metal center.

amido NNO Ligand: Design and Synthesis

Our group has demonstrated that bis(phenoxide)pyridyl complexes⁷ and bis(anilide)pyridyl complexes⁸ produce regioregular (and stereoirregular) polypropylene; a related aryl(pyridine)phenoxide complex (**19**) presented here also polymerizes propylene in a regioregular sense. These data perhaps suggest that incorporation of an anionic nitrogen donor into an asymmetric ligand framework impacts the regioselectivity of the resulting catalytic species; thus, we were interested in investigating the polymerization behavior of metal complexes with other dianionic asymmetric NNO-coordinating ligands. For a first target, we selected an amido(pyridine)phenoxide ligand due to its straightforward synthesis and literature precedent for this framework supporting a Hf propylene

polymerization catalyst; unfortunately, the microstructure of the PP produced by the known Hf catalyst was only probed by FT-IR, which does not allow for analysis of the regiostructure of the polymer.³⁹

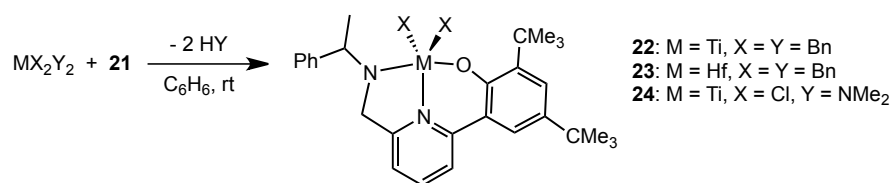
The amido(pyridine)phenoxide ligand **21** was synthesized using protocols similar to those reported for other 2-phenoxy-6-(methanamino)pyridines.⁴⁰ A Suzuki coupling reaction between boronic ester **1** and 6-bromo-2-pyridinecarboxaldehyde yielded 6-(3,5-di-*t*-butyl-2-(methoxymethoxy)phenyl)-picolinaldehyde. A condensation reaction with the desired amine, 1-phenylethylamine, generated a 2-phenoxy-6-iminopyridine intermediate, which underwent a one-pot reduction with sodium triacetoxyborohydride to yield the MOM-protected amido(pyridine)ligand **21-MOM**. Deprotection with acidic MeOH gave the desired ligand **21** in good yield (Scheme 3.23).



Scheme 3.23 Synthesis of amido(pyridine)phenoxide ligand **21**.

amido NNO Ligand: Metalation

Reaction of the amido(pyridine)phenoxide ligand **21** with tetrabenzyltitanium and tetrabenzylhafnium led to clean (by ^1H NMR spectroscopy) dibenzyl Ti and Hf complexes **22** and **23** (Scheme 3.24); the related reaction with tetrabenzylzirconium did not yield a clean product. Although the crude reaction mixtures of **22** and **23** appear to be very clean, we have been unable to isolate solids of the complexes; solutions of **22** and **23** decompose when concentrated by removal of solvent in vacuo, potentially because of the highly electrophilic nature of these metal complexes. We were able to obtain the molecular structure of a related Ti complex (**21**)TiCl₂ **24**, synthesized by reaction of ligand **21** with TiCl₂(NMe₂)₂, by single crystal X-ray diffraction (Scheme 3.24). **24** was crystallized as the THF adduct from slow vapor diffusion of pentane into a concentrated THF solution. The X-ray structure of **24** reveals pseudo-octahedral geometry around the Ti metal center and a typical Ti–(amido)N bond length, as well as other standard bond lengths and angles for an octahedral Ti(IV) complex (Figure 3.16).



Scheme 3.24 Synthesis of amido(pyridine)phenoxide complexes **23-24**.

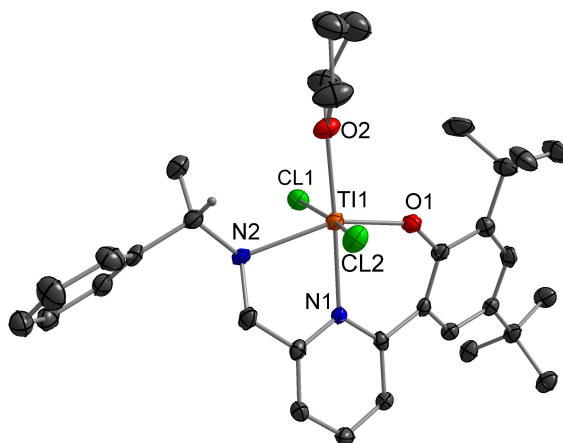


Figure 3.16 Probability ellipsoid diagram (50%) of the X-ray structure of the THF adduct of **24**. Selected bond lengths (Å) and angles (°): Ti(1)–Cl(1) = 2.4135(12), Ti(1)–Cl(2) = 2.4167(12), Ti(1)–O(1) = 1.852(2), Ti(1)–O(2) = 2.133(3), Ti(1)–N(1) = 2.183(3), Ti(1)–N(2) = 2.272(3); Cl(1)–Ti(1)–Cl(2) = 167.97(4), O(1)–Ti(1)–N(2) = 156.94(11), O(2)–Ti(1)–N(1) = 176.38(11), N(1)–Ti(1)–N(2) = 74.16(10), O(1)–Ti(1)–N(1) = 83.06(10).

amido NNO Ligand: Polymerization Behavior

Since we were unable to isolate clean metal complexes containing the amido(pyridine)phenoxide ligand **21**, we tested the polymerization activity of **22** and **23** by preparing the catalysts in situ; a freshly prepared solution of **21** and either tetrabenzyltitanium or tetrabenzylhafnium was loaded into a syringe and injected directly into the polymerization vessel. The in situ prepared hafnium complex **22** did not yield any polymer; however, recall that in our hands the anilide(pyridine)phenoxide Hf complex **7** also did not polymerize propylene. The Ti complex **23**, however, did yield PP and the activity at 0 °C was determined to be 1.6×10^4 g PP (mol cat)⁻¹ h⁻¹. Investigation of the polymer with ¹³C NMR spectroscopy revealed regioregular stereoirregular polypropylene, identical to that obtained from the (CNO)TiBn₂ catalyst **19** (Figure 3.17, see Figure 3.13).

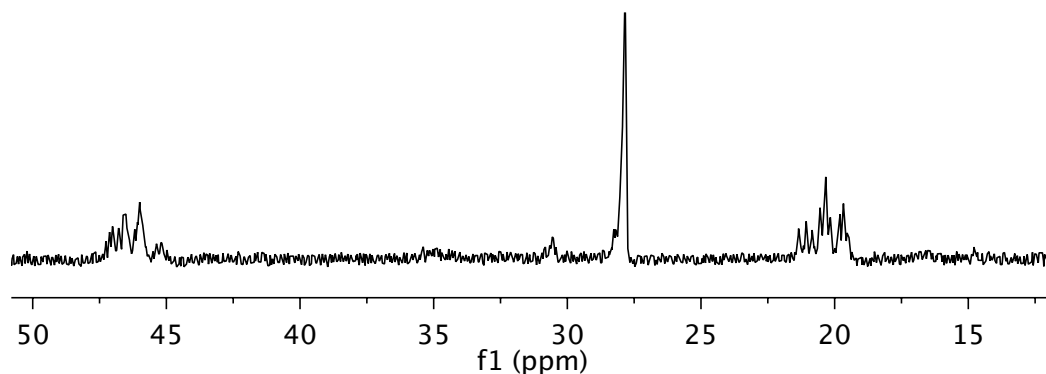


Figure 3.17 ^{13}C NMR spectrum of stereoirregular regioregular PP from in situ formed Ti complex **23** at 120 °C in TCE- d_2 .

This preliminary polymerization data suggests that a group 4 polymerization catalysts with a dianionic NNO ligand motif is not enough to give regioregular PP. We recognize that the anionic nitrogen donor in the amido(pyridine)phenoxide ligand is in a 5-membered ring compared to a 6-membered ring in the anilide(pyridine)phenoxide ligands. Additionally, by incorporating a dialkyl amido donor, the ligand motif is no longer a triaryl pincer framework, and the potential impact of these changes alone on polymerization behavior should be noted. Nevertheless, our polymerization results taken together clearly indicate that only the tridentate anilide(pyridine)phenoxide ligands **5**, **10**, and **11** support group 4 catalysts that exhibit nearly random regioselectivity for propylene polymerization. Furthermore, closely related tridentate dianionic ligand frameworks, whether incorporating symmetric anilide groups or pyridine(phenoxide) moieties, all lead to catalysts that produce regioregular PP, such that only the specific combination of an anilide, pyridine and a phenoxide together seems to result in regiorandom polymerization activity.

(NNO)TiCl₂: Further Polymerization Studies

Our studies with various post-metallocene polymerization catalysts up to this point suggest that anilide(pyridine)phenoxide catalysts are quite unique in their regioselectivity and that this regioselectivity may somehow be inherent in the catalyst structure; however, we thought it worthwhile to test these catalysts under different polymerization reaction conditions to investigate whether temperature or co-catalyst/activator had any effect on regioselectivity. With help from our collaborators at King Fahd University of Petroleum and Minerals (KFUPM) and Dow Chemical, we were able to test propylene polymerization with precatalyst **8** under different sets of conditions.

*Polymerization with (NNO)TiCl₂ **8** at (KFUPM)*

Ti complex **8** was tested in a 1 L glass reactor, which allowed for testing propylene polymerization at higher temperatures (22-25 °C) and higher pressures of propylene (8-9 atm) compared to the Fisher–Porter setup employed in the Bercaw laboratories (0 °C, 5 atm). A polymerization reaction using complex **8** as a catalyst, along with triisobutyl aluminum (TIBA) and MAO in toluene at room temperature yielded very sticky non-solid PP (Figure 3.17). We were not able to calculate an accurate activity for the reaction, but we estimate the activity to be on the order of $\sim 9 \times 10^5$ g PP (mol cat)⁻¹ h⁻¹.



Figure 3.17 Sticky non-solid PP produced at KFUPM (rt, 8–9 atm propylene) with precatalyst **8** (left) and nonsticky solid PP produced at Caltech (0 °C, 5 atm propylene) also with precatalyst **8** (right).

Investigation of the PP with ^{13}C NMR spectroscopy revealed stereoirregular and regioirregular PP (Figure 3.18). Notably, this sample of PP had a slightly different microstructure than the PP obtained from **8** in our reactor at 0 °C with 5 atm of propylene and dry MAO as the co-catalyst. We thought that the addition of free aluminum (TIBA) to the polymerization might affect the speciation of the catalyst and subsequently the polymer microstructure; the MAO used in our polymerizations is dried in vacuo to remove free trimethylaluminum (TMA). To test the possibility of TIBA affecting the polymerization, we set up a polymerization reaction with **8** in chlorobenzene using MMAO at 0 °C in our reactor. MMAO or modified MAO is a more stable version of MAO made from careful hydrolysis of TIBA. As we used the solution directly, it presumably contained free TIBA. Polymerization with MMAO as a co-catalyst yielded sticky non-solid PP; the activity was determined to be $1.0 \times 10^5 \text{ g PP (mol cat)}^{-1} \text{ h}^{-1}$. ^{13}C NMR spectroscopy on the PP from the reaction of **8**/MMAO revealed a microstructure identical to that from the PP synthesized at KFUPM with

8/MAO/TIBA (Figure 3.18). These results suggest that the polymerization reaction is very sensitive to free aluminum, but importantly shows that the regiorandom behavior of catalyst **8** is not affected by reaction temperatures between 0 and 22 °C.

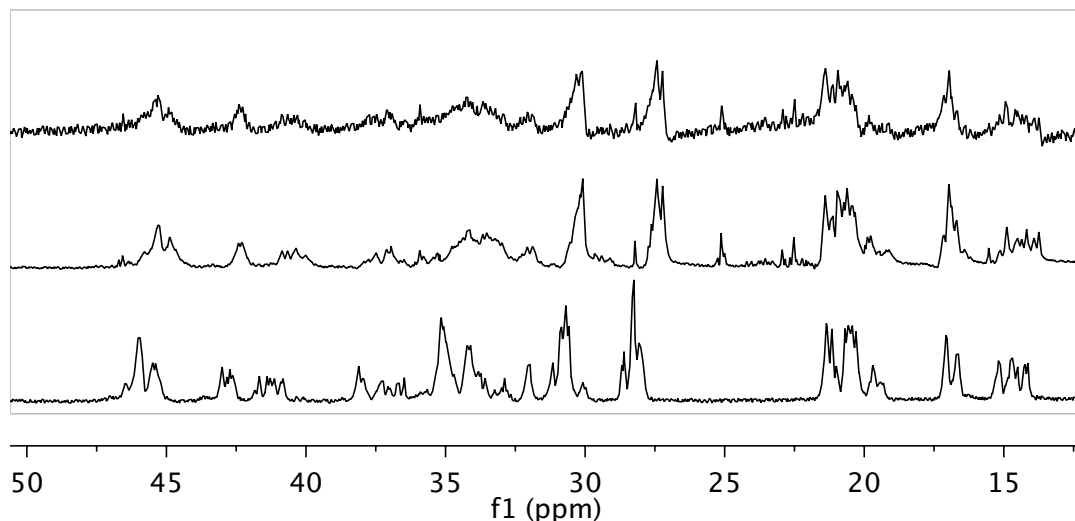


Figure 3.18 ^{13}C NMR spectra of PP from complex **8**/MAO/TIBA run at rt at KFUPM (top), PP from **8**/MMAO run at 0 °C at Caltech (middle), and PP from **8**/dry MAO run at 0 °C at Caltech (bottom). Spectra were taken at 120 °C in $\text{TCE-}d_2$.

Notably, GPC on the polymer obtained from **8**/MAO/TIBA at KFUPM revealed lower molecular weight PP compared to the polymers obtained at Caltech with the same precatalyst under different polymerization conditions; the PP from **8**/MAO/TIBA has a M_w value of only 4,076 g/mol, while the molecular weights of PP from **8**/dry MAO ranged from 93,190 g/mol to 400,810 g/mol (see Table 3.2). The molecular weight distribution for the polymer was still rather narrow with a M_w/M_n of 2.45. As expected, the PP had no observable T_m and a T_g of -26.11 °C. The GPC of PP from **8**/MMAO run at 0 °C showed a bimodal distribution with a low molecular weight peak of 3,975 g/mol and a high molecular weight peak of 195,372 g/mol. The low molecular weight polymers observed in

polymerizations with **8**/MAO/TIBA and **8**/MMAO may be a result of free aluminum present in the reaction, as aluminum alkyls are known to act as chain-transfer agents;⁴¹ only higher molecular weight PP was obtained when dry MAO with minimal free TMA was used (Table 3.2).

*Polymerization with (NNO)TiCl₂ **8** at Dow Chemical Company.*

Ti complex **8** was tested for propylene polymerization in a 1.8 L SS batch reactor. Polymerizations were run at 70 °C with 700 g of IsoparE, 150 g of propylene, 50 psi of hydrogen for 15 min. PMAO-IP or MAO were used as co-catalysts. These polymerizations yielded solid PP with excellent activities of 2.1×10^6 g PP (mol cat)⁻¹ h⁻¹ (**8**/PMAO-IP) and 9.6×10^5 g PP (mol cat)⁻¹ h⁻¹ (**8**/MAO) (Table 3.3), and broad molecular weight distributions, M_w/M_n , of 18.55 and 20.86, respectively; however, the GPC traces show trimodal distributions. Deconvolution of the GPC data for the PP from **8**/PMAO-IP reveals two low M_w peaks of 319 and 1,864 g/mol and a high M_w peak of 85,883 g/mol. Similarly, the deconvoluted GPC data for **8**/MAO has two low M_w peaks of 315 and 2,355 g/mol and a high M_w peak of 82,256 g/mol. Most interestingly, unlike the PP produced by our catalysts under any other condition, the PP produced with **8**/PMAO-IP or **8**/MAO at Dow had melting points of 158.2 °C and 155.3 °C, which is in the range expected for isotactic PP (Table 3.3). Indeed, ¹³C NMR spectroscopy on the polymers revealed peaks indicative of stereocontrolled isotactic PP (iPP), as well as peaks for stereoirregular and regioirregular PP (Figure 3.19 and Figure 3.20);

significantly, these results provide the first example of isotactic PP from a NNO-type catalyst. Consistent with the GPC data, the ^{13}C NMR spectra suggest that more than one type of polymer was made (presumably by different active species). Comparison of the ^{13}C NMR spectra for PP from **8**/PMAO-IP or **8**/MAO to the PP from **8**, **15**, or **16** activated with dry MAO shows identical regioirregular microstructures (Figure 3.21 and Figure 3.11).

Table 3.3 Propylene polymerization data for **8**/PMAO-IP and **8**/MAO.

Precatalyst	Precatalyst (mmol)	Time (h)	MAO (equiv)	PMAO-IP (equiv)	Yield PP (g) ^a	Activity (g PP (mol cat) ⁻¹ h ⁻¹)	T _g (°C)	T _m (°C)	M _w (g/mol)	M _w /M _n
8	0.010	0.25	-	10000	5.3	2.1 × 10 ⁶	-12.8	158.2	65599	18.55
8	0.010	0.25	10000	-	2.4	9.6 × 10 ⁶	-31.0	155.3	50041	20.86

^aPolymerizations were carried out with 700 g of IsoparE, 150 g of propylene, 50 psi of hydrogen at 70 °C for the time indicated.

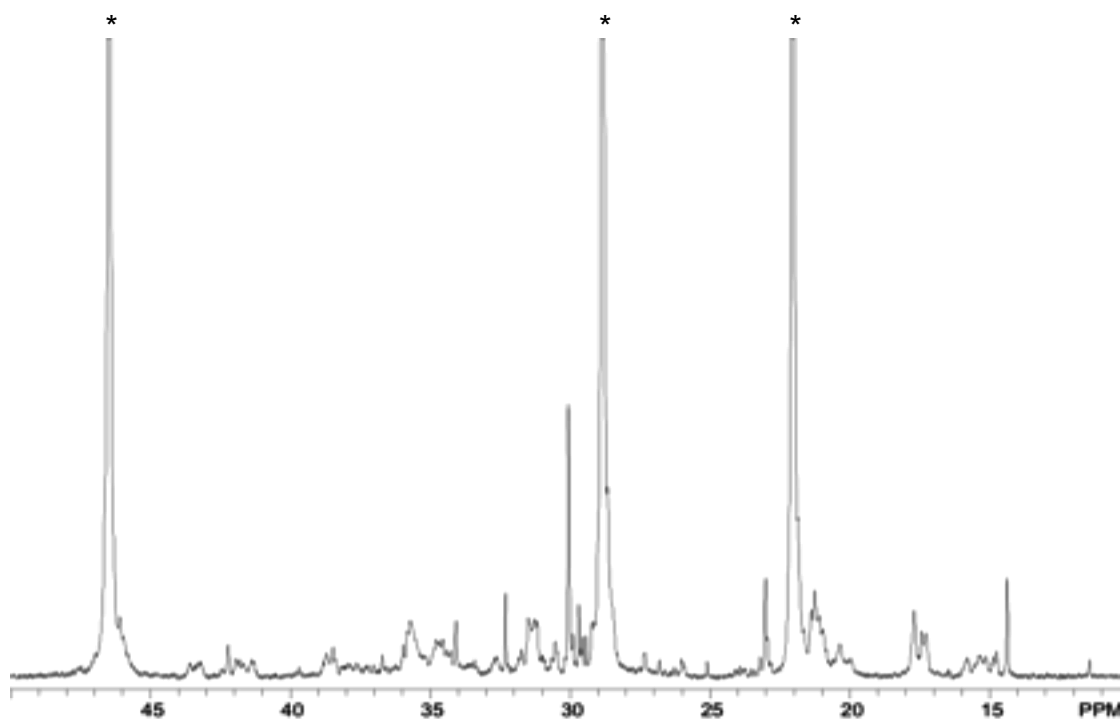


Figure 3.19 ^{13}C NMR spectrum of PP from **8**/PMAO-IP at 115 °C in TCE- d_2 . Resonances for iPP are indicated with asterisks.

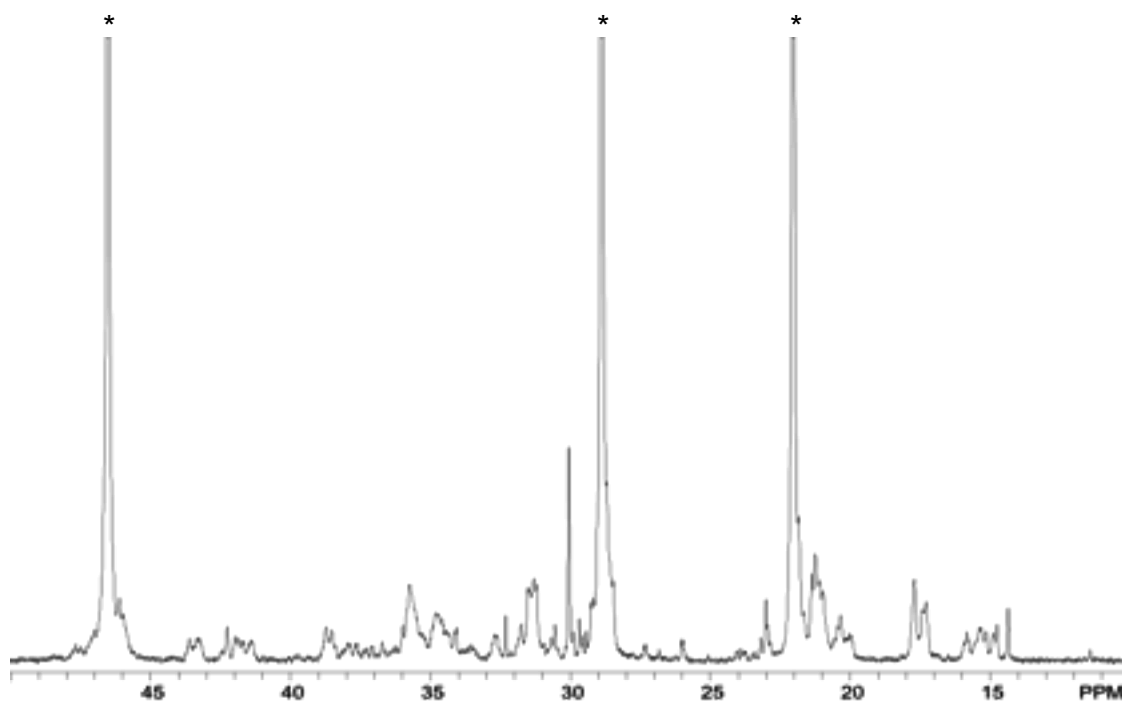


Figure 3.20 ^{13}C NMR spectrum of PP from **8**/MAO at 115 °C in $\text{TCE-}d_2$. Resonances for iPP are indicated with asterisks.

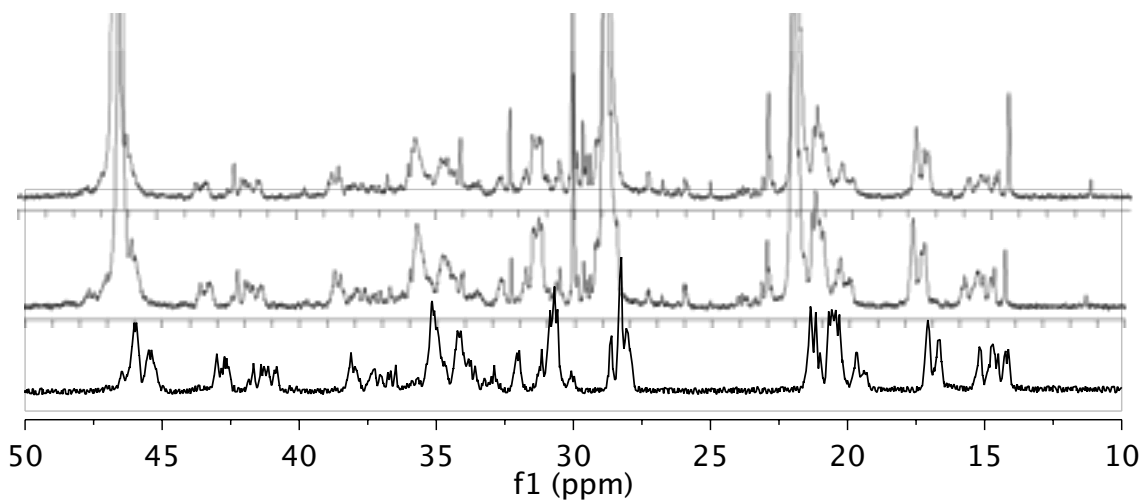


Figure 3.21 ^{13}C NMR spectra of PP from complex **8**/PMAO-IP (top), **8**/MAO (middle), and **8**/dry MAO/0 °C (bottom) at 115 or 120 °C in $\text{TCE-}d_2$.

These results seem to indicate that at least one new species is obtained from **8** under these polymerization conditions, which polymerizes propylene with

high stereo- and regioselectivity to yield iPP. At the same time, however, the species which was observed to yield regioirregular and stereoirregular PP at 0 or 22 °C is still active. Further studies are needed to separate the different types of PP in order to determine the yields of each polymer and to confirm that the isotactic fraction does not contain any regioerrors.

Conclusions and Future Work

A series of asymmetric post-metallocene group 4 complexes have been synthesized and tested for propylene polymerization activity. In most cases, the complexes were found to polymerize propylene upon activation with MAO with moderate to good activities. Interestingly, group 4 complexes based on a modular anilide(pyridine)phenoxide framework were discovered to produce highly regioirregular (and stereoirregular) polypropylene resulting from little apparent preference by these catalysts for 1,2- or 2,1-insertions of propylene; importantly, near regiorandom behavior is a new discovery for early metal polymerization catalysts, which typically polymerize propylene with a very high degree of regiocontrol. Furthermore, these NNO complexes feature a variable R-group on the anilide arm (R = 1-phenylethyl, benzyl, or adamantyl) close to the metal center (see Figures 3.4, 3.8, and 3.10 for X-ray structures), which has apparently no influence on monomer selectivity based on analysis of the PP obtained from different NNO catalysts by ^{13}C NMR spectroscopy (Figure 3.11). Subjecting the anilide(pyridine)phenoxide catalyst **8** to different polymerization conditions,

namely, higher pressures of propylene and higher reaction temperatures, revealed that the catalytically active species that produces regioirregular PP operates regardless of temperature or pressure, but also that at least one new polymerization species is formed at higher temperatures and pressures, which, surprisingly, produces apparently stereo- and regiocontrolled isotactic PP.

Catalyst modification pathways to explain the unusual regioselectivity of NNO-type catalysts were investigated through the synthesis of model complexes, as well as stoichiometric activation studies. These experiments seem to suggest that catalyst modification by dissociation of the anilide arm and subsequent C–H activation of an aryl C–H group, monomer insertion into a metal–ligand bond, or cleavage of the anilide arm R-group are unlikely under standard polymerization conditions. In fact, these studies imply that having an intact anilide(pyridine)phenoxide ligand is critical for regioirregular propylene polymerization and that the active species is coordinated to the NNO ligand. Unfortunately, the underlying factors influencing and ultimately leading to the unique regioselectivity of these interesting post-metallocene polymerization catalysts remain, at this time, a mystery, but perhaps future studies could lead to a better understanding of these complexes. For example, one path of inquiry that has not yet been explored is stoichiometric activations. If clean species could be obtained upon activation with typical stoichiometric activators (boranes, trityl or borate salts), then these studies could be carefully studied by NMR spectroscopy, which could perhaps lead to insights into the speciation of the

active catalyst, as well as the first insertions. Another potentially interesting future study would be to investigate anilide(pyridine)phenoxide species with aryl R-groups, as all of the NNO ligands described here had alkyl groups. Notably, the bis(anilide)pyridyl complexes investigated by our group for propylene polymerization had aryl groups.⁸ Although this seemingly small change is unlikely to be the cause of regioirregular polymerizations, it would be worth confirming that, indeed, the anilide R-group has no impact on regioselectivity whether it is a 1°, 2°, or 3° alkyl group or an aryl group.

Although these experiments together do not provide a satisfying explanation of the unusual polymerization behavior of group 4 anilide(pyridine)phenoxide complexes, they represent a small contribution to our understanding of the complex behavior of post-metallocene catalysts. As recently noted by Busico, “the common belief that ‘single-site’ olefin polymerization catalysis is easily amenable to rational understanding” does not hold true for post-metallocene catalysts and in fact, “it is clear that molecular catalysts are not necessarily simple nor foreseeable.”⁴² Nonetheless, these results importantly show that new discoveries are still possible in established fields like early metal α -olefin polymerization catalysis. Continued work in this area will undoubtedly lead to new breakthroughs in post-metallocene catalysts for olefin polymerization.

Acknowledgements

We thank Tonia Ahmed (SURF), Dr. Jerzy Klosin (Dow), and Professor John Bercaw for contributing experimental data to this chapter.

Experimental Section

General Considerations

All air- and moisture-sensitive compounds were manipulated using standard high-vacuum and Schlenk techniques or manipulated in a glovebox under a nitrogen atmosphere. Solvents for air- and moisture-sensitive reactions were dried over sodium benzophenone ketyl and stored over titanocene where compatible, or dried by the method of Grubbs.⁴³ $\text{TiCl}_2(\text{NMe})_2$ ⁴⁴, ZrBn_4 , HfBn_4 ⁴⁵, 2-bromo-N-(1-phenylethyl)aniline (**4**)¹⁵, N-benzyl-2-bromoaniline,²⁷ N-Adamant-1-yl-2-bromoaniline²⁸, and 2-bromo-6-(3,5-di-t-butylphenyl)pyridine³⁸ were prepared following literature procedures. 2-isopropoxy-4,4,5,5-tetramethyl-1,3,2-dioxaborolane was purchased from Sigma Aldrich and distilled prior to use. Butyllithium solution, potassium phosphate tribasic, barium hydroxide octahydrate and palladium(II)acetate were purchased from Sigma Aldrich and used as received. $\text{Pd}(\text{PPh}_3)_4$ and 2-(dicyclohexylphosphino)biphenyl were purchased from Strem and used as received. Pinacolborane was purchased from Alfa Aesar. 1,4-dioxane and pinacolborane were dried over 3 Å molecular sieves prior to use. Methylaluminoxane (MAO) was purchased as a toluene solution from Albemarle and was dried in vacuo at 150 °C overnight to remove free

trimethylaluminum before use. Propylene was dried by passage through a column of activated alumina and molecular sieves. Benzene-d₆, toluene-d₈, C₆D₅Cl, CDCl₃ and 1,1,2,2-tetrachloroethane-d₂ (TCE-d₂) were purchased from Cambridge Isotopes. Benzene-d₆ and toluene-d₈ were dried over sodium benzophenone ketyl then over titanocene. C₆D₅Cl was distilled from CaH₂ and passed through a plug of activated alumina prior to use. NMR spectra were recorded on Varian Mercury 300, Varian INOVA 500 or Varian INOVA 600 spectrometers and referenced to the solvent residual peak. High resolution mass spectra (HRMS) were obtained at the California Institute of Technology Mass Spectral Facility using a JEOL JMS-600H magnetic sector mass spectrometer. Elemental analyses were performed by Midwest Microlab LLC, Indianapolis, IN 46250. X-ray quality crystals were grown as indicated in the experimental procedures for each complex. The crystals were mounted on a glass fiber with Paratone-N oil. Data collection was carried out on a Bruker KAPPA APEX II diffractometer with a 0.71073 Å MoKα source. Structures were determined using direct methods with standard Fourier techniques using the Bruker AXS software package. In some cases, Patterson maps were used in place of the direct methods procedure. Some details regarding crystal data and structure refinement are available in Tables 3.3 and 3.4. Selected bond lengths and angles are supplied in the corresponding figures.

2-(3,5-di-*tert*-butyl-2-(methoxymethoxy)phenyl)-4,4,5,5-tetramethyl-1,3,2-dioxaborolane **1**. 26.20 g (0.0796 mol) of 1-bromo-3,5-di-*tert*-butyl-2-(methoxymethoxy)benzene was placed in a 250 mL Schlenk flask charged with a stir bar. The vessel was evacuated and refilled with Ar three times, and then 200 mL of dry Et₂O was added via cannula to the flask. The reaction solution was cooled to -78 °C in a dry ice/acetone bath, and 46.5 mL (1.5 eq) of *n*-BuLi (2.5 M in hexanes) was added dropwise using an addition funnel. The solution was stirred at -78 °C for 30 min, then 26.0 mL (1.6 eq) of 2-isopropoxy-4,4,5,5-tetramethyl-1,3,2-dioxaborolane was added via syringe. After 30 min at -78 °C, the flask was removed from the cooling bath and allowed to warm to room temperature while stirring; stirring was continued for an additional 2 hours. The reaction was quenched with saturated aqueous ammonium chloride and extracted with Et₂O (3 × 70 mL). The combined organics were dried over magnesium sulfate and rotovapped to yield a yellow white solid, which was further dried under vacuum. Recrystallization from hot MeOH yielded white microcrystals. 21.38 g, (0.0568 mol, 71% yield). ¹H NMR (500 MHz, CDCl₃) δ 1.31 (s, 9H, C(CH₃)₃), 1.36 (s, 12H, BOC(CH₃)₂), 1.44 (s, 9H, C(CH₃)₃), 3.57 (s, 3H, CH₂OCH₃), 5.16 (s, 2H, CH₂OCH₃), 7.47 (d, *J* = 2.6 Hz, 1H, aryl-CH), 7.53 (d, *J* = 2.6 Hz, 1H, aryl-CH). ¹³C NMR (126 MHz, CDCl₃) δ 25.00 (C(CH₃)₂), 30.91 (BOC(CH₃)₂), 31.68 (C(CH₃)₂), 34.54 (C(CH₃)₂), 35.34 (BOC(CH₃)₂), 57.58 (CH₂OCH₃), 83.72 (C(CH₃)₂), 100.59 (CH₂OCH₃), 120.98,

127.75, 130.97, 140.53, 144.58, 159.34 (aryl-C). HRMS (FAB+) m/z : calcd for $C_{22}H_{37}O_4B$ $[M]^+$ 376.2785; found 376.2776.

2-bromo-6-(3,5-di-*tert*-butyl-2-(methoxymethoxy)phenyl)pyridine 2. An oven-dried 350 mL Schlenk bomb was charged with a stirbar, evacuated and refilled with Ar. Under positive Ar pressure, 6.88 g (0.0292 mol) of 2,6-dimethylpyridine, 10.02 g (0.0266 mol) of 2-(3,5-di-*tert*-butyl-2-(methoxymethoxy)phenyl)-4,4,5,5-tetramethyl-1,3,2-dioxaborolane, 1.55 g (0.00134 mol) of $Pd(PPh_3)_4$ and 11.33 g (0.0534 mol) of K_3PO_4 crushed with a mortar and pestle were added and the vessel was sealed with a septum. The vessel was evacuated and refilled with Ar three times. 100 mL of dry toluene was added via syringe and the vessel was sealed with a Kontes valve. The reaction mixture was stirred at room temperature for 25 min, during which time the bright yellow color faded to pale yellow (with insoluble white K_3PO_4). The vessel was placed in a 115 °C oil bath for 7 days, then cooled to room temperature, and the suspension filtered through celite with the aid of Et_2O . Solvent was removed in vacuo and the resulting residue was purified by column chromatography on SiO_2 using 1:3 Et_2O /hexanes ($R_f = 0.625$). 9.52 g (82% yield). (This product contains 7% of the bis-arylated pyridine product 2,6-bis(3,5-di-*tert*-butyl-2-(methoxymethoxy)phenyl)pyridine reported previously^{7a}, but we have found that we can carry this product on and remove the impurity completely during a later purification step.) 1H NMR (500 MHz, $CDCl_3$) δ 1.33 (s, 9H, $C(CH_3)_3$), 1.46 (s, 9H, $C(CH_3)_3$), 3.32 (s, 3H, CH_2OCH_3), 4.56 (s, 2H,

CH_2OCH_3), 7.39 (d, $J = 2.5$ Hz, 1H, aryl-CH), 7.47 – 7.41 (m, 2H, aryl-CH), 7.56 (t, $J = 7.7$ Hz, 1H, aryl-CH), 7.66 (d, $J = 7.7$ Hz, 1H, aryl-CH). ^{13}C NMR (126 MHz, CDCl_3) δ 31.05 ($\text{C}(\text{CH}_3)_3$), 31.61 ($\text{C}(\text{CH}_3)_3$), 34.80 ($\text{C}(\text{CH}_3)_2$), 35.58 ($\text{C}(\text{CH}_3)_2$), 57.51 (CH_2OCH_3), 99.85 (CH_2OCH_3), 124.11, 125.69, 126.12, 126.48, 132.68, 138.28, 141.90, 142.63, 146.34, 151.40, 159.83 (aryl-C). HRMS (FAB+) m/z : calcd for $\text{C}_{21}\text{H}_{29}\text{O}_2\text{NBr}$ [$\text{M} + \text{H}$] $^+$ 406.1382; found 406.1385.

2-(6-(3,5-di-*tert*-butyl-2-(methoxymethoxy)phenyl)pyridin-2-yl)-*N*-(1-phenylethyl)aniline NNO-MOM 5-MOM. This synthesis is based on reported procedures.¹⁶ To a 350 mL Schlenk bomb charged with a stirbar was added 1.50 g (0.00544 mol) of 2-bromo-*N*-(1-phenylethyl)aniline, and the bomb was evacuated and refilled with Ar. Under positive Ar pressure, 0.0611 g (0.272 mmol) of $\text{Pd}(\text{OAc})_2$ and 0.382 g (1.09 mmol) of 2-(dicyclohexylphosphino)biphenyl were added and the vessel was sealed with a septum. The reaction vessel was then evacuated and refilled with Ar three times and 15 mL of dry dioxane was added via syringe, followed by 3.79 mL triethylamine (0.0272 mol) and 2.37 mL pinacolborane (0.0163 mol). The reaction vessel was sealed with a Kontes valve and placed in an 80 °C oil bath for 1.5 h, during which time the color changed to olive green, then cooled to room temperature and 3.75 mL of H_2O was added via syringe. Under positive Ar pressure, 5.15 g of $\text{Ba}(\text{OH})_2 \cdot 8 \text{H}_2\text{O}$ (0.0163 mol) and 2.38 g (1 eq) **2** were added successively. The reaction vessel was sealed with a Kontes valve and placed in

a 90 °C oil bath overnight (~16 h), then cooled to room temperature and the mixture filtered through celite with the aid of Et₂O. Brine was added to the filtrate, which was extracted with additional Et₂O (3 × 50 mL). The combined extracts were dried over magnesium sulfate and rotovapped to yield a brown oil, which was further purified by passage through SiO₂ with dichloromethane to yield a yellow oil. (2.6558 g, 0.00508 mol, crude yield 93%; some impurities were subsequently removed following deprotection). ¹H NMR (500 MHz, CDCl₃) δ 1.33 (s, 9H, C(CH₃)₃), 1.43 (d, *J* = 6.7 Hz, 3H, CH(CH₃)), 1.51 (s, 9H, C(CH₃)₃), 3.27 (s, 3H, CH₂OCH₃), 4.61 – 4.52 (m, 3H, CH(CH₃), CH₂OCH₃), 6.55 (d, *J* = 8.4 Hz, 1H, aryl-CH), 6.70 (t, *J* = 7.5 Hz, 1H, aryl-CH), 7.14 – 7.09 (m, 1H, aryl-CH), 7.16 (d, *J* = 7.1 Hz, 1H, aryl-CH), 7.19 (t, *J* = 7.1 Hz, 2H, aryl-CH), 7.33 (d, *J* = 6.9 Hz, 2H, aryl-CH), 7.49 – 7.46 (m, 2H, aryl-CH), 7.53 (dd, *J* = 7.7, 0.9 Hz, 1H, aryl-CH), 7.68 (dd, *J* = 7.9, 1.4 Hz, 1H, aryl-CH), 7.73 (d, *J* = 8.1 Hz, 1H, aryl-CH), 7.83 (t, *J* = 7.9 Hz, 1H, aryl-CH), 9.37 (d, *J* = 6.0 Hz, 1H, NH). ¹³C NMR (126 MHz, CDCl₃) δ 25.37 (CH(CH₃)), 31.11 (C(CH₃)₃), 31.68 (C(CH₃)₃), 34.78 (C(CH₃)₃), 35.62 (C(CH₃)₃), 53.15 (CH(CH₃)), 57.57 (CH₂OCH₃), 99.69 (CH₂OCH₃), 112.96, 115.61, 119.96, 120.60, 122.21, 124.95, 125.99, 126.28, 126.62, 128.58, 129.23, 130.36, 134.32, 136.99, 142.36, 145.86, 145.96, 147.33, 151.52, 156.55, 159.70 (aryl-C). HRMS (FAB+) *m/z*: calcd for C₃₅H₄₃O₂N₂ [M + H]⁺ 523.3325; found 523.3299.

2,4-di-*tert*-butyl-6-(6-(2-((1-phenylethyl)amino)phenyl)pyridin-2-yl)phenol 5-H₂. 3.150 g of **5-MOM** was placed in a 250 mL round bottom flask charged with a stir bar, and 30-mL of THF was added to give a yellow solution. The flask was cooled to 0 °C using a water-ice bath; a 30 mL solution of 2:1 conc. HCl/THF was added dropwise; the reaction mixture was stirred for 30 minutes at 0 °C, then removed from the ice bath and allowed to reach room temperature while stirring was continued overnight. The reaction was re-cooled again to 0 °C and quenched with a 2 M aq. NaOH solution to give a solution with neutral pH. The organic layer was extracted with Et₂O (3 × 50 mL) and the combined organics were dried over magnesium sulfate and rotovapped to yield a yellow-white solid, which was redissolved and passed through a SiO₂ plug, using 10% Et₂O/hexanes as an eluent, to give an off-white solid. Recrystallization by dissolving in hot hexanes followed by cooling in the freezer yielded a clean off-white powder (868.4 mg, 0.00181 mol, yield: 34%). ¹H NMR (500 MHz, CDCl₃) δ 1.40 (s, 9H, C(CH₃)₃), 1.45 (d, *J* = 6.7 Hz, 3H, CH(CH₃)), 1.50 (s, 9H C(CH₃)₃), 4.57 – 4.47 (m, 1H, CH(CH₃)), 6.00 (d, *J* = 4.6 Hz, 1H, NH), 6.51 (d, *J* = 8.3 Hz, 1H, aryl-CH), 6.78 – 6.69 (m, 1H, aryl-CH), 7.13 (t, *J* = 7.8 Hz, 1H, aryl-CH), 7.22 (t, *J* = 7.3 Hz, 1H, aryl-CH), 7.31 (t, *J* = 7.6 Hz, 2H, aryl-CH), 7.36 (dd, *J* = 7.6, 1.5 Hz, 1H, aryl-CH), 7.44 (d, *J* = 2.3 Hz, 1H, aryl-CH), 7.51 – 7.46 (m, 3H, aryl-CH), 7.73 (d, *J* = 2.3 Hz, 1H, aryl-CH), 7.89 (d, *J* = 8.2 Hz, 1H, aryl-CH), 7.96 (t, *J* = 8.0 Hz, 1H, aryl-CH), 14.03 (s, 1H, OH). ¹³C NMR (126 MHz, CDCl₃) δ 25.43 (CH(CH₃)), 29.81 (C(CH₃)₃), 31.80 (C(CH₃)₃), 34.55 (C(CH₃)₃), 35.46 (C(CH₃)₃), 53.89 (CH(CH₃)),

112.58, 116.56, 118.13, 118.41, 121.38, 121.69, 123.05, 126.07, 126.47, 126.89, 128.79, 130.44, 130.61, 137.85, 139.09, 140.16, 145.09, 145.55, 156.31, 156.41, 158.24 (aryl-C). HRMS (FAB+) m/z : calcd for $C_{33}H_{38}N_2O$ $[M]^+$ 478.2984; found 478.2993.

(5)ZrBn₂ 6. A 2 mL benzene solution of **5-H₂** (95.0 mg, 0.198 mmol) was added to a 2 mL benzene solution of ZrBn₄ (91.0 mg, 0.200 mmol) and stirred for ten minutes under inert atmosphere in the glovebox. Benzene was removed in vacuo from the resulting yellow-brown solution to yield a yellow-brown oil, which was redissolved in pentane and pumped dry several times to remove residual toluene, before being filtered through celite with pentane. The resulting solution was cooled to -30 °C resulting in precipitation of bright yellow solid. (131.2 mg, 0.174 mmol, yield: 88%.) ¹H NMR (500 MHz, toluene-*d*₈, -20 °C) δ 1.48 (s, 9H, C(CH₃)₃), 1.63 (s, 9H, C(CH₃)₃), 1.74 (d, $J = 6.5$ Hz, 3H, CH(CH₃)), 1.90 (d, $J = 10.3$ Hz, 1H, ZrCH₂), 2.02 (d, $J = 10.3$ Hz, 1H, ZrCH₂), 2.61 (d, $J = 10.7$ Hz, 1H, ZrCH₂), 2.73 (d, $J = 10.7$ Hz, 1H, ZrCH₂), 4.63 (q, $J = 6.4$ Hz, 1H, CH(CH₃)), 6.23 (d, $J = 7.4$ Hz, 2H, aryl-CH), 6.37 (d, $J = 7.7$ Hz, 1H, aryl-CH), 6.52 (t, $J = 6.5$ Hz, 3H, aryl-CH), 6.63 (t, $J = 7.6$ Hz, 2H, aryl-CH), 6.68 (t, $J = 7.6$ Hz, 2H, aryl-CH), 6.75 (t, $J = 7.3$ Hz, 1H, aryl-CH), 6.80 (t, $J = 7.5$ Hz, 1H, aryl-CH), 7.22 – 7.11 (m, 3H, aryl-CH), 7.29 (d, $J = 7.3$ Hz, 2H, aryl-CH), 7.33 (d, $J = 8.2$ Hz, 1H, aryl-CH), 7.37 (t, $J = 7.6$ Hz, 2H, aryl-CH), 7.46 (d, $J = 2.1$ Hz, 1H, aryl-CH), 7.57 (d, $J = 2.2$ Hz, 1H, aryl-CH). ¹³C NMR (126 MHz, toluene-*d*₈, -20 °C) δ 24.87

(CH(CH₃)), 30.46 (C(CH₃)₃), 32.26 (C(CH₃)₃), 34.97 (C(CH₃)₃), 36.15 (C(CH₃)₃), 64.06 (ZrCH₂), 65.45 (CH(CH₃)), 66.19 (ZrCH₂), 120.07, 121.83, 122.40, 124.02, 124.52, 124.82, 126.35, 126.65, 126.77, 126.86, 127.14, 128.40, 128.61, 128.90, 129.55, 129.75, 130.42, 132.52, 132.75, 134.95, 138.65, 138.87, 142.00, 144.56, 145.89, 149.79, 155.00, 155.11, 158.71 (aryl-C). Anal. Calcd for C₄₇H₅₀N₂OZr (%): C, 75.25; H, 6.72; N, 3.73. Found (1): C, 73.39; H, 6.72; N, 3.68. (2): C, 73.62; H, 6.50; N, 3.68. (This compound is air- and moisture-sensitive and despite repeated attempts satisfactory %C analysis could not be obtained.)

(5)HfBn₂ 7. A 2 mL benzene solution of **5-H₂** (54.6 mg, 0.114 mmol) was added to a 2 mL benzene solution of HfBn₄ (62.5 mg, 0.115 mmol) and stirred for ten minutes under inert atmosphere in the glovebox. Benzene was removed in vacuo from the resulting yellow solution to yield a yellow solid, which was redissolved in pentane and pumped dry several times to remove residual toluene to give a fine pale yellow powder (62.7 mg, 0.075 mmol, yield: 66%). ¹H NMR (500 MHz, toluene-*d*₈, -20 °C) δ 1.48 (s, 9H, C(CH₃)₃), 1.64 (s, 9H, C(CH₃)₃), 1.67 (d, *J* = 11.3 Hz, 1H, HfCH₂), 1.80 – 1.74 (m, 4H, HfCH₂, CH(CH₃)), 2.40 (d, *J* = 11.5 Hz, 1H, HfCH₂), 2.55 (d, *J* = 11.5 Hz, 1H, HfCH₂), 4.79 (q, *J* = 6.4 Hz, 1H, CH(CH₃)), 6.27 (d, *J* = 7.4 Hz, 2H, aryl-CH), 6.42 (d, *J* = 7.7 Hz, 1H, aryl-CH), 6.53 – 6.45 (m, 3H, aryl-CH), 6.67 (dd, *J* = 17.0, 7.7 Hz, 4H, aryl-CH), 6.76 (dd, *J* = 13.9, 7.1 Hz, 2H, aryl-CH), 6.88 (d, *J* = 8.2 Hz, 1H, aryl-CH), 6.93 (d, *J* = 7.7 Hz, 1H, aryl-CH), 7.16 – 7.11 (m, 3H, aryl-CH), 7.30 (d, *J* = 7.5 Hz, 2H, aryl-CH), 7.35 (d, *J* =

8.2 Hz, 1H, aryl-CH), 7.39 (d, $J = 7.5$ Hz, 2H, aryl-CH), 7.43 (d, $J = 2.2$ Hz, 1H, aryl-CH), 7.60 (d, $J = 2.2$ Hz, 1H, aryl-CH). ^{13}C NMR (126 MHz, toluene- d_8 , -20 C°) δ 25.13 (CH(CH₃)), 30.43 (C(CH₃)₃), 32.25 (C(CH₃)₃), 34.95 (C(CH₃)₃), 36.07 (C(CH₃)₃), 64.57 (CH(CH₃)), 71.19 (HfCH₂), 72.13 (HfCH₂), 120.55, 121.76, 122.37, 124.41, 124.62, 124.86, 125.57, 125.78, 126.73, 126.85, 126.92, 127.16, 128.41, 128.63, 128.94, 129.56, 129.60, 129.66, 131.56, 132.55, 135.73, 138.97, 139.02, 142.12, 145.14, 146.61, 149.61, 154.94, 155.12, 158.14 (aryl-C). Anal. Calcd for C₄₇H₅₀HfN₂O (%): C, 67.41; H, 6.02; N, 3.35. Found (1): C, 61.82; H, 5.65; N, 3.55. (2): C, 59.22; H, 5.68; N, 3.55. (This compound is air- and moisture-sensitive and despite repeated attempts satisfactory %C analysis could not be obtained.)

(5)TiCl₂ 8. A 4 mL benzene solution of **5-H₂** (301.1 mg, 0.629 mmol) was added to a 4 mL benzene solution of TiCl₂(NMe₂)₂ (130.8 mg, 0.632 mmol) and stirred for ten minutes under inert atmosphere in the glovebox. Benzene was removed in vacuo from the resulting dark red solution to yield a dark orange solid, which was triturated several times with pentane to remove free dimethylamine (373.6 mg, 0.627 mmol, quantitative yield). ^1H NMR (500 MHz, C₅D₅Cl) δ 1.34 (s, 9H, C(CH₃)₃), 1.78 (s, 9H, C(CH₃)₃), 2.31 (d, $J = 6.7$ Hz, 3H, CH(CH₃)), 5.12 – 5.06 (m, 1H, CH(CH₃)), 6.36 (dd, $J = 7.7, 1.7$ Hz, 2H, aryl-CH), 6.77 – 6.72 (m, 2H, aryl-CH), 7.04 – 7.00 (m, 1H, aryl-CH), 7.06 (d, $J = 7.7$ Hz, 1H, aryl-CH), 7.23 – 7.19 (m, 4H, aryl-CH), 7.39 (d, $J = 7.5$ Hz, 1H, aryl-CH), 7.51 (t, $J = 8.0$ Hz, 1H,

aryl-CH), 7.79 – 7.72 (m, 3H, aryl-CH). ^{13}C NMR (126 MHz, $\text{C}_5\text{D}_5\text{Cl}$) δ 25.20 (CH(CH₃)), 30.50 (C(CH₃)₃), 31.44 (C(CH₃)₃), 34.78 (C(CH₃)₃), 35.80 (C(CH₃)₃), 72.23 (CH(CH₃)), 121.70, 123.57, 123.77, 124.01, 126.20, 127.03, 128.11, 128.33, 128.53, 128.62, 129.53, 132.94, 133.91, 135.26, 137.92, 139.03, 144.16, 145.45, 151.46, 152.70, 158.24 (aryl-C). Anal. Calcd for $\text{C}_{33}\text{H}_{36}\text{Cl}_2\text{N}_2\text{OTi}$ (%): C, 66.57; H, 6.09; N, 4.70. Found: C, 66.43; H, 5.93; N, 4.78.

(5)TiBn₂ 9. To a 5 mL toluene solution of **8** (12.0 mg, 0.020 mmol) was added 42.3 μL of a BnMgCl solution (2.1 equiv) via syringe and the resulting orange solution stirred for ten minutes under inert atmosphere in the glovebox. The reaction mixture was filtered through a plug of celite with the aid of toluene and then toluene was removed in vacuo to yield a red solid. The red solid was triturated several times with pentane. ^1H NMR (300 MHz, C_6D_6) δ 1.48 (s, 9H, C(CH₃)₃), 1.76 (s, 9H, C(CH₃)₃), 1.80 (d, $J = 6.6$ Hz, 3H, CH(CH₃)), 2.40 (d, $J = 9.0$ Hz, 1H, ZrCH₂), 2.86 (d, $J = 8.7$ Hz, 1H, ZrCH₂), 3.15 (d, $J = 9.8$ Hz, 1H, ZrCH₂), 3.25 (d, $J = 9.9$ Hz, 1H, ZrCH₂), 4.85 (q, $J = 6.6$ Hz, 1H, CH(CH₃)), 6.12 (d, $J = 7.1$ Hz, 2H, aryl-CH), 6.41 (d, $J = 7.3$ Hz, 2H, aryl-CH), 6.45 – 6.62 (m, 4H, aryl-CH), 6.69 (t, $J = 7.3$ Hz, 3H, aryl-CH), 6.82 (t, $J = 7.0$ Hz, 1H, aryl-CH), 6.97 – 7.04 (m, 2H, aryl-CH), 7.10 (dd, $J = 10.2, 6.2$ Hz, 2H, aryl-CH), 7.22 (td, $J = 7.6, 7.0, 1.6$ Hz, 1H, aryl-CH), 7.38 (dd, $J = 8.8, 6.0$ Hz, 5H, aryl-CH), 7.52 (d, $J = 1.9$ Hz, 1H, aryl-CH), 7.67 (d, $J = 2.2$ Hz, 1H, aryl-CH).

BⁿNNO-MOM 10-MOM. Followed the same procedure as **5-MOM** starting from *N*-benzyl-2-bromoaniline. Crude yield: 91% yellow oil; some impurities were subsequently removed following deprotection. ¹H NMR (500 MHz, CDCl₃) δ 1.33 (s, 9H, C(CH₃)₃), 1.50 (s, 9H, C(CH₃)₃), 3.23 (s, 3H, CH₂OCH₃), 4.49 (s, 2H, CH₂OCH₃), 4.50 (d, *J* = 4.3 Hz, 2H, benzyl-CH₂), 6.69 (dd, *J* = 8.3, 1.2 Hz, 1H, aryl-CH), 6.76 (ddd, *J* = 8.2, 7.3, 1.1 Hz, 1H, aryl-CH), 7.14 – 7.17 (m, 2H, aryl-CH), 7.20 – 7.24 (m, 1H, aryl-CH), 7.29 – 7.33 (m, 1H, aryl-CH), 7.42 (d, *J* = 2.5 Hz, 1H, aryl-CH), 7.47 (d, *J* = 2.6 Hz, 1H, aryl-CH), 7.54 (dd, *J* = 7.7, 0.9 Hz, 1H, aryl-CH), 7.69 – 7.74 (m, 2H, aryl-CH), 7.84 (t, *J* = 7.9 Hz, 1H, aryl-CH), 9.44 (s, 1H, NH). ¹³C NMR (126 MHz, CDCl₃) δ 31.02 (C(CH₃)₃), 31.63 (C(CH₃)₃), 34.71 (C(CH₃)₃), 35.58 (C(CH₃)₃), 47.39 (benzyl-CH₂), 57.56 (CH₂OCH₃), 99.73 (CH₂OCH₃), 112.07, 112.94, 115.80, 119.92, 121.57, 124.86, 126.35, 126.62, 126.88, 128.41, 129.25, 130.50, 134.14, 137.27, 139.93, 142.45, 145.99, 148.16, 151.72, 156.54, 159.50 (aryl-C). HRMS (FAB+) *m/z*: calcd for C₃₄H₄₀N₂O₂ [M + H]⁺ 508.3090; found 508.3081.

BⁿNNO-H₂ 10-H₂. 1.0010 g of **10-MOM** was placed in a 100 mL round bottom flask charged with a stirbar and 5 mL of THF and 2 mL of MeOH were added to give a yellow solution. The flask was cooled to 0 °C with a water-ice bath; a 6 mL solution of 1:1 MeOH/conc. HCl was added dropwise resulting in the solution turning brighter yellow. The reaction was stirred for 30 min at 0 °C, then removed from the ice bath and allowed to reach room temperature while stirring was

continued overnight. The solution was then quenched with 2 M aq. NaOH to give a solution with neutral pH. The organic layer was extracted with diethyl ether (3 × 70 mL) and the combined organics were dried over magnesium sulfate and rotovapped to reveal a yellow oil, which was redissolved in dichloromethane and passed through a SiO₂ plug to give an orange oil. Recrystallization by dissolving in hot hexanes followed by cooling in the freezer yielded bright yellow crystals. 412.7 mg (45% yield). ¹H NMR (500 MHz, CDCl₃) δ 1.40 (s, 9H, C(CH₃)₃), 1.49 (s, 9H, C(CH₃)₃), 4.42 (s, 2H, benzyl-CH₂), 6.08 (s, 1H, NH), 6.70 (dd, *J* = 8.3, 1.0 Hz, 1H, aryl-CH), 6.80 (td, *J* = 7.4, 1.1 Hz, 1H, aryl-CH), 7.18 – 7.32 (m, 4H, aryl-CH), 7.40 (dd, *J* = 7.6, 1.6 Hz, 1H, aryl-CH), 7.42 – 7.46 (m, 3H, aryl-CH), 7.48 (dd, *J* = 7.7, 0.9 Hz, 1H, aryl-CH), 7.69 (d, *J* = 2.4 Hz, 1H, aryl-CH), 7.85 (d, *J* = 7.7 Hz, 1H, aryl-CH), 7.95 (t, *J* = 8.0 Hz, 1H, aryl-CH), 13.88 (s, 1H, OH). ¹³C NMR (126 MHz, CDCl₃) δ 29.75 (C(CH₃)₃), 31.77 (C(CH₃)₃), 34.52 (C(CH₃)₃), 35.47 (C(CH₃)₃), 47.99 (benzyl-CH₂), 111.79, 116.88, 118.29, 118.63, 121.42, 121.56, 123.50, 126.41, 127.01, 127.08, 128.71, 130.52, 130.61, 137.79, 139.12, 139.54, 140.26, 146.02, 156.18, 156.20, 158.35 (aryl-C). HRMS (FAB+) *m/z*: calcd for C₃₂H₃₆ON₂ [M]⁺ 464.2828; found 464.2817.

^{Ad}NNO-MOM 11-MOM. Followed the same procedure as **5-MOM** starting from *N*-Adamant-1-yl-2-bromoaniline. Precipitate forms while stirring overnight. Crude yield: 62% golden foamy oil; some impurities were subsequently removed following deprotection. ¹H NMR (500 MHz, CDCl₃) δ 1.35 (s, 9H, C(CH₃)₃), 1.51

(s, 9H, C(CH₃)₃), 1.57 – 1.75 (m, 6H, Ad-CH₂), 1.90 (dd, *J* = 7.1, 2.9 Hz, 6H, Ad-CH₂), 1.99 – 2.16 (m, 3H, Ad-CH), 3.30 (s, 3H, CH₂OCH₃), 4.56 (s, 2H, CH₂OCH₃), 7.12 – 7.19 (m, 1H, aryl-CH), 7.22 (ddd, *J* = 8.6, 7.0, 1.7 Hz, 1H, aryl-CH), 7.34 – 7.42 (m, 1H, aryl-CH), 7.45 (d, *J* = 2.5 Hz, 1H, aryl-CH), 7.48 (d, *J* = 2.6 Hz, 1H), 7.56 (dd, *J* = 7.7, 0.9 Hz, 1H, aryl-CH), 7.61 (ddd, *J* = 6.8, 5.1, 1.3 Hz, 2H, aryl-CH), 7.78 (t, *J* = 7.9 Hz, 1H, aryl-CH), 8.35 (s, 1H, NH). ¹³C NMR (126 MHz, CDCl₃) δ 29.77 (Ad-CH), 31.03 (C(CH₃)₃), 31.69 (C(CH₃)₃), 34.79 (C(CH₃)₃), 35.58 (C(CH₃)₃), 36.66 (Ad-CH₂), 43.01 (Ad-CH₂), 51.89 (Ad-quat), 57.56 (CH₂OCH₃), 99.61 (CH₂OCH₃), 119.35, 120.76, 122.31, 124.86, 126.34, 127.43, 128.86, 129.35, 130.12, 133.97, 136.87, 142.29, 145.82, 151.47, 156.17, 158.29, 159.93 (aryl-C). HRMS (FAB+) *m/z*: calcd for C₃₇H₄₉N₂O₂ [M + H]⁺ 553.3794; found 553.3790.

Ad^dNNO-H₂ 11-H₂. Followed the same procedure as **10-H₂** except used diethyl ether as the eluent through the SiO₂ plug instead of dichloromethane. An off-white powder precipitated from a hot hexanes solution cooled in the freezer. Yield: 42% off-white powder. ¹H NMR (500 MHz, CDCl₃) δ 1.39 (s, 9H, C(CH₃)₃), 1.49 (s, 9H, C(CH₃)₃), 1.62 – 1.70 (m, 6H, Ad-CH₂), 1.98 (d, *J* = 3.0 Hz, 6H, Ad-CH₂), 2.07 (s, 3H, Ad-CH), 5.44 (s, 1H, NH), 6.74 (td, *J* = 7.4, 1.1 Hz, 1H, aryl-CH), 7.12 (dd, *J* = 8.5, 1.2 Hz, 1H, aryl-CH), 7.22 – 7.26 (m, 1H, aryl-CH), 7.30 (dd, *J* = 7.6, 1.7 Hz, 1H, aryl-CH), 7.39 (dd, *J* = 7.7, 1.0 Hz, 1H, aryl-CH), 7.42 (d, *J* = 2.4 Hz, 1H, aryl-CH), 7.71 (d, *J* = 2.4 Hz, 1H, aryl-CH), 7.86 (d, *J* = 7.6 Hz,

1H, aryl-CH), 7.91 (dd, $J = 8.2, 7.6$ Hz, 1H, aryl-CH), 13.96 (s, 1H, OH). ^{13}C NMR (126 MHz, CDCl_3) δ 29.82 (Ad-CH), 29.87 ($\text{C}(\text{CH}_3)_3$), 31.79 ($\text{C}(\text{CH}_3)_3$), 34.52 ($\text{C}(\text{CH}_3)_3$), 35.45 ($\text{C}(\text{CH}_3)_3$), 36.60 (Ad-CH₂), 42.57 (Ad-CH₂), 51.87 (Ad-quat), 115.33, 116.22, 117.82, 118.15, 121.24, 121.90, 124.88, 126.38, 129.69, 131.21, 137.80, 138.93, 139.90, 144.59, 156.49, 156.62, 158.12 (aryl-C). HRMS (FAB+) m/z : calcd for $\text{C}_{35}\text{H}_{44}\text{ON}_2$ $[\text{M}]^+$ 508.3454; found 508.3441.

2-bromo-N-methoxyethylaniline 12. Copper (I) iodide (2.38 g, 0.0125 mol) and potassium phosphate (12.81 g, 0.0603 mol) were placed in a round bottom bomb charged with a stir bar. The bomb was sealed with a septum and placed under vacuum, then backfilled with Ar and isopropanol (30.0 ml), ethylene glycol (4.0 mL, 0.0717 mol), 2-methoxyethylamine (3.2 mL, 0.0368 mol) and 2-bromiodobenzene (3.9 mL, 0.0304 mol) were added via syringe. The flask was sealed with a Kontes valve and the reaction vessel was placed in a 90 °C oil bath to give a yellow suspension, which then turned green-blue within 30 min. The reaction was kept at 90 °C for 2 d then allowed to cool to room temperature and 30 mL of diethyl ether and 30 mL of water were added to the reaction mixture. The organic layer was extracted with diethyl ether (3 × 100 mL) and the combined organic phases were washed with water and brine until the aqueous layer was colorless (the first washes with water were teal). The combined organics were dried over sodium sulfate and the solvent was removed by rotary evaporation to give a brown oil. The oil was further purified by column

chromatography on silica gel using 10% ethyl acetate/hexanes ($R_f = 0.33$). 2.273 g brown oil (0.00989 mol, Yield: 33% yield). ^1H NMR (500 MHz, CDCl_3) δ 3.34 (t, $J = 5.3$ Hz, 2H, $\text{CH}_2\text{CH}_2\text{OCH}_3$), 3.42 (s, 3H, $\text{CH}_2\text{CH}_2\text{OCH}_3$), 3.65 (dd, $J = 5.7, 5.0$ Hz, 2H, $\text{CH}_2\text{CH}_2\text{OCH}_3$), 4.65 (s, 1H, NH), 6.58 (ddd, $J = 7.9, 7.4, 1.5$ Hz, 1H, aryl-CH), 6.65 (dd, $J = 8.1, 1.5$ Hz, 1H, aryl-CH), 7.18 (ddd, $J = 8.1, 7.3, 1.5$ Hz, 1H, aryl-CH), 7.43 (dd, $J = 7.9, 1.5$ Hz, 1H, aryl-CH). ^{13}C NMR (126 MHz, CDCl_3) δ 43.54 ($\text{CH}_2\text{CH}_2\text{OCH}_3$), 58.99 ($\text{CH}_2\text{CH}_2\text{OCH}_3$), 70.87 ($\text{CH}_2\text{CH}_2\text{OCH}_3$), 110.13, 111.49, 118.02, 128.54, 132.57, 145.11 (aryl-C). HRMS (FAB+) m/z : calcd for $\text{C}_9\text{H}_{12}\text{ONBr}$ $[\text{M}]^+$ 229.0102; found 229.0110.

MeOEt^{NO-MOM} 13-MOM. Followed the same procedure as **5-MOM** starting from 2-bromo-*N*-methoxyethylaniline **12**. Estimated yield: 81% brown oil. ^1H NMR (500 MHz, CDCl_3) δ 1.34 (s, 9H, $\text{C}(\text{CH}_3)_3$), 1.51 (s, 9H, $\text{C}(\text{CH}_3)_3$), 3.06 (s, 3H, $\text{CH}_2\text{CH}_2\text{OCH}_3$), 3.28 (s, 3H, OCH_2OCH_3), 3.40 – 3.43 (m, 2H, $\text{CH}_2\text{CH}_2\text{OCH}_3$), 3.51 – 3.55 (m, 2H, $\text{CH}_2\text{CH}_2\text{OCH}_3$), 4.57 (s, 2H, OCH_2OCH_3), 6.74 (td, $J = 7.5, 1.1$ Hz, 1H, aryl-CH), 6.79 (dd, $J = 8.3, 1.1$ Hz, 1H, aryl-CH), 7.27 – 7.31 (m, 1H, aryl-CH), 7.40 (d, $J = 2.5$ Hz, 1H, aryl-CH), 7.44 (d, $J = 2.5$ Hz, 1H, aryl-CH), 7.50 (dd, $J = 7.6, 0.9$ Hz, 1H, aryl-CH), 7.66 (ddd, $J = 7.8, 3.2, 1.3$ Hz, 2H, aryl-CH), 7.80 (t, $J = 7.9$ Hz, 1H, aryl-CH), 8.94 (t, $J = 5.6$ Hz, 1H, NH). ^{13}C NMR (126 MHz, CDCl_3) δ 31.06 ($\text{C}(\text{CH}_3)_3$), 31.69 ($\text{C}(\text{CH}_3)_3$), 34.76 ($\text{C}(\text{CH}_3)_3$), 35.60 ($\text{C}(\text{CH}_3)_3$), 43.02 ($\text{CH}_2\text{CH}_2\text{OCH}_3$), 57.62 (OCH_2OCH_3), 58.59 ($\text{CH}_2\text{CH}_2\text{OCH}_3$), 71.31 ($\text{CH}_2\text{CH}_2\text{OCH}_3$), 99.88 (OCH_2OCH_3), 111.43, 115.66, 119.94, 121.03,

121.73, 124.78, 126.42, 129.35, 129.42, 130.51, 137.09, 142.32, 145.89, 148.23, 151.77, 156.48, 159.47 (aryl-C). HRMS (FAB+) m/z : calcd for $C_{30}H_{41}O_3N_2$ [M + H]⁺ 477.3117; found 477.3115.

MeOEt **NNO-H₂ 13-H₂**. 1.4004 g of **13-MOM** was placed in a 100 mL round bottom flask charged with a stir bar, and 50-mL of THF was added to give a brown solution. The flask was cooled to 0 °C using a water-ice bath; a 50 mL solution of 4:1 v/v conc. HCl/THF was added dropwise; the reaction mixture was stirred for 30 minutes at 0 °C, then removed from the ice bath and allowed to reach room temperature while stirring was continued overnight. The reaction was quenched with a 2 M aq. NaOH solution to give a solution with neutral pH. The organic layer was extracted with Et₂O (3 × 50 mL) and the combined organics were dried over magnesium sulfate and rotovapped to yield a yellow-white solid, which was redissolved and passed through a SiO₂ plug, using 3:2 dichloromethane/hexanes as an eluent, to give a yellow crystalline solid. (428.6 mg, 0.991 mol, yield: 34%).
¹H NMR (500 MHz, CDCl₃) δ 1.38 (s, 9H, C(CH₃)₃), 1.49 (s, 9H, C(CH₃)₃), 3.16 (s, 3H, CH₂CH₂OCH₃), 3.38 (d, $J = 5.7$ Hz, 2H, CH₂CH₂OCH₃), 3.60 (t, $J = 5.8$ Hz, 2H, CH₂CH₂OCH₃), 5.80 (s, 1H, NH), 6.77 – 6.85 (m, 2H, aryl-CH), 7.30 – 7.35 (m, 1H, aryl-CH), 7.40 (dd, $J = 7.9, 1.6$ Hz, 1H, aryl-CH), 7.42 (d, $J = 2.4$ Hz, 1H, aryl-CH), 7.45 (dd, $J = 7.8, 0.9$ Hz, 1H, aryl-CH), 7.68 (d, $J = 2.3$ Hz, 1H, aryl-CH), 7.82 (d, $J = 8.1$ Hz, 1H, aryl-CH), 7.92 (t, $J = 7.9$ Hz, 1H, aryl-CH), 13.69 (s, 1H, OH). ¹³C NMR (126 MHz, CDCl₃) δ 29.78 (C(CH₃)₃), 31.77 (C(CH₃)₃), 34.50

(C(CH₃)₃), 35.43 (C(CH₃)₃), 43.24 (CH₂CH₂OCH₃), 58.72 (CH₂CH₂OCH₃), 71.01 (CH₂CH₂OCH₃), 111.41, 116.85, 118.21, 118.75, 121.44, 121.49, 123.57, 126.22, 130.57, 130.60, 137.57, 138.91, 140.16, 146.15, 156.02, 156.12, 158.34 (aryl-C). HRMS (FAB+) *m/z*: calcd for C₂₈H₃₇O₂N₂ [M + H]⁺ 433.2855; found 433.2869.

(10)ZrBn₂ 14. A 2 mL benzene solution of **10-H₂** (66.5 mg, 0.143 mmol) was added to a 2 mL benzene solution of ZrBn₄ (65.0 mg, 0.143 mmol) and stirred for ten minutes under inert atmosphere in the glovebox. Benzene was removed in vacuo from the resulting yellow solution to yield a yellow oil, which was redissolved in pentane and pumped dry several times to remove residual toluene to reveal a yellow powder. (90.8 mg, 0.123 mmol, yield: 86%). ¹H NMR (500 MHz, toluene-*d*₈) δ 1.40 (s, 9H, C(CH₃)₃), 1.64 (s, 9H, C(CH₃)₃), 2.06 (d, *J* = 10.2 Hz, 2H, Zr-CH₂), 2.22 (d, *J* = 10.3 Hz, 2H, Zr-CH₂), 4.85 (s, 2H, NCH₂Ph), 6.64 – 6.74 (m, 7H, aryl-CH), 6.77 – 6.81 (m, 1H, aryl-CH), 6.80 – 6.89 (m, 11H, aryl-CH), 7.07 (dd, *J* = 7.9, 1.6 Hz, 1H, aryl-CH), 7.25 (ddd, *J* = 8.5, 7.1, 1.6 Hz, 1H, aryl-CH), 7.35 (dd, *J* = 8.2, 1.2 Hz, 1H, aryl-CH), 7.40 (d, *J* = 2.3 Hz, 1H, aryl-CH), 7.60 (d, *J* = 2.2 Hz, 1H, aryl-CH). ¹³C NMR (126 MHz, toluene-*d*₈) δ 30.90 (C(CH₃)₃), 32.24 (C(CH₃)₃), 34.97 (C(CH₃)₃), 36.14 (C(CH₃)₃), 55.96 (NCH₂), 65.65 (ZrCH₂), 121.70, 121.92, 122.33, 122.38, 123.75, 124.91, 125.00, 126.94, 127.35, 127.58, 127.92, 128.08, 128.67, 129.59, 131.74, 133.00, 138.49, 138.96, 140.76, 141.64, 142.29, 143.84, 156.24, 156.30, 157.26 (aryl-C). Anal. Calcd for

$C_{46}H_{48}N_2OZr$ (%): C, 75.06; H, 6.57; N, 3.81. Found (1): C, 68.19; H, 6.23; N, 3.79. (2) C, 66.65; H, 6.08; N, 4.24. (This compound is air- and moisture-sensitive and despite repeated attempts satisfactory analysis could not be obtained.)

(10)TiCl₂ 15. A 3 mL benzene solution of **10-H₂** (60.4 mg, 0.130 mmol) was added to a 3 mL benzene solution of TiCl₂(NMe₂)₂ (26.9 mg, 0.131 mmol) and stirred for ten minutes under inert atmosphere in the glovebox. Benzene was removed in vacuo from the resulting dark red solution to yield a deep purple solid, which was triturated several times with pentane to remove free dimethylamine (77.6 mg, 0.133 mmol, quantitative yield). ¹H NMR (300 MHz, C₆H₅Cl) δ 1.30 (s, 9H, C(CH₃)₃), 1.66 (s, 9H, C(CH₃)₃), 4.95 (s, 1H, NCH₂), 6.12 (s, 1H, NCH₂), 6.60 – 6.85 (m, 6H, aryl-CH), 7.02 – 7.12 (m, 2H, aryl-CH), 7.17 (dd, *J* = 7.8, 1.0 Hz, 1H, aryl-CH), 7.25 – 7.34 (m, 1H, aryl-CH), 7.48 (t, *J* = 8.0 Hz, 1H, aryl-CH), 7.56 (dd, *J* = 8.0, 1.5 Hz, 1H, aryl-CH), 7.63 – 7.72 (m, 3H, aryl-CH). ¹³C NMR (126 MHz, C₆D₅Cl, –15 °C) δ 31.41 C(CH₃)₃, 32.45 (C(CH₃)₃), 35.69 (C(CH₃)₃), 36.63 C(CH₃)₃, 117.29, 123.11, 123.98, 126.02, 128.18, 129.55, 130.64, 132.98, 138.48, 139.58, 139.67, 145.83, 153.52, 155.43, 159.48 (aryl-C). Anal. Calcd for C₃₂H₃₄Cl₂N₂OTi (%): C, 66.11; H, 5.89; N, 4.82. Found: C, 65.98; H, 6.06; N, 4.87.

(11)TiCl₂ 16. A 3 mL benzene solution of **11-H₂** (67.6 mg, 0.133 mmol) was added to a 3 mL benzene solution of TiCl₂(NMe₂)₂ (27.5 mg, 0.133 mmol) and stirred for ten minutes under inert atmosphere in the glovebox. Benzene was removed in vacuo from the resulting dark red solution to yield a light orange solid, which was triturated several times with pentane to remove free dimethylamine (86.4 mg, 0.134 mmol, quantitative yield). ¹H NMR (500 MHz, C₆D₅Cl) δ 1.30 (s, 9H, C(CH₃)₃), 1.33 – 1.39 (m, Ad-CH₂, 6H), 1.63 – 1.71 (m, 6H, Ad-CH₂), 1.78 (s, 9H, C(CH₃)₃), 1.79 (br s, 3H, Ad-CH), 7.24 (dd, *J* = 7.7, 1.0 Hz, 1H, aryl-CH), 7.36 – 7.43 (m, 2H, aryl-CH), 7.48 – 7.55 (m, 2H, aryl-CH), 7.58 – 7.62 (m, 1H, aryl-CH), 7.71 (q, *J* = 2.4 Hz, 2H, aryl-CH), 7.77 (dd, *J* = 8.3, 1.1 Hz, 1H, aryl-CH). ¹³C NMR (126 MHz, C₆D₅Cl) δ 29.93 (Ad-CH), 30.36 (C(CH₃)₃), 31.31 (C(CH₃)₃), 34.60 (C(CH₃)₃), 35.69 (C(CH₃)₃), 35.87 (Ad-CH₂), 42.62 (Ad-CH₂), 69.51 (Ad-quat), 122.09, 122.25, 123.34, 123.72, 127.83, 128.65, 130.31, 131.13, 132.03, 133.17, 134.16, 137.90, 139.15, 144.77, 152.18, 153.39, 158.07 (aryl-C). Anal. Calcd for C₃₅H₄₂Cl₂N₂OTi (%): C, 67.21; H, 6.77; N, 4.48. Found (1): C, 66.53; H, 6.80; N, 4.20. (2) C, 66.37; H, 6.73; N, 4.36. (This compound is air- and moisture-sensitive and despite repeated attempts satisfactory %C analysis could not be obtained.)

(13)ZrBn₂ 17. A 2 mL benzene solution of **13-H₂** (62.2 mg, 0.143 mmol) was added to a 2 mL benzene solution of ZrBn₄ (65.5 mg, 0.143 mmol) and stirred for ten minutes under inert atmosphere in the glovebox. Benzene was removed in

vacuo from the resulting yellow solution to yield a yellow oil, which was redissolved in pentane and pumped dry several times to remove residual toluene to reveal a yellow powder. (100.7 mg, 0.143 mmol, quantitative yield: 86%). This complex is fluxional at rt. Upon cooling, the pendant L-donor appears to coordinate irreversibly to Zr leading to a C_1 complex with diastereotopic benzyl and ethyl protons. ^1H NMR (500 MHz, toluene- d_8 , $-40\text{ }^\circ\text{C}$) δ 1.44 (s, 9H, $\text{C}(\text{CH}_3)_3$), 1.60 (s, 9H, $\text{C}(\text{CH}_3)_3$), 2.11 – 2.16 (m, 1H, ethyl- CH_2), 2.32 (d, $J = 9.5$ Hz, 1H, Zr- CH_2), 2.39 (d, $J = 10.4$ Hz, 1H, Zr- CH_2), 2.58 (t, $J = 7.1$ Hz, 2H, ethyl- CH_2 , Zr- CH_2), 2.77 (td, $J = 11.6, 5.3$ Hz, 1H, ethyl- CH_2), 2.82 – 2.92 (m, 2H, ethyl- CH_2 , Zr- CH_2), 3.30 (s, 3H, OCH_3), 6.48 (d, $J = 7.5$ Hz, 2H, aryl- CH), 6.54 (dd, $J = 8.3, 1.2$ Hz, 1H, aryl- CH), 6.70 (t, $J = 7.3$ Hz, 1H, aryl- CH), 6.74 (dd, $J = 7.8, 1.1$ Hz, 1H, aryl- CH), 6.84 (t, $J = 7.4$ Hz, 2H, aryl- CH), 6.88 (d, $J = 9.5$ Hz, 1H, aryl- CH), 6.90 (t, $J = 8.8$ Hz, 1H, aryl- CH), 7.07 (s, 1H, aryl- CH), 7.20 (dd, $J = 8.0, 1.2$ Hz, 1H, aryl- CH), 7.26 (d, $J = 2.4$ Hz, 1H, aryl- CH), 7.40 (t, $J = 7.4$ Hz, 3H, aryl- CH), 7.71 (d, $J = 2.5$ Hz, 1H, aryl- CH).

2-(3,5-di-*t*-butyl-2-(methoxymethoxy)phenyl)-6-(*o*-tolyl)pyridine CNO-MOM

18-MOM. An oven-dried 25 mL Schlenk bomb was charged with a stirbar, evacuated and refilled with Ar. Under positive Ar pressure, 0.750 g of **2**, 0.251 g of *o*-tolyl-boronic acid, 0.107 g of $\text{Pd}(\text{PPh}_3)_4$ and 0.784 g of K_3PO_4 crushed with a mortar and pestle were added and the vessel was sealed with a septum. The vessel was evacuated and refilled with Ar three times, and then 5 mL of dry

toluene was added via syringe and the vessel was sealed with a Kontes valve. The reaction mixture was stirred at room temperature for 10 min, then the vessel was placed in a 100 °C oil bath for 18 h, then cooled to room temperature, and the suspension filtered through celite with the aid of Et₂O. Solvent was removed in vacuo and the resulting residue was redissolved in dichloromethane and passed through a SiO₂ plug using 1:9 Et₂O/hexanes as the eluent. 0.742 g (96% crude yield). ¹H NMR (500 MHz, CDCl₃) δ 1.35 (s, 9H, C(CH₃)₃), 1.50 (s, 9H, C(CH₃)₃), 2.53 (s, 3H, tolyl-CH₃), 3.37 (s, 3H, CH₂OCH₃), 4.61 (s, 2H, CH₂OCH₃), 7.28 – 7.34 (m, 3H, aryl-CH), 7.38 (dd, *J* = 7.7, 1.0 Hz, 1H, aryl-CH), 7.44 (d, *J* = 2.6 Hz, 1H, aryl-CH), 7.48 – 7.52 (m, 1H, aryl-CH), 7.52 (dd, *J* = 2.6, 0.8 Hz, 1H, aryl-CH), 7.69 (dd, *J* = 7.9, 0.9 Hz, 1H, aryl-CH), 7.79 (t, *J* = 7.7 Hz, 1H, aryl-CH). ¹³C NMR (126 MHz, CDCl₃) δ 20.87 (tolyl-CH₃), 31.03 (C(CH₃)₃), 31.61 (C(CH₃)₃), 34.73 (C(CH₃)₃), 35.55 (C(CH₃)₃), 57.52 (CH₂OCH₃), 99.60 (CH₂OCH₃), 122.05, 123.03, 124.96, 125.99, 126.65, 128.35, 129.89, 131.02, 134.23, 136.19, 136.33, 140.54, 142.34, 146.00, 151.36, 157.76, 160.16 (aryl-C). HRMS (FAB+) *m/z*: calcd for C₂₈H₃₆O₂N [M + H]⁺ 418.2746; found 418.2726.

2,4-di-*t*-butyl-6-(6-(*o*-tolyl)pyridin-2-yl)phenol CNO-H₂ 18-H₂. 0.355 g of **18-MOM** was placed in a 50 mL round bottom flask charged with a stirbar and 20 mL of THF was added to give a colorless solution. The flask was cooled to 0 °C with a water-ice bath; a 15 mL solution of 1:1 THF/conc. HCl was added dropwise. The reaction was stirred for 30 min at 0 °C, then removed from the ice

bath and allowed to reach room temperature while stirring, which resulted in the reaction solution turning pale translucent yellow. Stirring was continued overnight, and then the solution was quenched with 2 M aq. NaOH to give a solution with neutral pH. The organic layer was extracted with diethyl ether (3 × 30 mL) and the combined organics were dried over magnesium sulfate and rotovapped to reveal a yellow oil, which was precipitated from hot hexanes followed by cooling in the freezer to give a pale yellow powder. 0.173 g (54% yield). ¹H NMR (500 MHz, CDCl₃) δ 1.39 (s, 9H, C(CH₃)₃), 1.48 (s, 9H, C(CH₃)₃), 2.42 (s, 3H, tolyl-CH₃), 7.29 – 7.41 (m, 4H, aryl-CH), 7.43 (d, *J* = 2.4 Hz, 1H, aryl-CH), 7.46 (dt, *J* = 7.0, 1.4 Hz, 1H, aryl-CH), 7.74 (d, *J* = 2.4 Hz, 1H, aryl-CH), 7.87 – 7.94 (m, 2H, aryl-CH), 14.67 (s, 1H, OH). ¹³C NMR (126 MHz, CDCl₃) δ 20.59 (tolyl-CH₃), 29.71 (C(CH₃)₃), 31.79 (C(CH₃)₃), 34.51 (C(CH₃)₃), 35.45 (C(CH₃)₃), 117.75, 117.95, 120.99, 121.68, 126.18, 126.36, 128.81, 129.73, 131.13, 136.07, 137.80, 137.90, 139.35, 139.79, 156.42, 157.16, 158.55 (aryl-C). HRMS (FAB+) *m/z*: calcd for C₂₆H₃₁ON [M]⁺ 373.2406; found 373.2424.

(18)TiBn₂ 19. To a stirring slurry of **18-H₂** (30.2 mg, 0.081 mmol) in 5:1 pentane/ether was added to a 3 mL solution of TiBn₄ (33.4 mg, 0.081 mmol) and the resulting red solution was stirred for ten minutes under inert atmosphere in the glovebox. The reaction solution was passed through a pad of celite to remove impurities and with 5:1 pentane/ether, then solvent was removed in vacuo to yield a dark red solid, which was triturated several times with pentane before being

redissolved in 5:1 pentane/ether and recrystallized by cooling in the freezer. (30.2 mg, 0.050 mmol, 62% yield). ^1H NMR (300 MHz, toluene- d_8) δ 1.37 (s, 9H, $\text{C}(\text{CH}_3)_3$), 1.85 (s, 9H, $\text{C}(\text{CH}_3)_3$), 2.21 (s, 3H, Ar- CH_3), 3.88 (d, $J = 8.3$ Hz, 2H, Ti- CH_2), 4.15 (d, $J = 8.3$ Hz, 2H, Ti- CH_2), 6.33 – 6.44 (m, 2H, aryl- CH), 6.54 (t, $J = 7.7$ Hz, 4H, aryl- CH), 6.63 – 6.71 (m, 4H, aryl- CH), 6.82 (d, $J = 4.7$ Hz, 2H, aryl- CH), 7.13 (d, $J = 5.4$ Hz, 1H, aryl- CH), 7.23 (t, $J = 7.1$ Hz, 1H, aryl- CH), 7.37 (d, $J = 2.4$ Hz, 1H, aryl- CH), 7.69 (d, $J = 2.4$ Hz, 1H, aryl- CH), 8.51 (d, $J = 6.9$ Hz, 1H, aryl- CH). ^{13}C NMR (126 MHz, C_6D_6) δ 23.59 (tolyl- CH_3), 30.99 ($\text{C}(\text{CH}_3)_3$), 31.84 ($\text{C}(\text{CH}_3)_3$), 34.66 ($\text{C}(\text{CH}_3)_3$), 35.80 ($\text{C}(\text{CH}_3)_3$), 92.42 (Ti- CH_2), 119.61, 121.77, 123.32, 124.72, 125.70, 126.58, 127.75, 128.57, 129.33, 131.13, 132.54, 132.65, 133.00, 136.76, 137.81, 138.66, 142.08, 157.60, 158.15, 165.17, 204.42 (aryl-C). Anal. Calcd for $\text{C}_{40}\text{H}_{43}\text{NOTi}$ (%): C, 79.85; H, 7.20; N, 2.33. Found (1): C, 74.91; H, 6.99; N, 2.33. (2) C, 74.74; H, 6.86; N, 2.32. (This compound is air- and moisture-sensitive and despite repeated attempts satisfactory %C analysis could not be obtained.)

Recovery of Ligand 5 from Small Scale Polymerization Reaction with 8 and 1-Hexene. To a 20 mL vial in the glovebox was added 1 mL of 1-hexene and 50 equiv (0.193 g) of dry MAO. The 1-hexene/MAO solution was stirred for 5 min, then a solution of **8** dissolved in 1 mL of PhCl was added to the vial and the reaction was stirred for 25 min at room temperature. The vial was then removed from the glovebox and 2 mL of D_2O were added slowly, followed by 5 drops of

conc. HCl, and 4 mL of D₂O, which resulted in de-colorization of the dark red solution. The organic layer was extracted with hexanes (3 × 4 mL) and the combined organics were dried over magnesium sulfate and solvent removed *in vacuo* to reveal a pale yellow solid. 44.9 mg (5-D₂ and poly-1-hexene). MS (FAB+) *m/z*: calcd for C₃₃H₃₈ON₂ [M]⁺ 478.2984; found 478.3524.

2-(3,5-di-*t*-butyl-2-(methoxymethoxy)phenyl)-6-(3,5-di-*t*-butylphenyl)pyridine

ArNO-MOM 20-MOM. An oven-dried 50 mL Schlenk bomb was charged with a stirbar, evacuated and refilled with Ar. Under positive Ar pressure, 0.501 g of 2-bromo-6-(3,5-di-*t*-butylphenyl)pyridine, 0.547 g of **1**, 67.8 mg of Pd₂dba₃, 62.2 mg SPhos and 0.624 g of K₃PO₄ crushed with a mortar and pestle were added and the vessel was sealed with a septum. The vessel was evacuated and refilled with Ar three times, and then 10 mL of dry toluene was added via syringe and the vessel was sealed with a Kontes valve. The reaction mixture was stirred at room temperature for 10 min, then the vessel was placed in a 100 °C oil bath for 42 h, then cooled to room temperature, and the suspension filtered through celite with the aid of Et₂O. Solvent was removed *in vacuo* and the resulting residue was redissolved in dichloromethane and passed through a SiO₂ plug using 1:9 Et₂O/hexanes as the eluent. 0.749 g (quantitative crude yield). ¹H NMR (500 MHz, CDCl₃) δ 1.39 (s, 9H, C(CH₃)₃), 1.42 (s, 18H, C(CH₃)₃), 1.53 (s, 9H, C(CH₃)₃), 3.42 (s, 3H, CH₂OCH₃), 4.65 (s, 2H, CH₂OCH₃), 7.46 (d, *J* = 2.6 Hz, 1H, aryl-CH), 7.53 (t, *J* = 1.8 Hz, 1H, aryl-CH), 7.69 (dd, *J* = 7.5, 1.3 Hz, 1H, aryl-CH), 7.73 (d,

$J = 2.6$ Hz, 1H, aryl-CH), 7.75 (dd, $J = 7.8, 1.4$ Hz, 1H, aryl-CH), 7.78 (d, $J = 7.6$ Hz, 1H, aryl-CH), 7.98 (d, $J = 1.8$ Hz, 2H, aryl-CH). ^{13}C NMR (126 MHz, CDCl_3) δ 31.04 ($\text{C}(\text{CH}_3)_3$), 31.63 ($\text{C}(\text{CH}_3)_3$), 31.65 ($\text{C}(\text{CH}_3)_3$), 34.77 ($\text{C}(\text{CH}_3)_3$), 35.15 ($\text{C}(\text{CH}_3)_3$), 35.60 ($\text{C}(\text{CH}_3)_3$), 57.59 (CH_2OCH_3), 99.53 (CH_2OCH_3), 118.65, 121.50, 122.92, 123.31, 124.91, 127.08, 128.54, 129.11, 134.05, 136.66, 139.06, 142.38, 145.91, 151.14, 151.49, 157.72, 158.21 (aryl-C). HRMS (FAB+) m/z : calcd for $\text{C}_{35}\text{H}_{50}\text{O}_2\text{N}$ $[\text{M} + \text{H}]^+$ 516.3842; found 516.3836.

2,4-di-*t*-butyl-6-(6-(3,5-di-*t*-butylphenyl)pyridin-2-yl)phenol ArNO-H 20-H.

Followed the same procedure as **18-H₂**. A yellow powder precipitated from a hot hexanes solution cooled in the freezer. Yield: 53% yellow powder. ^1H NMR (500 MHz, CDCl_3) δ 1.39 (s, 9H, $\text{C}(\text{CH}_3)_3$), 1.43 (s, 18H, $\text{C}(\text{CH}_3)_3$), 1.52 (s, 9H, $\text{C}(\text{CH}_3)_3$), 7.44 (d, $J = 2.4$ Hz, 1H, aryl-CH), 7.57 (t, $J = 1.8$ Hz, 1H, aryl-CH), 7.65 (dd, $J = 7.0, 1.5$ Hz, 1H, aryl-CH), 7.73 (d, $J = 2.3$ Hz, 1H, aryl-CH), 7.85 – 7.93 (m, 4H, aryl-CH), 15.19 (s, 1H, OH). ^{13}C NMR (126 MHz, CDCl_3) δ 29.70 ($\text{C}(\text{CH}_3)_3$), 31.60 ($\text{C}(\text{CH}_3)_3$), 31.81 ($\text{C}(\text{CH}_3)_3$), 34.51 ($\text{C}(\text{CH}_3)_3$), 35.24 ($\text{C}(\text{CH}_3)_3$), 35.52 ($\text{C}(\text{CH}_3)_3$), 117.77, 118.00, 118.11, 120.95, 121.57, 123.80, 126.29, 137.62, 137.89, 138.40, 139.71, 151.69, 155.16, 157.37, 158.87 (aryl-C). HRMS (FAB+) m/z : calcd for $\text{C}_{33}\text{H}_{45}\text{ON}$ $[\text{M}]^+$ 471.3501; found 471.3508.

6-(3,5-di-*t*-butyl-2-(methoxymethoxy)phenyl)picolinaldehyde. A 100 mL Schlenk bomb was charged with a stirbar and 1.24 g (6.65 mmol) 6-

bromopyridine-2-carboxaldehyde, 2.50 g (6.65 mmol) 2-(3,5-di-*tert*-butyl-2-(methoxymethoxy)phenyl)-4,4,5,5-tetramethyl-1,3,2-dioxaborolane, and 0.385 g (0.333 mmol) Pd(PPh₃)₄ were added and the vessel was sealed with a septum. The bomb was evacuated and refilled with argon three times. 25 mL of dry toluene and 10 mL of 2 M Na₂CO₃ were injected into the vessel with a syringe, and the vessel was sealed with a Kontes valve. The reaction mixture was placed in an oil bath at 100°C and was stirred overnight. The organic layer was extracted using methylene chloride (4 x 30 mL), and the combined organics were dried with magnesium sulfate and rotovapped. The product, a white powder, was purified by chromatography on SiO₂ using 1:10 ethyl acetate/hexane. (2.1412 g, 6.0236 mmol, 91% yield). ¹H NMR (500 MHz, CDCl₃) δ 1.35 (s, 9H, C(CH₃)₃), 1.48 (s, 9H, C(CH₃)₃), 3.25 (s, 3H, CH₂OCH₃), 4.55 (s, 2H, CH₂OCH₃), 7.48 (s, 2H, aryl-CH), 7.68 – 8.03 (m, 3H, aryl-CH), 10.17 (s, CHO). ¹³C NMR (126 MHz, CDCl₃) δ 31.08 (C(CH₃)₃), 31.60 (C(CH₃)₃), 34.83 (C(CH₃)₃), 35.60 (C(CH₃)₃), 57.40 (CH₂OCH₃), 100.02 (CH₂OCH₃), 119.67, 125.80, 126.34, 129.75, 133.17, 136.90, 142.83, 146.62, 151.63, 152.98, 159.41 (aryl-C), 194.00 (CHO).

Amido(pyridine)phenoxide N-((6-(3,5-di-*t*-butyl-2-(methoxymethoxy)phenyl)pyridin-2-yl)methyl)-1-phenylethanamine 21-MOM. To a 100 mL round-bottom flask charged with a stirbar was added a 1.00 g (2.81 mmol) slurry of 6-(3,5-di-*tert*-butyl-2-(methoxymethoxy)phenyl)picolinaldehyde in 15 mL of acetonitrile, and 363 μL of DL- α -methylbenzylamine (2.81 mmol) was added via syringe.

The reaction mixture was stirred for 30 minutes, then 0.924 g of NaHB(OAc)₃ was added and stirring was continued for one hour. The reaction was then quenched with 60 mL saturated sodium bicarbonate solution, and the organic layer was extracted with ether (3 x 50 mL). The combined organics were dried over magnesium sulfate and rotovapped to yield a colorless oil. (1.0947 g, 2.3764 mmol, 85% yield). ¹H NMR (500 MHz, CDCl₃) δ 1.36 (s, 9H, C(CH₃)₃), 1.47 (d, *J* = 6.5 Hz, 3H, CH(CH₃)), 1.50 (s, 9H, C(CH₃)₃), 2.34 (s, 1H, NH), 3.33 (s, 3H, CH₂OCH₃), 3.86 (s, 1H, CH₂), 3.91 (q, *J* = 6.6 Hz, 1H, CH(CH₃)), 4.55 (s, 2H, CH₂OCH₃), 7.17 (dd, *J* = 7.6, 1.0 Hz, 1H, aryl-CH), 7.22 – 7.30 (m, 1H, aryl-CH), 7.36 (t, *J* = 7.6 Hz, 2H, aryl-CH), 7.38 – 7.48 (m, 4H, aryl-CH), 7.58 (dd, *J* = 7.8, 1.1 Hz, 1H, aryl-CH), 7.66 (t, *J* = 7.7 Hz, 1H, aryl-CH). ¹³C NMR (126 MHz, CDCl₃) δ 24.44 (CH(CH₃)), 31.03 (C(CH₃)₃), 31.63 (C(CH₃)₃), 34.77 (C(CH₃)₃), 35.58 (C(CH₃)₃), 53.04 (CH₂), 57.46 (CH₂OCH₃), 58.09 (CH(CH₃)), 99.52 (CH₂OCH₃), 120.51, 123.40, 125.10, 126.46, 127.00, 127.16, 128.62, 133.99, 136.46, 142.49, 145.33, 146.07, 151.41, 158.06, 159.52 (aryl-C). HRMS (FAB+) *m/z*: calcd for C₃₀H₄₁N₂O₂ [M + H]⁺ 461.3168; found 461.3161.

Amido(pyridine)phenoxide 2,4-di-tert-butyl-6-(6-(((1-phenylethyl)amino)-methyl)pyridin-2-yl)phenol 21-H₂. To a 250 mL round-bottom flask charged with a stirbar was added 1.0947 g (0.00263 mol) of N-((6-(3,5-di-tert-butyl-2-(methoxymethoxy)phenyl)pyridin-2-yl)methyl)-1-phenylethylamine and 10.5 mL of THF. To the stirring solution was added 10.5 mL of a 2:1 conc. HCl/THF

solution, and stirring was continued at room temperature overnight. Solvent was removed in vacuo to yield the hydrochloride salt, which was washed with ether. The salt was then dissolved in 10 mL methylene chloride and a saturated sodium bicarbonate solution was added until the aqueous layer reached a neutral pH. The organic layer was extracted with methylene chloride (4 x 20 mL) and the combined organics were dried over magnesium sulfate and solvent was removed in vacuo to yield a yellow oil. (0.9700 g, 2.3284 mmol, 88% yield) ^1H NMR (500 MHz, CD_2Cl_2) δ 1.44 (s, 9H, $\text{C}(\text{CH}_3)_3$), 1.45 (d, $J = 6.8$ Hz, 3H, $\text{CH}(\text{CH}_3)$), 1.58 (s, 9H, $\text{C}(\text{CH}_3)_3$), 1.96 (s, 1H, NH), 3.80 – 3.95 (m, 3H, $\text{CH}(\text{CH}_3)$, CH_2), 7.28 (d, $J = 8.0$ Hz, 1H, aryl- CH), 7.31 (d, $J = 7.2$ Hz, 1H, aryl- CH), 7.37 – 7.42 (m, 2H, aryl- CH), 7.43 – 7.47 (m, 2H, aryl- CH), 7.49 (d, $J = 2.4$ Hz, 1H, aryl- CH), 7.76 (d, $J = 2.4$ Hz, 1H, aryl- CH), 7.81 (t, $J = 7.9$ Hz, 1H, aryl- CH), 7.87 (d, $J = 8.1$ Hz, 1H, aryl- CH), 14.83 (s, 1H, OH). ^{13}C NMR (126 MHz, CD_2Cl_2) δ 24.98 ($\text{CH}(\text{CH}_3)$), 30.08 ($\text{C}(\text{CH}_3)_3$), 32.07 ($\text{C}(\text{CH}_3)_3$), 34.91 ($\text{C}(\text{CH}_3)_3$), 35.87 ($\text{C}(\text{CH}_3)_3$), 52.83 ($\text{CH}(\text{CH}_3)$), 58.16 (CH_2), 118.36, 118.56, 120.22, 121.58, 126.67, 127.40, 127.58, 129.08, 138.07, 138.70, 140.44, 146.14, 157.51, 157.88, 159.03, 171.28 (aryl-C). HRMS (FAB+) m/z : calcd for $\text{C}_{33}\text{H}_{38}\text{N}_2\text{O}$ $[\text{M}]^+$ 446.3297; found 446.3286.

(21)TiBn₂ 22. A solution of 11.3 mg (0.0274 mmol) of TiBn_4 in C_6D_6 was added to a solution of 11.4 mg (0.0274 mmol) of **21-H₂** in C_6D_6 in the glovebox to produce the deep-red complex. The identity of the complex was confirmed by ^1H NMR spectroscopy. ^1H NMR (300 MHz, C_6D_6) δ 1.38 (s, 9H), 1.74 (d, $J = 6.8$ Hz, 3H),

2.00 (s, 9H), 3.32 (d, $J = 9.6$ Hz, 1H), 3.35 (d, $J = 8.5$ Hz, 1H), 3.53 (d, $J = 9.1$ Hz, 1H), 3.60 (d, $J = 8.5$ Hz, 1H), 4.37 (d, $J = 20.9$ Hz, 1H), 4.54 (d, $J = 21.0$ Hz, 1H), 6.21 (d, $J = 7.6$ Hz, 1H), 6.33 (t, $J = 7.1$ Hz, 1H), 6.39 – 6.45 (m, 2H), 6.48 – 6.61 (m, 2H), 6.79 (td, $J = 7.8, 3.6$ Hz, 4H), 7.22 (t, $J = 7.5$ Hz, 3H), 7.41 – 7.51 (m, 3H), 7.60 (d, $J = 2.4$ Hz, 1H), 7.81 (d, $J = 2.4$ Hz, 1H).

(21)HfBn₂ 23. A solution of 21.6 mg (0.0398 mmol) HfBn₄ in C₆D₆ was added to a solution of 16.6 mg (0.0398 mmol) **21-H₂** in C₆D₆ in the glovebox to yield a gold-colored solution. The identity of the metal complex was confirmed by ¹H NMR spectroscopy.

(21)TiCl₂ 24. A solution of 52.00 mg (0.051 mmol) TiCl₂(NMe₂)₂ in C₆D₆ was added to a solution of 21.2 mg (0.051 mmol) **21-H₂** in C₆D₆ in the glovebox to produce the deep purple solution. Solvents were removed in vacuo. (137.6 mg, quantitative yields). 15 mg of the compound were recrystallized in THF/DCM. The identity of the resulting metal complex was confirmed by X-ray crystallography and ¹H NMR spectroscopy.

Polymerization of 8 at KFUPM. To the new glass reactor of the new computer controlled polymerization instrument was added 50 mL of dry toluene, 1 mL triisobutylaluminum, and 24.2 mL 10 wt% MAO in toluene (1000 equiv) at about 10 °C. The temperature was adjusted to 10 °C and the nitrogen was replaced

with propylene (2 bar). A 30 μmol (18 mg) sample of catalyst **8** was transferred to a small vial in the Ar-filled glovebox and capped with a septum. The sample was dissolved in 10 mL of toluene and transferred to the reactor against a propylene flow at 10 °C. The reactor was closed, and propylene was rapidly added to give a total volume of approximately 150 mL at 10 °C, whereupon the temperature increased to approx. 20 °C and pressure to approx. 6 bar. Propylene addition was stopped, and stirring increased to 800 rpm, T = 25 °C and p = 7.2 bar (8.2 atm). The reaction was run for 30 min to give approx. 2:1 liquid propylene:toluene. The reactor was vented and opened when most liquid propylene had evaporated. A film of polymer formed on evaporation from the stainless steel pan that we decanted the toluene and polymer solution into. A solid polymer formed on addition of a couple of mL of methanol. Air drying overnight yielded crude weight of PP of about 14 g. Crude polymer was dissolved in toluene, washed with HCl/methanol (about 1:10) and placed in a separatory funnel. Toluene layer was placed in flask and reduced by half in volume, then transferred to stainless steel pan to evaporate remaining toluene. The polymer did not crystallize. Transferred with some toluene to flask and pumped mostly dry. Gave oily uncrystalline product.

Polymerization of 8 at Dow Chemical. Reactor Procedures: Propylene polymerizations were conducted in a 1.8 L SS batch reactor. This reactor was manufactured by Buchi AG and sold by Mettler, and is heated/cooled via the

vessel jacket and reactor head. Syltherm™ 800 is the heat transfer fluid used and is controlled by a separate heating/cooling skid. Both the reactor and the heating/cooling system are controlled and monitored by a Camile TG process computer. The bottom of the reactor is fitted with a large orifice bottom dump valve, which empties the reactor contents into a 6 L SS dump pot. The dump pot is vented to a 30 gal. blowdown tank, with both the pot and the tank N₂ purged. All chemicals used for polymerization or catalyst makeup are run through purification columns, to remove any impurities that may affect polymerization. The propylene and toluene were passed through 2 columns, the first containing A2 alumina, the second containing Q5 reactant. The N₂ was passed through a single Q5 reactant column. The reactor was cooled to 50°C for chemical additions. The Camile then controlled the addition of 700 g. of IsoparE, using a micro-motion flowmeter to add accurately the desired amount. The 150 g. of propylene was then added through the micro-motion flowmeter. The reactor is then preloaded with MMAO to scavenge any impurities in the feeds. After the chemicals are in the reactor, the reactor was heated up to 70°C for polymerization. The catalyst solution (0.005 M in toluene) is mixed with the desired activator and transferred into the catalyst shot tank. This is followed by 3 rinses of toluene, 5 mL each. Immediately after catalyst addition to the reactor, the run timer begins. For successful polymerizations, exotherm and pressure drops were observed. These polymerizations were run for 15 min., then the agitator was stopped, the reactor pressured up to ~500 psi with N₂, and the

bottom dump valve opened to empty reactor contents to the dump pot. The dump pot contents are poured into trays that are set in a vacuum oven, where they are heated up to 140°C under vacuum to remove any remaining solvent. After the trays cool to ambient temperature, the polymers are weighed for yields and submitted for polymer testing.

Procedure for GPC Analysis performed by Dow Chemical. Molecular weight distribution (M_w , M_n) information was determined by analysis on a custom Dow-built Robotic-Assisted Dilution High-Temperature Gel Permeation Chromatographer (RAD-GPC). Polymer samples were dissolved for 90 minutes at 160°C at a concentration of 30mg/mL in 1,2,4-trichlorobenzene (TCB) stabilized by 300ppm BHT, while capped and with stirring. They were then diluted to 1mg/mL immediately before a 400 μ L aliquot of the sample was injected. The GPC utilized two (2) Polymer Labs PLgel 10 μ m MIXED-B columns (300x10mm) at a flow rate of 2.0mL/minute at 150°C. Sample detection was performed using a PolyChar IR4 detector in concentration mode. A conventional calibration of narrow Polystyrene (PS) standards was utilized, with apparent units adjusted to homo-polyethylene (PE) using known Mark-Houwink coefficients for PS and PE in TCB at this temperature. Absolute M_w information was calculated using a PDI static low-angle light scatter detector.

Procedure for DSC Analysis performed by Dow Chemical. Melting and crystallization temperatures of polymers were measured by differential scanning calorimetry (DSC 2910, TA Instruments, Inc.). Samples were first heated from room temperature to 210 °C at 10°C /min. After being held at this temperature for 4 min, the samples were cooled to -40 °C at 10/min and were then heated to 215 °C at 10/min after being held at -40°C for 4 min.

Table 3.4 Crystal data and structure refinement for **8**, **14**, and **16**.

	8	14	16
CCDC Number	877737		
Empirical formula	C ₃₃ H ₃₆ Cl ₂ N ₂ OTi	C ₄₆ H ₄₈ N ₂ OZr	C _{36.83} H _{46.32} Cl _{2.34} N ₂ OTi
Formula weight	595.44	736.08	663.77
T (K)	100(2)	100(2)	100(2)
a, Å	9.955(2)	11.0188(4)	10.387(2)
b, Å	11.603(3)	13.6909(5)	15.918(4)
c, Å	25.865(5)	15.0870(6)	21.740(5)
α, deg	90	64.169(2)	76.406(5)
β, deg	96.160(9)	68.942(2)	79.036(5)
γ, deg	90	75.522(2)	87.948(5)
Volume, Å ³	2970.6(11)	1899.90(13)	3429.9(14)
Z	4	2	4
Crystal system	Monoclinic	Triclinic	Triclinic
Space group	P2 ₁ /n	P -1	P -1
<i>d</i> _{calc} , g/cm ³	1.331	1.287	1.285
θ range, deg	1.58 to 24.71	2.0 to 39.6	1.447 to 30.637
Abs. coefficient, mm ⁻¹	0.497	0.33	0.463
Abs. correction	None	Semi Emp.	Semi Emp.
GOF	1.057	1.25	1.026
<i>R</i> ₁ , <i>wR</i> ₂ [<i>I</i> > 2σ(<i>I</i>)]	0.0384, 0.1052	0.0379, 0.0764	0.0387, 0.0950

Table 3.5 Crystal data and structure refinement for **7** and **24**(THF).

	17	24 (THF)
CCDC Number		
Empirical formula	C ₄₀ H ₄₃ NO ₃ Ti	C _{39.67} H _{57.34} Cl ₂ N ₂ O _{3.92} Ti
Formula weight	601.65	743.73
T (K)	100(2)	100(2)
a, Å	10.5475(6)	11.0051(7)
b, Å	11.5064(6)	12.9025(9)
c, Å	14.7987(8)	14.9598(10)
α, deg	67.224(2)	70.820(3)
β, deg	86.953(3)	77.256(3)
γ, deg	76.102(3)	85.136(3)
Volume, Å ³	1605.91(15)	1956.7(2)
Z	2	2
Crystal system	Triclinic	Triclinic
Space group	P -1	P -1
<i>d</i> _{calc} , g/cm ³	1.244	1.262
θ range, deg	2.44 to 41.64	1.9 to 26.2
Abs. coefficient, mm ⁻¹	0.30	0.40
Abs. correction	Semi Emp.	Semi Emp.
GOF	1.71	1.63
<i>R</i> ₁ , <i>wR</i> ₂ [<i>I</i> > 2σ(<i>I</i>)]	0.0415, 0.1014	0.0642, 0.1328

References

1. Hustad, P. D. *Science* **2009**, *325*, 704-707.
2. Natta, G.; Pino, P.; Corradini, P.; Danusso, F.; Mantica, E.; Mazzanti, G.; Moraglio, G. *J. Am. Chem. Soc.* **1955**, *77*, 1708-1710.
3. Gibson, V. C.; Spitzmesser, S. K. *Chem. Rev.* **2003**, *103*, 283-315.
4. (a) Brintzinger, H. H.; Fischer, D.; Mülhaupt, R.; Rieger, B.; Waymouth, R. M. *Angew. Chem. Int. Ed.* **1995**, *34*, 1143-1170. (b) Coates, G. W. *Chem. Rev.* **2000**, *100*, 1223-1252. (c) Resconi, L.; Cavallo, L.; Fait, A.; Piemontesi, F. *Chem. Rev.* **2000**, *100*, 1253-1346.
5. (a) Domski, G. J.; Rose, J. M.; Coates, G. W.; Bolig, A. D.; Brookhart, M. *Prog. Polym. Sci.* **2007**, *32*, 30-92. (b) Anderson-Wile, A. M.; Edson, J. B.; Coates, G. W. In *Complex Macromolecular Architectures*; John Wiley & Sons (Asia) Pte Ltd: Singapore, 2011, p 267-316.
6. Arriola, D. J.; Carnahan, E. M.; Hustad, P. D.; Kuhlman, R. L.; Wenzel, T. T. *Science* **2006**, *312*, 714-719.
7. (a) Agapie, T.; Henling, L. M.; DiPasquale, A. G.; Rheingold, A. L.; Bercaw, J. E. *Organometallics* **2008**, *27*, 6245-6256. (b) Golisz, S. R.; Bercaw, J. E. *Macromolecules* **2009**, *42*, 8751-8762.
8. Tonks, I. A.; Tofan, D.; Weintrob, E. C.; Agapie, T.; Bercaw, J. E. *Organometallics* **2012**, *31*, 1965-1974.
9. Alfa Aesar, H34478 2-Bromo-6-iodopyridine, 97%, 2013. <http://www.alfa.com/en/GP100W.pgm?DSSTK=H34478&rnd=060431362> (accessed June 25, 2013).
10. Alfa Aesar, A15397 2,6-Dibromopyridine, 98%, 2013. <http://www.alfa.com/en/GP100W.pgm?DSSTK=A15397&rnd=1911298042> (accessed June 25, 2013).
11. Alfa Aesar, H26961 2-Bromo-6-chloropyridine, 95%, 2013. <http://www.alfa.com/en/GP100W.pgm?DSSTK=H26961&rnd=664437533> (accessed June 25, 2013).
12. (a) Snégaroff, K.; Nguyen, T. T.; Marquise, N.; Halauko, Y. S.; Harford, P. J.; Roisnel, T.; Matulis, V. E.; Ivashkevich, O. A.; Chevallier, F.; Wheatley, A. E. *Chem. Eur. J.* **2011**, *17*, 13284-13297. (b) Chau, N. T. T.; Meyer, M.; Komagawa, S.; Chevallier, F.; Fort, Y.; Uchiyama, M.; Mongin, F.; Gros, P. C. *Chem. Eur. J.* **2010**, *16*, 12425-12433.
13. Zhang, H.; Tse, M. K.; Chan, K. S. *Synth. Commun.* **2001**, *31*, 1129-1139.
14. Agapie, T.; Bercaw, J. E. *Organometallics* **2007**, *26*, 2957-2959.

15. Rivas, F. M.; Riaz, U.; Giessert, A.; Smulik, J. A.; Diver, S. T. *Org. Lett.* **2001**, *3*, 2673-2676.
16. (a) Rebstock, A. S.; Mongin, F.; Trécourt, F.; Quéguiner, G. *Org. Biomol. Chem.* **2003**, *1*, 3064-3068. (b) Baudoin, O.; Guénard, D.; Guéritte, F. *J. Org. Chem.* **2000**, *65*, 9268-9271.
17. Tsukahara, T.; Swenson, D. C.; Jordan, R. F. *Organometallics* **1997**, *16*, 3303-3313.
18. (a) Xu, T.; Liu, J.; Wu, G.-P.; Lu, X.-B. *Inorg. Chem.* **2011**, *50*, 10884-10892.
19. See for example: (a) Boussie, T. R.; Diamond, G. M.; Goh, C.; Hall, K. A.; LaPointe, A. M.; Leclerc, M.; Lund, C.; Murphy, V.; Shoemaker, J. A. W.; Tracht, U.; Turner, H.; Zhang, J.; Uno, T.; Rosen, R. K.; Stevens, J. C. *J. Am. Chem. Soc.* **2003**, *125*, 4306-4317. (b) Frazier, K. A.; Froese, R. D.; He, Y.; Klosin, J.; Theriault, C. N.; Vosejka, P. C.; Zhou, Z.; Abboud, K. A. *Organometallics* **2011**, *30*, 3318-3329.
20. Passaglia, E.; Kevorkian, H. K. *J. Appl. Phys.* **1963**, *34*, 90-97.
21. For ^{13}C NMR assignment of 2,1-insertions see: (a) Asakura, T.; Nishiyama, Y.; Doi, Y. *Macromolecules* **1987**, *20*, 616-620. (b) Grassi, A.; Zambelli, A.; Resconi, L.; Albizzati, E.; Mazzocchi, R. *Macromolecules* **1988**, *21*, 617-622. (c) Cheng, H. N.; Ewen, J. A. *Makromol. Chem.* **1989**, *190*, 1931-1943. (d) Asakura, T.; Nakayama, N.; Demura, M.; Asano, A. *Macromolecules* **1992**, *25*, 4876-4881. (e) Zhou, Z.; Stevens, J. C.; Klosin, J.; Kummerle, R.; Qiu, X. H.; Redwine, D.; Cong, R. J.; Taha, A.; Mason, J.; Winniford, B.; Chauvel, P.; Montanez, N. *Macromolecules* **2009**, *42*, 2291-2294.
22. Busico, V.; Cipullo, R.; Chadwick, J. C.; Modder, J. F.; Sudmeijer, O. *Macromolecules* **1994**, *27*, 7538-7543.
23. Hustad, P. D.; Tian, J.; Coates, G. W. *J. Am. Chem. Soc.* **2002**, *124*, 3614-3621.
24. Resconi has reported a zirconocene catalyst that polymerizes propylene with 2,1-insertions on the order of 3 mol%: Resconi, L.; Camurati, I.; Sudmeijer, O. *Top. Catal.* **1999**, *7*, 145-163. A Ti thio(bisphenoxy) complex has been reported by Miyatake et al. that gives a regioirregular polypropylene (the mol% of 2,1-insertions was not reported): Miyatake, T.; Mizunuma, K.; Kakugo, M. *Makromol. Chem., Macromol. Symp.* **1993**, *66*, 203-214.
25. For exemplary ^{13}C NMR of polypropylene from a late-metal catalyst see: McCord, E. F.; McLain, S. J.; Nelson, L. T. J.; Arthur, S. D.; Coughlin, E. B.; Ittel, S. D.; Johnson, L. K.; Tempel, D.; Killian, C. M.; Brookhart, M. *Macromolecules* **2001**, *34*, 362-371.

26. Ewart, S. W.; Sarsfield, M. J.; Jeremic, D.; Tremblay, T. L.; Williams, E. F.; Baird, M. C. *Organometallics* **1998**, *17*, 1502-1510.
27. Würtz, S.; Lohre, C.; Fröhlich, R.; Bergander, K.; Glorius, F. *J. Am. Chem. Soc.* **2009**, *131*, 8344-8345.
28. Aluri, B. R.; Kindermann, M. K.; Jones, P. G.; Dix, I.; Heinicke, J. *Inorg. Chem.* **2008**, *47*, 6900-6912.
29. (a) Tshuva, E. Y.; Goldberg, I.; Kol, M.; Weitman, H.; Goldschmidt, Z. *Chem. Commun.* **2000**, 379-380. (b) Tshuva, E. Y.; Goldberg, I.; Kol, M.; Goldschmidt, Z. *Organometallics* **2001**, *20*, 3017-3028. (c) Tshuva, E. Y.; Groysman, S.; Goldberg, I.; Kol, M.; Goldschmidt, Z. *Organometallics* **2002**, *21*, 662-670.
30. (a) Segal, S.; Goldberg, I.; Kol, M. *Organometallics* **2005**, *24*, 200-202. (b) Yeori, A.; Goldberg, I.; Shuster, M.; Kol, M. *J. Am. Chem. Soc.* **2006**, *128*, 13062-13063.
31. Tshuva, E. Y.; Goldberg, I.; Kol, M. *J. Am. Chem. Soc.* **2000**, *122*, 10706-10707.
32. Kwong, F. Y.; Klapars, A.; Buchwald, S. L. *Org. Lett.* **2002**, *4*, 581-584.
33. Bassi, I.; Allegra, G.; Scordamaglia, R.; Chioccola, G. *J. Am. Chem. Soc.* **1971**, *93*, 3787-3788.
34. Giesbrecht, G. R.; Whitener, G. D.; Arnold, J. *Organometallics* **2000**, *19*, 2809-2812.
35. (a) Chan, M. C.; Kui, S. C.; Cole, J. M.; McIntyre, G. J.; Matsui, S.; Zhu, N.; Tam, K. H. *Chem. Eur. J.* **2006**, *12*, 2607-2619. (b) Tam, K.-H.; Lo, J. C.; Guo, Z.; Chan, M. C. *J. Organomet. Chem.* **2007**, *692*, 4750-4759. (c) Tam, K.-H.; Chan, M. C.; Kaneyoshi, H.; Makio, H.; Zhu, N. *Organometallics* **2009**, *28*, 5877-5882. (d) Liu, C.-C.; So, L.-C.; Lo, J. C.; Chan, M. C.; Kaneyoshi, H.; Makio, H. *Organometallics* **2012**, *31*, 5274-5281. (e) Lo, J. C.; Chan, M. C.; Lo, P.-K.; Lau, K.-C.; Ochiai, T.; Makio, H. *Organometallics* **2013**, *32*, 449-459.
36. Murray, M. C.; Baird, M. C. *Can. J. Chem.* **2001**, *79*, 1012-1018.
37. (a) Boussie, T. R.; Diamond, G. M.; Goh, C.; Hall, K. A.; LaPointe, A. M.; Leclerc, M. K.; Murphy, V.; Shoemaker, J. A.; Turner, H.; Rosen, R. K. *Angew. Chem. Int. Ed.* **2006**, *45*, 3278-3283. (b) Froese, R. D.; Hustad, P. D.; Kuhlman, R. L.; Wenzel, T. T. *J. Am. Chem. Soc.* **2007**, *129*, 7831-7840.
38. Hintermann, L.; Dang, T. T.; Labonne, A.; Kribber, T.; Xiao, L.; Naumov, P. *Chem. Eur. J.* **2009**, *15*, 7167-7179.
39. Diamond, G. M.; Hall, K. A.; LaPointe, A. M.; Leclerc, M. K.; Longmire, J.; Shoemaker, J. A.; Sun, P. *ACS Catalysis* **2011**, *1*, 887-900.

40. Davies, C. J.; Gregory, A.; Griffith, P.; Perkins, T.; Singh, K.; Solan, G. A. *Tetrahedron* **2008**, *64*, 9857-9864.
41. (a) Resconi, L.; Bossi, S.; Abis, L. *Macromolecules* **1990**, *23*, 4489-4491. (b) Chien, J. C. W.; Wang, B. P. *J. Polym. Sci., A: Polym. Chem.* **1988**, *26*, 3089-3102. (c) Chien, J. C. W.; Razavi, A. *J. Polym. Sci., A: Polym. Chem.* **1988**, *26*, 2369-2380. (d) Chien, J. C. W.; Wang, B. P. *J. Polym. Sci., A: Polym. Chem.* **1990**, *28*, 15-38.
42. Busico, V.; Cipullo, R.; Pellicchia, R.; Rongo, L.; Talarico, G.; Macchioni, A.; Zuccaccia, C.; Froese, R. D. J.; Hustad, P. D. *Macromolecules* **2009**, *42*, 4369-4373.
43. Pangborn, A. B.; Giardello, M. A.; Grubbs, R. H.; Rosen, R. K.; Timmers, F. J. *Organometallics* **1996**, *15*, 1518-1520.
44. Benzing, E.; Kornicker, W. *Chem. Ber.* **1961**, *94*, 2263-2267.
45. Felten, J. J.; Anderson, W. P. *J. Organomet. Chem.* **1972**, *36*, 87-92.

Chapter 4

Improved Synthesis of Fujita's Ti Phenoxy–Imine Catalyst and Initial Studies of 1-Hexene Trimerization

Chapter 4

Introduction

α -Olefins are important building blocks for many valuable products including detergents, polymers, and lubricants.¹ Currently, the primary industrial route to even carbon number α -olefins is oligomerization of ethylene, which generates a statistical mixture (Schulz–Flory distribution) of olefins. For many applications, however, a pure olefin feedstock is required, such as in copolymerizations of 1-hexene and ethylene to generate linear low density polyethylene (LLDPE);² thus, costly fractional distillation is often necessary to separate olefin products generated through nonselective oligomerization.³

Selective trimerization of ethylene and other olefins by homogeneous catalysts may offer a more cost effective route to obtain some linear α -olefins. Indeed, interest in this field has grown and selective olefin oligomerization systems are now known for chromium, titanium, and tantalum, with Cr systems generally being the most active and selective.⁴ For example, a PNP/CrCl₃(THF)₃ (PNP = *N,N*-bis(bis(*o*-methoxyphenyl)phosphino)methylamine) is known that can be activated with 300 equiv of MAO at 20 atm ethylene and 80 °C to produce 90% C₆ with 99.9% 1-hexene with a productivity of 1,033,200 g (g of Cr)⁻¹ h⁻¹ (Figure 4.1).⁵ In fact, a chromium system is currently used by Chevron–Phillips for the commercial production of 1-hexene.⁶

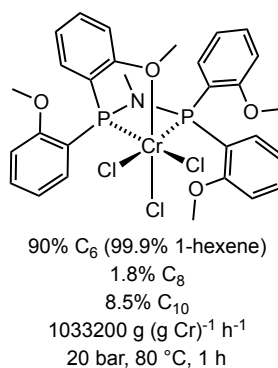


Figure 4.1 PNP/CrCl₃(THF)₃ system for selective ethylene trimerization. See ref. 5.

Our group is interested in upgrading simple feedstocks to liquid hydrocarbon fuels through co-oligomerization of heavy and light olefins. An ideal catalytic system for this process would be selective for fuel range hydrocarbons, which for diesel fuel is typically C₈–C₁₈. If a catalyst could trimerize a potentially renewable feedstock such as ethylene and then subsequently incorporate the resulting α -olefin product effectively into new catalytic cycles, then a selective route to hydrocarbons larger than C₆ or C₈ could be obtained using a simple feedstock as a starting material.

Recently, Fujita and co-workers reported a Ti complex supported by a phenoxy–imine (FI) ligand with a pendant donor arm that upon activation with methylaluminoxane (MAO) trimerizes ethylene to 1-hexene with excellent activity and selectivity (Figure 4.2).⁷ Fujita proposes selective trimerization involves a metallacycle mechanism with Ti(II) and Ti(IV) species, rather than linear chain growth (Cossee-Arman mechanism). β -hydride elimination and reductive elimination are proposed to form an intermediate Ti(II) species from a starting Ti(IV) dialkyl species (Scheme 4.1). This proposed Ti(II) intermediate species can

then oxidatively couple ethylene to form a Ti(IV) metallacycle, which can insert another ethylene to form a metallacycloheptane. β -hydride elimination and reductive elimination or a concerted 3,7-H transfer from the metallacycloheptane intermediate leads to 1-hexene (Scheme 4.2). Indeed, studies in our laboratory using deuterium labeled ethylene (C_2H_4 and C_2D_4) have confirmed a metallacycle mechanism;⁸ only products with even numbers of deuterium were observed to form when a 1:1 mixture of C_2H_4 and C_2D_4 were trimerized (a Cossee-Arman mechanism is expected to lead to products with odd numbers of deuterium).

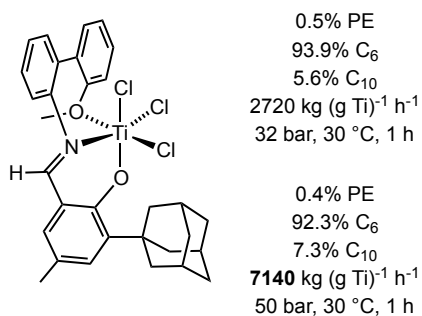
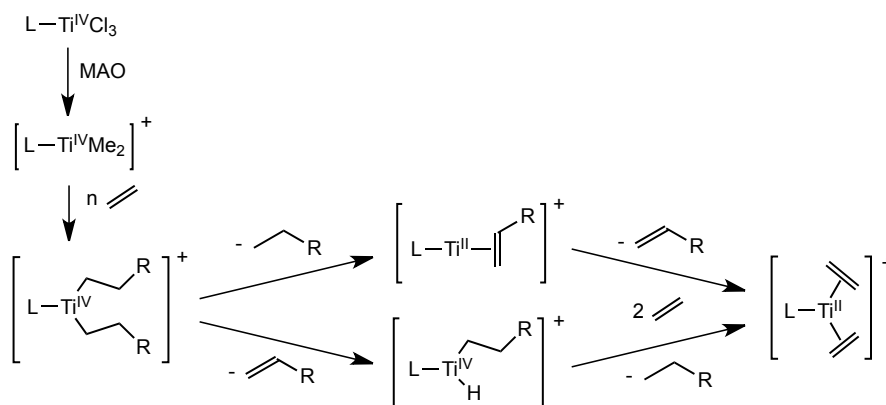
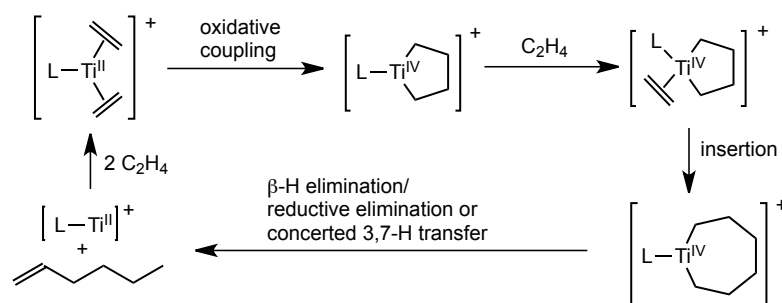


Figure 4.2 Trimerization of ethylene with a (FI)Ti complex at different ethylene pressures. See ref. 7.



Scheme 4.1 Proposed mechanism for formation of Ti(II) from starting Ti(IV) complex upon activation with MAO. (Adapted from ref. 7).



Scheme 4.2 Proposed mechanism for selective trimerization of ethylene to 1-hexene by (FI)Ti complexes. (Adapted from ref. 7).

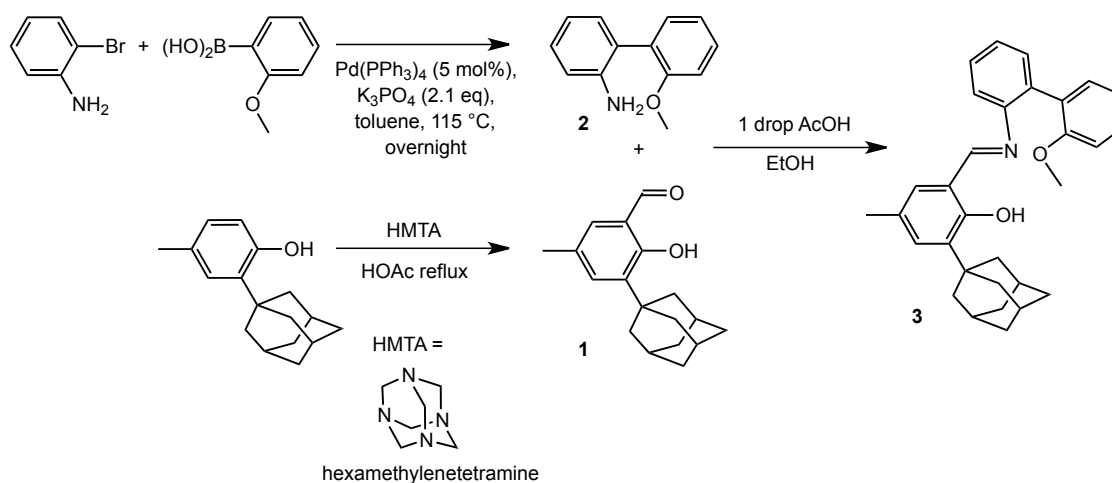
Interestingly, Fujita reports the formation of C_{10} products during the trimerization of ethylene with (FI)Ti complexes. These products result from incorporation of newly formed 1-hexene into the ethylene trimerization catalytic cycle. Furthermore, Fujita has identified primarily one major C_{10} product: 2-butyl-hex-1-ene, with only minor branched decene products, which may suggest that 1-hexene is incorporated selectively. Based on these results, we were interested in investigating (FI)Ti complexes as potential candidates for trimerization of higher α -olefins for selective formation of fuel range liquid hydrocarbons.

Results and Discussion

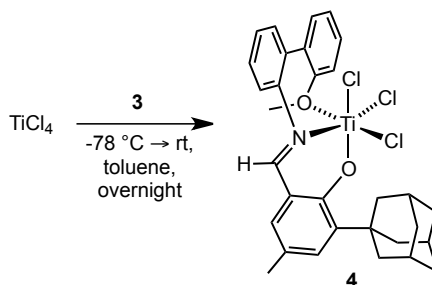
Improved Synthesis of Fujita Catalyst

The synthesis for phenoxy–imine ligand reported by Fujita et al., seemed unnecessarily cumbersome, so we first sought to design a more straightforward synthesis that would also be easier to scale up. Formylation of 2-adamantyl-*p*-cresol⁹ was achieved via a Duff reaction with hexamethylenetetramine (HMTA) in refluxing acetic acid to yield 3-admantyl-2-hydroxy-5-methylbenzaldehyde **1**

(Scheme 4.3).¹⁰ For comparison, Fujita employed a magnesium-mediated ortho-formylation reaction, which requires more steps and is less amenable to large-scale reactions.^{7,11} The aniline 2-(2'-methoxyphenyl)aniline **2** was synthesized by a Suzuki coupling reaction between commercially available 2-bromoaniline and 2-methoxyphenylboronic acid. In our hands, the Suzuki coupling reaction conditions reported by Fujita and co-workers did not lead to any C–C bond coupling;⁷ for our conditions, see the Experimental Section. Finally, a condensation reaction between **1** and **2** led to the desired phenoxy–imine ligand **3** (Scheme 4.3). Metalation of **3** with TiCl_4 in toluene yielded the Ti phenoxy–imine complex (**3**) TiCl_3 **4** (Scheme 4.4). Notably, we did not observe precipitation of **4** from the reaction mixture as described by Fujita et al.,⁷ but were able to obtain complex **4** by removal of solvent in vacuo and washing the solid with diethyl ether.



Scheme 4.3 Improved synthesis of phenoxy–imine ligand **3**.



Scheme 4.4 Synthesis of (FI)Ti complex **4**.

Trimerization of 1-Hexene in Different Solvents and Neat

We were interested in testing the ability of **4** to trimerize linear α -olefins higher than ethylene. We have previously observed significant solvent effects on trimerization activity for a Cr trimerization precatalyst $[\text{CrCl}_3(\text{PNP})]$.¹² Thus, we were interested in investigating the potential of **4** to trimerize 1-hexene in different solvents. For our initial investigations, we tested activation of **4** with 1000 equivalents of MMAO in cyclohexane – the solvent used for ethylene trimerization studies by Fujita – and chlorobenzene. Unfortunately, at somewhat dilute concentrations of 1-hexene (~ 0.2 M) in either cyclohexane or chlorobenzene, we observed disappointing productivities for 1-hexene oligomerization: $2.7 \text{ g of C}_{12} + \text{C}_{18} (\text{g of Ti})^{-1} \text{ h}^{-1}$ and $17.1 \text{ g of C}_{12} + \text{C}_{18} (\text{g of Ti})^{-1} \text{ h}^{-1}$, respectively. By comparison, the reported productivity of **4** for ethylene trimerization under only 7.9 atm of ethylene is $155 \text{ kg of 1-hexene (g of Ti)}^{-1} \text{ h}^{-1}$ (productivity is dependent on ethylene pressure). Since we still observed some conversion of 1-hexene to C_{12} and C_{18} products, we decided to test trimerization of neat 1-hexene; activation of **4** with 1000 equiv of MMAO led to oligomerization of 1-hexene with a productivity of $730 \text{ g of C}_{12} + \text{C}_{18} (\text{g of Ti})^{-1} \text{ h}^{-1}$. Analysis of the

oligomerization products by GC suggests that at least five different C₁₈ products formed and indicates that more C₁₈ products formed than C₁₂ products: 0.29 g and 0.01 g, respectively (Figure 4.3). Notably, eight different C₁₈ products are possible, which may indicate that the formation of some products are unfavorable or the products may not be sufficiently separated by GC (see Scheme 4.5 for all possible C₁₈ products).

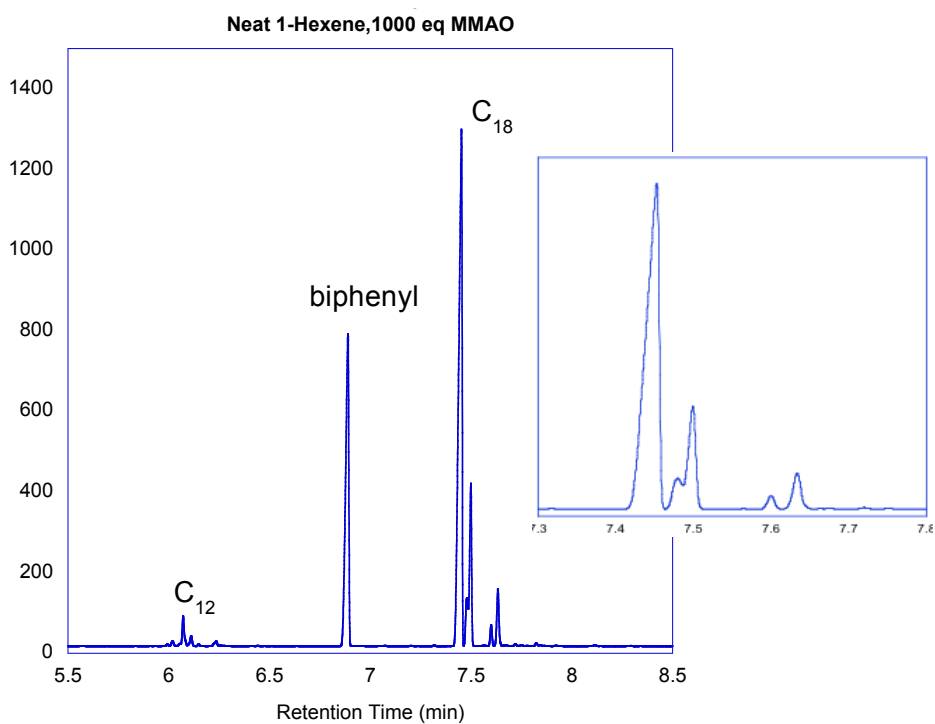
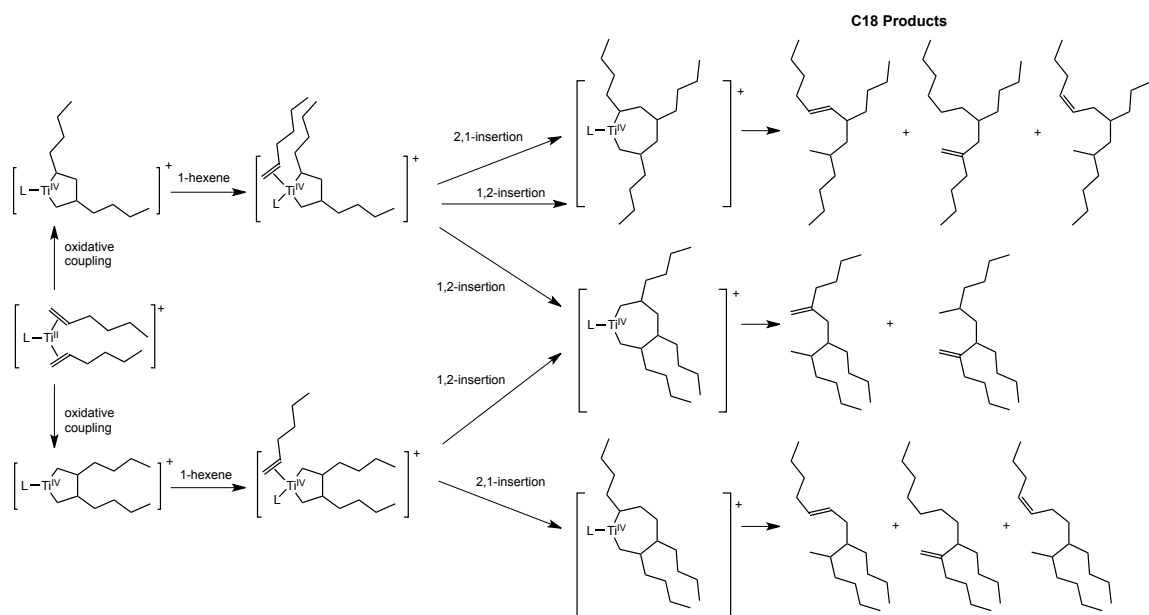


Figure 4.3 GC trace of 1-hexene oligomerization products from **4**/MMAO with close-up of C₁₈ product peaks (biphenyl is an internal standard).



Scheme 4.5 Possible C₁₈ products from trimerization of 1-hexene.

Investigation of MAO Equivalents

In the initial ethylene trimerization report, Fujita employs a rather high Al/4 ratio of 10,000:1. We were interested in investigating the effect of different ratios of Al (MMAO)/4 on oligomerization activity and to determine if less MAO could be used in the reaction. Accordingly, oligomerization of neat 1-hexene was tested with Al/4 ratios of 250:1 and 5000:1. These data along with the data for 1000:1 are shown in Table 4.1. The productivity of the reaction was significantly lower when only 250 equiv of MMAO were employed: 4.5 g of C₁₂ + C₁₈ (g of Ti)⁻¹ h⁻¹; however, the productivity did not significantly increase upon increasing the MMAO equivalents from 1000 to 5000. These results suggest that 1000 equiv of MMAO may be sufficient for activation of **4** for oligomerization.

Table 4.1 Data for trimerization of 1-hexene with different equivalents of MMAO.

1-Hexene Concentration ^a	MMAO (equiv)	Selectivity (g product)		C ₁₂ and C ₁₈ productivity ((g of C ₁₂ + g of C ₁₈)/(g of Ti)·h)
		C ₁₂	C ₁₈	
neat	250	4.9 × 10 ⁻⁴	1.4 × 10 ⁻³	4.5
neat	1000	1.0 × 10 ⁻²	2.9 × 10 ⁻¹	750
neat	5000	5.0 × 10 ⁻²	3.6 × 10 ⁻¹	962

^aOligomerization were carried out with 1 mL of PhCl at 22 °C for 1 h.

Conclusions and Future Work

An improved synthesis of the phenoxy–imine ligand reported by Fujita has been described and oligomerization of 1-hexene by a (FI)Ti complex is reported. Oligomerization of 1-hexene was found to be inefficient at dilute concentrations of 1-hexene, but C₁₂ and C₁₈ products were observed to form with good productivities when 1-hexene was used as the solvent. The influence of Al equivalents on oligomerization productivity was also investigated. Although these results represent only preliminary data, they importantly indicate that the (FI)Ti complex **4** can trimerize higher α -olefins, which is promising for the development of a catalytic system to upgrade light olefins into liquid fuel range hydrocarbons. Future experiments will investigate the catalyst lifetime, as well the rate of incorporation of linear α -olefins (e.g. 1-heptene) vs. ethylene.

Experimental Section

General Considerations

All air- and moisture-sensitive compounds were manipulated using standard high-vacuum and Schlenk techniques or manipulated in a glovebox

under a nitrogen atmosphere. Solvents for air- and moisture-sensitive reactions were dried over sodium benzophenone ketyl and stored over titanocene where compatible, or dried by the method of Grubbs.¹³ 3-admantyl-2-hydroxy-5-methylbenzaldehyde (**1**) and **3** were prepared following literature procedures.¹⁰ 2-adamantyl-*p*-cresol, hexamethylenetetramine (HMTA), 2-bromoaniline, 2-methoxyphenylboronic acid and TiCl₄ as a 1.0 M solution in toluene were purchased from Sigma Aldrich and used as received. Modified methylaluminoxane (MMAO) was purchased from Albemarle as a 7 wt% Al solution in isohexanes (MMAO-C4). 1-Hexene was distilled from CaH₂. C₆D₅Cl and CDCl₃ were purchased from Cambridge Isotopes. C₆D₅Cl was distilled from CaH₂ and passed through a plug of activated alumina prior to use. NMR spectra were recorded on Varian Mercury 300, Varian INOVA 500 or Varian INOVA 600 spectrometers and referenced to the solvent residual peak. Gas chromatography–mass spectrometry (GC-MS) analyses were performed on an Agilent 6890N system with an HP-5MS capillary column (30 m length, 0.25 mm diameter, and 0.5 μm film) that was equipped with an Agilent 5973N mass selective detector. Gas chromatography (GC) analyses were performed on an Agilent 6890N instrument with a flame ionization detector (FID). Routine runs were performed using a DB-1 capillary column (10 m length, 0.10 mm diameter, 0.40 μm film) with the following heating program: hold at 40 °C for 3 min, ramp temperature at 50 °C/min to 290 °C and then hold for 3 min (total run time 13 min). The amount of products in each oligomerization experiment was

determined by comparison of the integrated areas of the peaks to the integrated area of a biphenyl internal standard as a reference.

2-(2'-methoxyphenyl)aniline 2. An oven-dried 350 mL Schlenk bomb was charged with a stirbar, evacuated and refilled with Ar. Under positive Ar pressure, 2.955 g (0.0171 mol) of 2-bromoaniline, 2.871 g (0.189 mol) 2-methoxyphenylboronic acid, 0.998 g (0.864 mmol) of Pd(PPh₃)₄ and 10.933 g (0.515 mol) of K₃PO₄ crushed with a mortar and pestle were added and the vessel was sealed with a septum. The vessel was evacuated and refilled with Ar three times. 70 mL of dry toluene was added via syringe and the vessel was sealed with a Kontes valve. The reaction mixture was stirred at room temperature for 2 min, then the vessel was placed in a 115 °C oil bath overnight. The following day the vessel was cooled to room temperature, and the suspension filtered through celite with the aid of dichloromethane. Solvent was removed in vacuo and the resulting residue was purified by column chromatography on silica gel using 5:1 hexanes/ethyl acetate as the eluent to afford **2** as a white solid. 2.568 g (0.0129 mol) yellow-white powder (75% yield). The identity of the compound was confirmed by comparison with the reported spectroscopic data.

Modified Procedure for Synthesis of (3)TiCl₃ 4. A toluene solution of **3** was added via cannula to a solution of TiCl₄ in toluene at -78 °C under Ar on the Schlenk line. The reaction mixture was allowed to warm to room temperature and

stirred overnight. No solid was observed to precipitate, so the solvent was removed *in vacuo* to reveal a red-brown sludge, and the reaction vessel was taken into a glovebox. The sludge was taken up in diethyl ether and filtered through a glass frit to reveal a red brown powder. The identity of the compound was confirmed by comparison with the reported spectroscopic data.

General Procedure for Oligomerization Reactions in Neat 1-Hexene. To a 20-mL vial in the glovebox was added 4.0 mL (0.032 mol) of 1-hexene and 0.579 g (1000 eq) of MMAO. 5.2 mg (0.0086 mmol) of **4** was dissolved in 1.0 mL of chlorobenzene and taken up into a syringe and then added slowly to the solution of 1-hexene and MMAO while stirring. The vial was capped and stirring was continued at room temperature for 1 h. The reaction was then removed from the glovebox and quenched with a 10% v/v HCl/H₂O solution, then 50.0 mg (0.32 mmol) of biphenyl was added to the reaction mixture as a GC standard. The organic layer was carefully separated and a 2.0 mL aliquot of the organic phase was filtered through a short silica plug and then subjected to analysis by GC.

General Procedure for Oligomerization Reactions with 1-Hexene and a Co-Solvent. The same procedure as above for neat 1-hexene was followed, except 0.210 g of 1-hexene (2.5 mmol) and 10.0 mL of the co-solvent (cyclohexane or chlorobenzene) were added to the MMAO solution.

References

1. Lappin, G. R.; Nemeč, L. H.; Sauer, J. D.; Wagner, J. D. In *Kirk–Othmer Encyclopedia of Chemical Technology*; Wiley & Sons, Inc: 2005.
2. Vogt, D. Oligomerization of Ethylene to Higher Linear α -Olefins. In *Applied Homogeneous Catalysis with Organometallic Compounds*; Cornils, B., Herrmann, W. A., Eds.; VCH: New York, 1996; Vol. 1, pp 245-258.
3. Skupinska, J. *Chem. Rev.* **1991**, *91*, 613-648.
4. Agapie, T. *Coord. Chem. Rev.* **2011**, *255*, 861-880.
5. Carter, A.; Cohen, S. A.; Cooley, N. A.; Murphy, A.; Scutt, J.; Wass, D. F. *Chem. Commun.* **2002**, 858-859.
6. (a) Reagen, W. K.; Conroy, B. K. (Phillips Petroleum Co.). Canadian Patent 2020509, 1991. (b) Chemical Week Editorial Staff. *Chem. Eng. (N.Y.)* **2005**, *112*, 28.
7. Suzuki, Y.; Kinoshita, S.; Shibahara, A.; Ishii, S.; Kawamura, K.; Inoue, Y.; Fujita, T. *Organometallics* **2010**, *29*, 2394-2396.
8. For details on the experimental procedure for trimerization with deuterated ethylene see: (a) Agapie, T.; Schofer, S. J.; Labinger, J. A.; Bercaw, J. E. *J. Am. Chem. Soc.* **2004**, *126*, 1304-1305. (b) Agapie, T.; Labinger, J. A.; Bercaw, J. E. *J. Am. Chem. Soc.* **2007**, *129*, 14281-14295.
9. Although we purchased 2-adamantyl-*p*-cresol, it can be easily synthesized on a large scale from *p*-cresol and 1-adamantanol. See: Gademann, K.; Chavez, D. E.; Jacobsen, E. N. *Angew. Chem., Int. Ed.* **2002**, *41*, 3059-3061.
10. Chen, C. T.; Kao, J. Q.; Salunke, S. B.; Lin, Y. H. *Org. Lett.* **2011**, *13*, 26-29.
11. Aldred, R.; Johnston, R.; Levin, D.; Neilan, J. *J. Chem. Soc., Perkin Trans. 1* **1994**, 1823-1831.
12. Do, L. H.; Labinger, J. A.; Bercaw, J. E. *Organometallics* **2012**, *31*, 5143-5149.
13. Pangborn, A. B.; Giardello, M. A.; Grubbs, R. H.; Rosen, R. K.; Timmers, F. J. *Organometallics* **1996**, *15*, 1518-1520.

Appendix A

Compound Numbers by Chapter: A Handy Guide

A p p e n d i x A

Chapter 2 Compounds

- 1 $(\text{CO})_5\text{Cr}\{(\text{OMe})(p\text{-CF}_3\text{-C}_6\text{H}_4)\}$
- 2 $(\text{CO})_5\text{Cr}\{(\text{OMe})(p\text{-OMe-C}_6\text{H}_4)\}$
- 3 $(\text{CO})_5\text{Cr}\{(\text{OMe})(p\text{-NMe}_2\text{-C}_6\text{H}_4)\}$
- 4 (*E/Z*)-1,2-dimethoxy-1,2-bis(4-methoxyphenyl)ethane
- 5 $\text{Cp}(\text{CO})(\text{NO})\text{Cr}\{\text{C}(\text{OMe})(\text{C}_6\text{H}_5)\}$
- 6 $\text{Cp}(\text{CO})(\text{NO})\text{Cr}\{\text{C}(\text{OMe})(p\text{-CF}_3\text{-C}_6\text{H}_4)\}$
- 7 (triphos)(PPh₃)Pd
- 8 (triphos)(PPh₃)Pt
- 9 $\text{Cl}_2\text{Pt}\{\text{C}(\text{OMe})\text{Me}\}_2$
- 10 $\text{Br}_2\text{Pt}\{\text{C}(\text{OMe})\text{Me}\}_2$
- 11 $\text{Cl}_2\text{Pt}\{\text{C}(\text{O}^i\text{Pr})\text{Me}\}_2$
- 12 (*E/Z*)-2,3-dimethoxybut-2-ene
- 13 (*E/Z*)-2,3-diisopropoxybut-2-ene
- 14 *cis*-dichlorobis(triphenylphosphine)platinum(II)
- 15 2,3-dimethoxybut-1-ene **15**
- 16 *cis*-dibromobis(triphenylphosphine)platinum(II)
- 17 2,3-diisopropoxybut-1-ene
- 18 $\text{Cl}(\text{py})\text{Pt}(\text{COMe})\{\text{C}(\text{OMe})\text{Me}\}$
- 19 $\text{Br}(\text{py})\text{Pt}(\text{COMe})\{\text{C}(\text{OMe})\text{Me}\}$
- 20 $\text{Cl}(\text{py})\text{Pt}(\text{COMe})\{\text{C}(\text{O}^i\text{Pr})\text{Me}\}$
- 21 dichloride(but-2-yl)platinum(II) intermediate
- 22 $[\text{Cl}_2\text{Pt}(\text{COMe})\{\text{C}(\text{OMe})(\text{Me})\}]n\text{Bu}_4\text{NCl}$

Chapter 3 Compounds

- 1 2-(3,5-di-*t*-butyl-2-(methoxymethoxy)phenyl)-4,4,5,5-tetramethyl-1,3,2-dioxaborolane (boronic ester)
- 2 2-bromo-6-(3,5-di-*t*-butyl-2-(methoxymethoxy)phenyl)pyridine (monoarylated pyridine)
- 3 6,6'-(pyridine-2,6-diyl)bis(2,4-di-*tert*-butylphenol) (Bis-arylated pyridine)
- 4 2-bromo-*N*-(1-phenylethyl)aniline
- 5 2,4-di-*t*-butyl-6-(6-(2-((1-phenylethyl)amino)phenyl)pyridin-2-yl)phenol (NNO)
- 6 (5)ZrBn₂
- 7 (5)HfBn₂
- 8 (5)TiCl₂
- 9 (5)TiBn₂
- 10 ^{Bn}NNO
- 11 ^{Ad}NNO
- 12 2-bromo-*N*-methoxyethylaniline
- 13 ^{MeOEt}NNO
- 14 (10)ZrBn₂
- 15 (10)TiCl₂
- 16 (11)TiCl₂
- 17 (13)ZrBn₂
- 18 2,4-di-*t*-butyl-6-(6-(*o*-tolyl)pyridin-2-yl)phenol (CNO)
- 19 (18)TiBn₂
- 20 2,4-di-*t*-butyl-6-(6-(3,5-di-*t*-butylphenyl)pyridin-2-yl)phenol (ArNO)
- 21 2,4-di-*t*-butyl-6-(6-(((1-phenylethyl)amino)-methyl)pyridin-2-yl)phenol (amido(pyridine)phenoxide)
- 22 (21)TiBn₂
- 23 (21)HfBn₂
- 24 (21)TiCl₂

Chapter 4 Compounds

- 1 3-admantyl-2-hydroxy-5-methylbenzaldehyde
- 2 2-(2'-methoxyphenyl)aniline
- 3 phenoxy-imine ligand
- 4 (3)TiCl₃

Appendix B

Comparison of ^{13}C NMR Data of Polypropylene from $(\text{NNO})\text{TiCl}_2$ (**8**)
and Reported ^{13}C NMR Data for Regioirregular Propylene

A p p e n d i x B

Analysis of Polypropylene Regiospecificity by ^{13}C NMR Spectroscopy

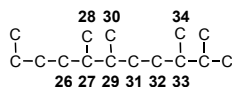
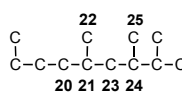
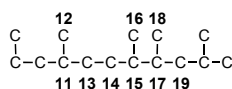
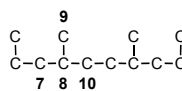
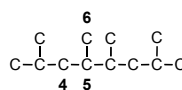
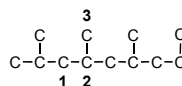
The following table compares peaks observed in the ^{13}C spectra of polypropylene (PP) from $(\text{NNO})\text{TiCl}_2$ (Chapter 3, **8**) with known literature values. The ^{13}C chemical shifts of PP from $(\text{NNO})\text{TiCl}_2$ are listed in the column “Expt'l Data.” The column to the right of the experimental data shows a range of chemical shifts reported in the literature and the corresponding type of insertion. The number in bold (1-44) corresponds to a carbon atom in the chemdraws to the right of the table, which show all of the possible sequences obtained from 1,2-, 2,1- and 3,1-insertion modes. The S, T and P in parentheses next to the bold carbon numbers indicate secondary, tertiary, and primary carbons, respectively, and the number range indicates the chemical shift range reported in the references listed at the top of the table. Finally, the colored blocks (orange, pink, and blue) represent the chemical shift ranges for secondary (orange), tertiary (pink), and primary (blue) carbons in polypropylene as reported in the literature. These color blocks show that chemical shift range for secondary and tertiary carbons overlap in the region of $\sim 32\text{-}40$ ppm in ^{13}C NMR spectroscopy.

This table allows for three important observations: 1) The methyl region of the ^{13}C spectra is well separated from the methine and methylene regions. 2) Since the data for PP from complex **8** has peaks in the overlapping region for secondary and tertiary carbons, we are not able to assign methylene and

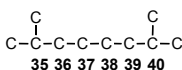
methine carbons by ^{13}C NMR data alone. 3) We observe peaks very close to the reported regions for 3,1-insertions (which overlap regions for 2,1-insertions), so we cannot rule out 3,1-insertions from our ^{13}C NMR data.

Expt'l Data	Macromolecules 1992, 25, 4876		Makromol. Chem. 1989, 190, 1931	
	2,1-insertions		3,1-insertion	n-propyl end group
46.49 46.01 45.94 45.49 45.39	1 (S) (45.7-47.7)	7 (S) (45.7-46.5)		
43.01 42.82 42.72 42.65	4, 19, 23 (S) (43.3-44.1)			
41.67 41.39 41.29 41.13	4 (S) (40.9-42.3)			
40.83				42 (S) (39.59-40.8)
38.11 37.23 37.06 36.76 36.65	15, 27, 29, 33 (T) (36.8-39.1)	Secondary (methylene)		36, 39 (S) (37.62-38.51)
36.48	13 (T) (36.5)			
35.16	5, 24 (T), 10, 13, 20 (S) (35.4-35.6)			
34.10 33.82 33.58 33.25 32.99	5, 17, 24 (T), 10, 20 (S) (34.2-34.8)			
32.88 32.06 31.97	31 (S) (33.4)			
31.16 30.90	14, 16 (S) (32.6)			
30.84 30.69 30.57 30.07	8, 11, 21 (T), 32 (S) (31.1-31.3)			
28.67 28.60 28.25 28.07	2 (T) (28.3-28.4)			
28.00 21.35 21.16				35, 40 (T) (30.8-30.92)
21.00 20.69 20.57 20.43 20.29	9, 12, 22 (P) (20.1-20.9)			41 (T) (30.3-30.8)
19.65 17.06 16.71 16.63 15.19 15.12	3 (P) (20.1-20.7)			
14.69 14.50 14.23 14.12	6, 25, 34 (P) (16.6-17.2)			43 (S) (19.73-20.3)
	6, 16, 18, 25, 28, 30 (P) (14.7-15.1)			
		Primary (methyl)		44 (P) (14.3-14.51)

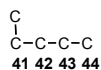
2,1-insertion modes



3,1-insertion



n-propyl end group



Secondary Carbon (methylene) = S
Tertiary Carbon (methine) = T
Primary Carbon (methyl) = P

